Karlsruhe Institute of Technology

Plastic Concrete for Cut-Off Walls: Novel Insights into the Microstructural Properties and Uniaxial Mechanical Behaviour over Time

Zur Erlangung des akademischen Grades eines

Doktors der Ingenieurwissenschaften (Dr.-Ing.)

von der KIT-Fakultät für

Bauingenieur, Geo- und Umweltwissenschaften des

Karlsruher Instituts für Technologie (KIT)

genehmigte

Dissertation

von

David Alós Shepherd, M.Sc.

Tag der mündlichen Prüfung:	18. Dezember 2023
Referent:	Univ.-Prof. Dr.-Ing. Frank Dehn
Korreferent:	Univ.-Prof. Dr.-Ing. Harald Garrecht

Karlsruhe 2023

Abstract

The worldwide ageing infrastructure is a reason for concern in many countries. Unfortunately, only when a catastrophic failure of some infrastructure occurs, does this topic obtain public awareness. Various failure modes are possible for earthen dams, e.g. slope instability may occur through water seepage below the dam body, in turn reducing internal friction and causing the dam to slip. Therefore, various dam repair and remediation programs have been initiated worldwide to ensure the correct functionality and safety of these critical infrastructures. A standard solution to counter dam seepage is the design and construction of cut-off walls made out of backfill materials such as Plastic Concrete.

Despite its indisputably beneficial material properties, Plastic Concrete has not yet been thoroughly studied. To date, the design of cut-off walls considers Plastic Concrete to be a linear-elastic material. Its undoubtedly existing ductile and plastic behaviour is neglected, not least due to the lack of appropriate constitutive laws and substantiated scientific investigations. Few studies have been large enough to provide reliable estimates of material behaviour under load during a prolonged period of time. Therefore, no constitutive law specifically for Plastic Concrete exists to date. Especially the extent to which the mixture composition influences Plastic Concrete's microstructural and mechanical behaviour remains unclear. Furthermore, no comprehensive research has been conducted to review the existing literature on Plastic Concrete and establish possible similarities with varying mix designs. The present thesis, therefore, aims to close this gap and sets the first steps for a comprehensive understanding of Plastic Concrete material behaviour.

Firstly, an extensive literature study confirmed that the mix design, especially bentonite contents and type, significantly influences Plastic Concrete's microstructural and mechanical properties, which are in turn dependent on sample age, with significant material property changes far beyond the 28-day mark. The literature review further provided first insights into the material properties and highlighted the current research gaps on Plastic Concrete's material behaviour. Most importantly, the literature review proved that Plastic Concrete's material behaviour aligns with concrete technology and can, therefore, be studied using the established concrete investigation procedures.

The microstructural properties investigated through MIP and XRD show a significant pore refinement over an extended study period of 4 years, correlating with increased material strength. In addition, the pore size distribution depends on the mix design and correlates to the source materials used. The mineralogical study using XRD confirms the existence of typical crystalline products from cement hydration.

The mechanical properties investigated also correlate to the selected mix design, especially the water, cement and bentonite contents used. In addition, the compressive and tensile strength significantly increase with sample age. This thesis also develops, for the first time, Plastic Concrete specific mechanical property models. The compressive strength development over time can be estimated for a sample age of up to 4 years as a modification of the *fib* Model Code 2020 time development model. The tensile-to-compressive strength ratio has been established to be best correlated using a linear approximation. Finally, the stabilised elastic modulus $E_{C,S}$ has shown to be closely correlated to the Plastic Concrete mix design and can be estimated from the corresponding compressive strength. This thesis also highlights the major impact that the elastic modulus test set-up, most importantly sample deformation measurement techniques, has on the obtained elastic modulus.

Finally, these findings are of significant value for future Plastic Concrete cut-off wall design since a more realistic and accurate time-dependent design will be possible, addressing the specific material behaviour of Plastic Concrete. With the acquired knowledge, Plastic Concrete cut-off walls can safely guarantee seepage control inside and below dams with a controlled material behaviour.

Zusammenfassung

Das zunehmende Alter baulicher Infrastruktur ist in vielen Ländern ein Grund zur Sorge, welcher häufig erst dann ins öffentliche Bewusstsein rückt, wenn es zu einem katastrophalen Versagen eines Infrastrukturbauwerks kommt. Bei Erddämmen sind verschiedene Versagensarten möglich, z. B. kann ein Böschungsbruch durch das Eindringen von Wasser unterhalb des Dammkörpers auftreten, wodurch die innere Reibung verringert wird und die Böschung ins Gleiten geraten kann. Um dies zu vermeiden, wurden weltweit verschiedene Sanierungs- und Ertüchtigungsprogramme für Dämme eingeleitet, um die ordnungsgemäße Funktion und Sicherheit dieser kritischen Infrastrukturen zu gewährleisten. Eine in der Praxis etablierte Lösung, ist die Planung und der Bau von Dichtwänden aus Dichtwandmassen wie Plastic Concrete.

Trotz seiner unbestreitbar vorteilhaften Materialeigenschaften ist Plastic Concrete noch nicht umfassend erforscht worden. Bislang wird Plastic Concrete bei der Bemessung von Dichtwänden als linear-elastischer Werkstoff betrachtet. Sein zweifellos vorhandenes duktiles und plastisches Verhalten wird vernachlässigt, nicht zuletzt, weil es an geeigneten konstitutiven Gesetzen und fundierten wissenschaftlichen Untersuchungen fehlt. Nur wenige Studien waren umfangreich genug, um das Materialverhalten über einen längeren Zeitraum zuverlässig abzuschätzen. Daher ist es bisher nicht gelungen, systematisch ein Stoffmodell für Plastic Concrete zu entwickeln. Insbesondere das Ausmaß, in dem die Mischungszusammensetzung das mikrostrukturelle und mechanische Verhalten von Plastic Concrete beeinflusst, ist bisher unklar. Darüber hinaus wurden bisher keine umfassenden Untersuchungen durchgeführt, um die vorhandene Literatur über Plastic Concrete zu überprüfen und allgemeingültige Gesetzmäßigkeiten festzustellen . Die vorliegende Arbeit zielt daher darauf ab, diese Lücke zu schließen und die ersten Schritte für ein umfassendes Verständnis des Materialverhaltens von Plastic Concrete zu setzen.

Zunächst bestätigte eine umfangreiche Literaturstudie, dass der Mischungsentwurf, insbesondere der Bentonitgehalt und die Bentonitart, die mikrostrukturellen und mechanischen Eigenschaften von Plastic Concrete erheblich beeinflusst. Diese wiederum sind vom Probenalter abhängig, wobei sich die Materialeigenschaften deutlich über die 28-Tage-Marke hinaus verändern. Die Literaturstudie lieferte zudem erste Einblicke in die Materialeigenschaften und zeigte ebenfalls die aktuellen Forschungslücken zum Materialverhalten von Plastic Concrete auf. Vor allem aber zeigte die Literaturstudie, dass das Materialverhalten von Plastic Concrete mit den Grundzügen der Betontechnologie übereinstimmt und daher mit den etablierten Frisch- und Festbetonuntersuchungen beschrieben werden kann.

Die mikrostrukturellen Eigenschaften wurden mittels Quecksilberdruckporosimetrie und Röntgendiffraktometrie untersucht. Die Ergebnisse zeigen hierbei eine signifikante Po-

renverfeinerung über einen längeren Untersuchungszeitraum von 4 Jahren, die mit einer zunehmenden Festigkeit korrelieren. Darüber hinaus hängt die Porengrößenverteilung vom Mischungsentwurf ab und korreliert mit den verwendeten Ausgangsstoffen. Die mineralogische Untersuchung mittels Röntgendiffraktometrie bestätigt die Existenz typischer kristalliner Produkte aus der Zementhydratation.

Die untersuchten mechanischen Eigenschaften korrelieren ebenfalls mit dem gewählten Mischungsentwurf, insbesondere mit dem verwendeten Wasser-, Zement- und Bentonitgehalt. Darüber hinaus steigt die Druck- und Zugfestigkeit mit dem Alter der Proben deutlich an. In dieser Arbeit werden auch erstmals Plastic Concrete-spezifische Modelle zur Abschätzung der mechanischen Eigenschaften entwickelt. Die Druckfestigkeitsentwicklung über die Zeit kann für ein Probenalter von bis zu 4 Jahren durch eine Anpassung des *fib* Model Code 2020-Zeitentwicklungsmodells angenähert werden. Es wurde festgestellt, dass das Verhältnis von Zug- zu Druckfestigkeit am besten durch eine lineare Annäherung korreliert werden kann. Schließlich hat sich gezeigt, dass der stabilisierte Elastizitätsmodul $E_{C,S}$ mit dem gewählten Mischungsentwurf korreliert und aus der entsprechenden Druckfestigkeit abgeschätzt werden kann. Die E-Moduluntersuchungen verdeutlichen auch den signifikanten Einfluss, den der Prüfaufbau bzw. die Prüfnorm, insbesondere die gewählte Verformungsmessmethode, auf den ermittelten E-Modul hat.

Schließlich sind diese Ergebnisse von großem Wert für die zukünftige Bemessung von Dichtwänden aus Plastic Concrete, da damit eine realitätsnahe und präzisere zeitabhängige Bemessung in Zukunft möglich sein wird, die das spezifische Materialverhalten von Plastic Concrete berücksichtigt. Mit den gewonnenen Erkenntnissen können Dichtwände aus Plastic Concrete eine sichere Sickerwasserkontrolle innerhalb und unterhalb von Dämmen durch ein kontrolliertes Materialverhalten gewährleisten.

Danksagung

Die vorliegende Arbeit entstand berufsbegleitend zu meiner Tätigkeit als wissenschaftlicher Mitarbeiter, Arbeitsgruppenleiter und zuletzt Abteilungsleiter am Institut für Massivbau und Baustofftechnologie, Abt. Baustoffe und Betonbau bzw. der MPA Karlsruhe, des Karlsruher Instituts für Technologie.

Allen voran bedanke ich mich herzlichst bei meinem Doktorvater Herrn Prof. Dr.-Ing. Frank Dehn für die wertvollen Hinweise und kritischen Anmerkungen, die zum Ergebnis dieser Arbeit maßgeblich beigetragen haben. Insbesondere danke ich ihm auch für seine Förderung, Ausbildung und das entgegengebrachte Vertrauen, die ich im Rahmen meiner Tätigkeit an der MPA Karlsruhe erfahren habe.

Herrn Prof. Dr.-Ing. Harald Garrecht danke ich für die Übernahme des Korreferats. Insbesondere für die freundlichen Gespräche und seine konstruktive Hilfestellungen bedanke ich mich sehr.

Mein Dank geht auch an Prof. Frank Schilling, Prof. Hans Stutz und Prof. Katja Emmerich für ihre Mitwirkung in meiner Promotionskommission, sowie die fachlichen Austausche im Zuge meines Promotionsvorhabens.

Ebenfalls bedanke ich mich bei Herrn Prof. em. Harald S. Müller für das entgegengebrachte Vertrauen zu meiner Einstellung am Institut kurz vor seiner Emeritierung.

Auch möchte ich mich bei Herrn Dr.-Ing. Karsten Beckhaus für seine wertvolle fachliche Unterstützung zum Thema „Plastic Concrete“ bedanken, die wesentlichen Einfluss auf die Ausgestaltung und Qualität dieser Arbeit gehabt hat. Auch möchte ich mich für die angenehmen Gespräche bedanken, die wir über die Jahre bei diversen Treffen führen konnten.

Ein besonderes Dankeschön gilt an allen aktuellen und ehemaligen Kolleginnen und Kollegen, einschließlich in Verwaltung und Technik, die mich bei meiner Arbeit im Büro, im Labor oder auf der Baustelle tatkräftig unterstützt haben.

Insbesondere meinen „treuen“ Wegbegleitern Herrn Jan Höffgen und Frau Sarah Lamparter danke ich für die Unterstützung und das offene Ohr, vom Anfang bis zum Ende meiner Promotion.

Mein besonderer Dank gilt auch Herrn Marcel Weinhold und Herrn Patrick Wehres, ohne die die Planung und Durchführung der Versuche im Baustofflabor nicht möglich gewesen wäre.

An dieser Stelle danke ich auch Herrn Sebastian Bruckschlögl, Frau Julia Bruder, Frau Anja Husel, Herrn Stefan Weber, Frau Liv Wittkopf-Bertsch und Herrn Christoph Zacharias, die als Bacheloranden bzw. Masteranden unter meiner Betreuung große Teile der experimentellen Untersuchungen durchgeführt haben.

Mein Dank gilt auch an Frau Johanna Renner, Herrn Stefan Weber und Frau Emily Zeller die mich als Wissenschaftliche Hilfskräfte im Projektalltag am Institut vielseitig unterstützt haben.

Herrn Jack S. Moffatt danke ich sehr für die kritische, fachliche und sprachliche Durchsicht der vorliegenden Arbeit sowie der hier enthaltenen Papers.

Mein besonderer Dank geht auch an meine Eltern, ohne deren Unterstützung ich heute nicht in Deutschland wäre.

Mein unendlicher und liebster Dank gilt meiner Ehefrau und meiner Tochter, die mir tagtäglich und bedingungslos Kraft, Glückseligkeit und Liebe schenken.

Karlsruhe, im Herbst 2023

Contents

List of Publications

Some parts of this dissertation have already been published, as peer-reviewed journal articles:

- Alós Shepherd, D., Kotan, E., Dehn, F.; Plastic concrete for cut-off walls: A review *Construction and Building Materials* **255**, 119248 (2020).
  DOI: 10.1016/j.conbuildmat.2020.119248
- Alós Shepherd, D., Bogner, A., Bruder, J., Dehn, F.; Experimental Study into the Time Development of the Microstructural Properties of Plastic Concrete: Material Insights & Experimental Boundaries. *Case Studies in Construction Materials*
  (Submitted, in Review)
- Alós Shepherd, D., Dehn, F.; Experimental Study into the Mechanical Properties of Plastic Concrete: Compressive Strength Development over Time, Tensile Strength and Elastic Modulus. *Case Studies in Construction Materials* **19**, e02521 (2023).
  DOI: 10.1016/j.cscm.2023.e02521

In addition, other contributions on Plastic Concrete have been made within the framework of this dissertation.

Other journal articles and reports:

- Alós Shepherd, D., Kotan, E., Dehn, F. (2018); State-of-the-Art-Report on Plastic Concrete for Cut-Off Walls. (Hrsg.) Institut für Massivbau und Baustofftechnologie, Abt. Baustoffe und Betonbau. Karlsruher Institut für Technologie. Karlsruhe. DOI: 10.5445/IR/1000085901

- Alós Shepherd, D., Bruckschlögl, S., Kotan, E., Dehn, F. (2020); Untersuchungen zur Anwendbarkeit optischer Verformungsmessverfahren bei Plastic Concrete. In: *Bautechnik*, H.3, S. 171-179. DOI: 10.1002/bate.201900071

Conference papers:

- Alós Shepherd, D., Kotan, E., Dehn, F. (2022); Plastic Concrete for Cut-Off Walls: a review on material behaviour. In: *Proceedings of the DFI-EFFC International Conference on Deep Foundations and Ground Improvement: Smart Construction for the Future*, 18.–20. May 2022 – Berlin, Germany, S. 121-132

- Beckhaus, K., Kayser, J., Kleist, F., Quarg-Vonscheidt, J., Alós Shepherd, D. (2023); Bemessungskonzept für nachhaltige Dichtwände aus hochverformbaren Dichtwandmassen. In: *Beiträge zum 19. Geotechnik-Tag in München: Geotechnik Zusammenwirken von Forschung und Praxis*, 28. March 2023, Technische Universität München, Munich, Germany

- Beckhaus, K., Kayser, J., Kleist, F., Quarg-Vonscheidt, J., Alós Shepherd, D. (2023); Design concept for sustainable cut-off walls made of highly deformable filling materials. In: R. Boes, P. Droz, R. Leroy (Eds.), Role of Dams and Reservoirs in a Successful Energy Transition: Proceedings of the 12th ICOLD European Club Symposium 2023 (ECS 2023, Interlaken, Switzerland, 5-8 September 2023), Taylor & Francis Group, Milton, 2023. ISBN: 978-1-032-57668-8, pp. 641–650. DOI: 10.1201/9781003440420-72

Committee work:

- Member of the CEN/TC 288 TG on “Revision of Annex D of EN 206”.
  Chair of the Sub-Group “Plastic Concrete Requirements”.

- Member of the DWA TG WW-6.6 “Hochverformbare Dichtwandmassen”

Further contributions on other concrete-related research topics can be found on the author’s ORCiD profile at orcid.org/0000-0001-9966-7355.

1 Introduction

1.1 Importance of Dam Safety

The worldwide ageing infrastructure is a reason for concern in many countries. Unfortunately, only when a catastrophic failure of some infrastructure occurs, does this topic obtain public awareness. A key example of the systematic, catastrophic failure of embankment dams and levees occurred in 2005 during the Katrina and Rita Hurricanes in the North American Gulf Shore area [1]. Two independent technical reports into the effects of Hurricane Katrina in New Orleans proved that insufficient design specifications, as well as deficient construction execution, were the main reasons for the catastrophic failure of the critical infrastructure and could have been avoided [2, 3]. Consequently, significant efforts are currently in place by the US Army Corps of Engineers (USACE) to assess and manage risks for dams and levee systems across the United States. Most notably, the National Inventory of Dams (NID) [4] is continuously updated to actively manage life safety risk assessments. In Figure 1.1, an overview of the existing Dams in the US according to the NID is given. It should hereby be highlighted that approximately 18.7 % of all dams are categorised as "High Hazard Potential" where the loss of human life is deemed probable. Therefore, continuous efforts are necessary to ensure the correct functionality and safety of these critical infrastructures.

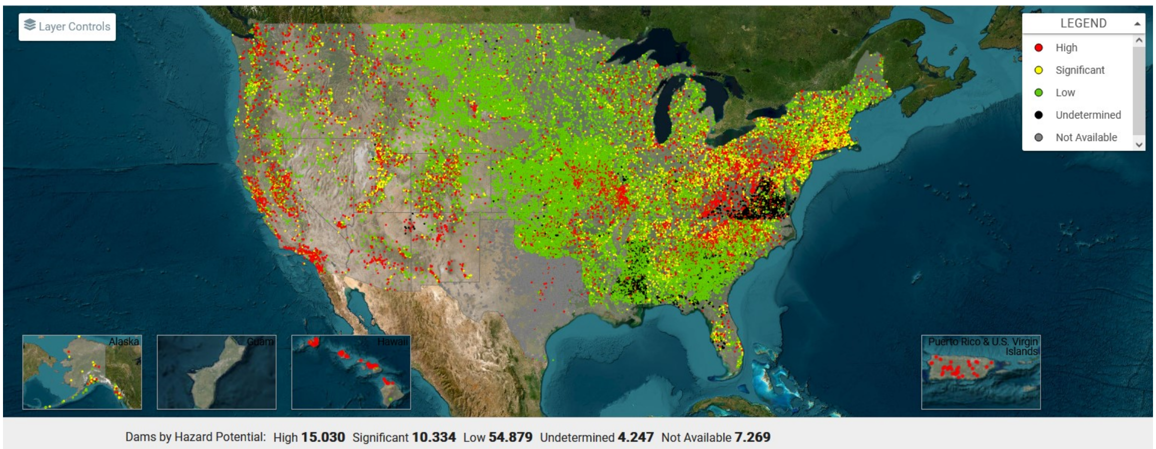

Figure 1.1: Overview of existing Dams in the US according to the National Inventory of Dams (NID) sorted by Dam Hazard Potential [4]

The exceptional flood event of July 2021 in central Europe, causing 188 deaths in Germany alone and with an estimated total damage of EUR 32 billion [5], also caused a mindset shift throughout Europe. The central Europe flooding in 2021 was clearly a cause of ever-increasing climate change [6], as also seen with the 2022-2023 European windstorm season. The confirmed windstorm increase in Europe in the 21st century [7] and the increased risk of hailstorms due to climate change [8], have also increased the likelihood of flash floods, which in turn also affect dam safety. Therefore, dam and levee safety has become of utmost importance for civil protection authorities since these are essential to avoid the loss of human life. In addition, the estimation of inundation areas and the derived damage assessments can only be forecast correctly if critical safety infrastructure such as dams and levees remain in place after catastrophic natural events.

Various failure modes are possible for earthen dams, ranging from dam over-topping and inadequate maintenance to foundation defects and slope instability [9]. The latter generally occurs through water seepage below the dam body, causing a reduction in internal friction and causing the dam to slip. Therefore, significant concern has been raised regarding dam safety and various dam repair and remediation programs have been initiated worldwide.

1.2 Dam Remediation with Cut-Off Walls

A standard solution to counter dam seepage is the design and construction of cut-off walls. The planned cut-off wall is hereby extended into an underlying impervious stratum, e.g. rock [1, 10]. In addition, cut-off walls may not only be placed to remediate but also to upgrade the storage capacity of an existing dam. In Figure 1.2, a schematic overview of the implemented cut-off wall remediation and the corresponding cut-off wall deformation is shown.

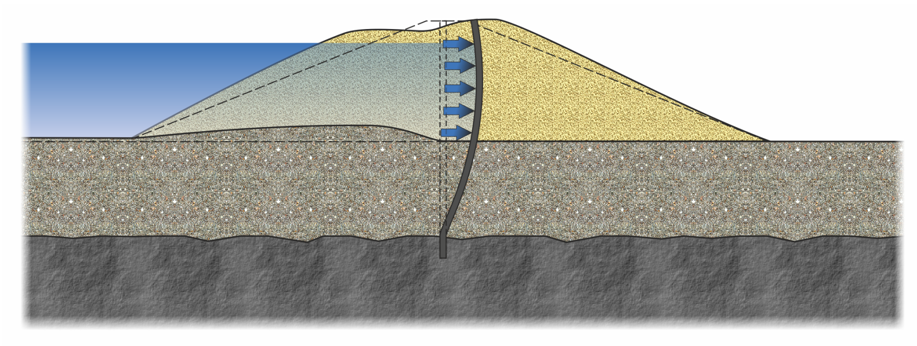

Figure 1.2: Schematic overview of cut-off wall deformation after dam consolidation and reservoir fluctuation, as well as original state (dashed lines) [11]

As can be seen in Figure 1.2, the cut-off wall is subject to large lateral loads through the reservoir water, causing dam settlement and cut-off wall bending strains. In addition, sizeable annual reservoir fluctuations or significant seismic events [1, 10] cause increased bending strains, which must be accounted for in cut-off wall design. The backfill material should, therefore, also be highly deformable to withstand significant bending strains and deformations and primarily ensure cut-off wall water tightness during the planned service life span since the cut-off wall has no further structural load-bearing function.

The most effective cut-off walls for seepage control can be constructed with excavated slurry-trench walls, especially for greater depths [12, 13]. In the first step, a slurry wall trench is excavated using clamshell excavators or hydromill trench cutters [14] (see Figure 1.3, left). The trench is hereby filled with a support fluid to stop the excavated trench from collapsing. Most commonly, bentonite or polymer support fluids are used. Before the backfill material can be placed, the support fluid used during excavation has to be replaced by a clean support fluid with defined material properties [15] (see Figure 1.3, centre). The backfill material is thereafter placed using the tremie method [16]. The backfill material is hereby placed through the so-called tremie pipe, whereby the lower end of the tremie pipe always remains below the concrete surface (see Figure 1.3, right).

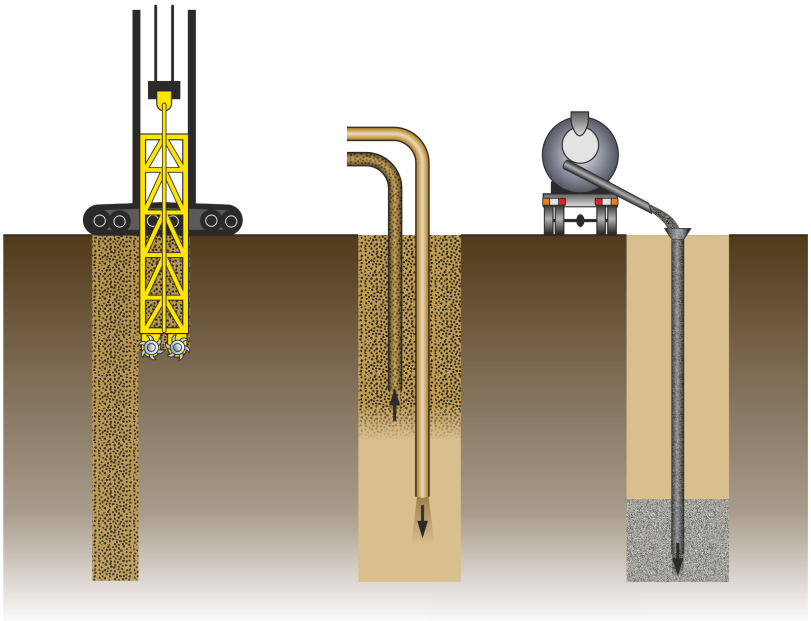

Figure 1.3: Overview of the construction of a slurry trench wall using a hydromill trench cutter (left) support fluid replacement (centre) and concrete placement using the tremie method (right) [11]

1.3 Cut-Off Wall Backfill Materials

As backfill materials, a wide range of possibilities exist. Firstly, self-hardening suspensions serve as a supporting liquid during excavation and, together with fine particles from the adjacent soil, form the final hardened filling material [17]. Since the placement occurs in a single phase, and thus tremie placement is not necessary, these materials are also commonly referred to as single-phase diaphragm wall materials [14]. However, due to the self-hardening properties, the processing window, as well as the depth of the cut-off wall, is limited. Self-hardening suspensions consist of cement, water and additions, without aggregate use, and can often be purchased as ready-mixed dry powders from material suppliers.

Secondly, a further possibility exists with deep soil grouting where the filling material is produced by mechanical disintegration of the soil by rotating mixing tools and subsequent mixing with cement suspension or cement without removing the support of the adjacent soil [17]. Due to its composition, this filling material can also be referred to in simplified terms as soilmix material. The properties of the adjacent soil hereby have a significant impact on the mechanical properties of the hardened filling material.

Finally, a growing interest has arisen in Plastic Concrete as a backfill material due to the materials' suitable characteristics. Plastic Concrete is hereby characterised by a high deformation capacity under load, which is of great advantage when ductile walls are needed to account for the aforementioned significant bending strains. Plastic Concrete has also been shown to be especially suited to withstand significant seismic events, unlike other backfill materials [18, 19]. The high deformation capacity of Plastic Concrete, in turn, decreases both rupture probability and crack opening width, which would incur material permeability increase [1, 19]. Plastic Concrete has therefore been widely used worldwide in dam construction and remediation for many years, with projects like the Sylvenstein Dam (Germany) [20], Hinze Dam (Australia) [21], Bagatalle Dam (Mauritius) [22, 23] or Karkheh Dam (Iran) [24].

1.4 Plastic Concrete in Standards and Guidelines

Plastic Concrete can be considered to be a low-strength, impervious concrete with a low elastic modulus capable of sustaining larger strains than standard concrete. These properties can be achieved through the targeted selection of raw materials and mix design. The key component differentiating Plastic Concrete from standard concrete is the far higher w/c-ratio, for which the fresh concrete stability has to be controlled by low amounts of physically water-binding additions (e.g. bentonite). However, to date, Plastic Concrete is not fully covered by existing standards.

Within EN 206:2017-01 [25], Annex D describes the "additional requirements for specification and conformity of concrete for special geotechnical works". However, within this Annex D, no specific requirements are set for Plastic Concrete. The current execution standard for diaphragm walls EN 1538:2015-10 [26] establishes that Plastic Concrete is considered a concrete with lower strength and lower elastic modulus capable of sustaining higher deformations than standard concrete. In addition, Plastic Concrete should have the required deformability and permeability combined with sufficient workability and strength [26]. EN1538:2015-10 [26], however, does not provide any specific mix design requirements and cross-references EN 206:2017-01 [25] for mix design. The German translation uses the term "clay concrete" (in German: Tonbeton); however, no requirements for the use of clay are given. Therefore, the current European standards do not provide sufficient regulations for Plastic Concrete.

The German Association for Water, Wastewater and Waste (in German: Deutsche Vereinigung für Wasserwirtschaft, Abwasser und Abfall e. V., hereinafter "DWA") uses within their guideline DWA-M 512-1 [27] the term "plastic earth concrete" to describe a cut-off wall material which can be used in particular when a low permeability coefficient is required in addition to high deformability. Whilst this accurately describes material properties, the term “earth concrete” may be confusing since Plastic Concrete does not use excavated soil as part of the mix design but instead uses concrete aggregates in the mix design.

The International Commission on Large Dams (ICOLD) gives within Bulletin 51 [28] some guideline values regarding Plastic Concrete mix design and corresponding reference values for material performance. However, since this bulletin is somewhat outdated, it can be safely assumed that reference values are no longer accurate due to the evolution of source materials and Plastic Concrete mix design over the past decades.

Finally, the United States Bureau of Reclamation defines within the design standard DS-13-(16):2014-07 [10] that Plastic Concrete can be used when a less stiff cutoff wall is constructed using concrete that uses the addition of bentonite, especially where strength may not be the primary design characteristic. Plastic Concrete cut-off walls can also undergo greater strains before cracking compared to traditional concrete walls [10]. Whilst the cited standard quotes the use of bentonite, Plastic Concrete mix design can also be achieved with other water-binding additions.

Overall, the term Plastic Concrete is not defined consistently within the civil engineering community and should, therefore, be clarified within the present thesis.

2 Research Scope and Objectives

Despite its indisputably beneficial material properties, Plastic Concrete has not yet been thoroughly studied. To date, the design of cut-off walls considers Plastic Concrete to be a linear-elastic material. Its undoubtedly existing ductile and plastic behaviour in the ultimate limit state and its clearly viscous behaviour during serviceability are neglected, not least due to the lack of appropriate constitutive laws and substantiated scientific investigations. Few studies have been large enough to provide reliable estimates of material behaviour under load during a prolonged period of time and, therefore, have failed to systematically develop a constitutive law specifically for Plastic Concrete. Especially the extent to which the mixture composition influences Plastic Concrete's microstructural and mechanical behaviour remains unclear. Furthermore, no comprehensive research has been conducted to review the existing literature on Plastic Concrete and establish possible similarities with varying mix designs.

Therefore, the present thesis aims to critically review the existing literature regarding Plastic Concrete and establish the state-of-the-art on Plastic Concrete material behaviour as well as Plastic Concrete cut-off wall design. Qualitative content analysis was used for this purpose. In addition, key knowledge gaps were identified from the literature review results.

To address these knowledge gaps, necessary experimental programmes were developed, coordinated and executed to obtain further insights into Plastic Concrete's microstructural and mechanical properties for varying mix designs. Due to Plastic Concrete's established long-term strength development, the corresponding tests were performed at varying ages, with this thesis providing data for a sample age of up to 4 years. The microstructural investigation primarily used mercury intrusion porosimetry (MIP) and X-ray diffractometry (XRD). The mechanical behaviour was studied in the fresh and hardened concrete state. Most notably, compressive strength, tensile strength and elastic modulus tests were performed for varying mix designs.

The mix designs were selected based on the aforementioned literature review. A total of three European sodium-activated bentonites were used in varying proportions within Plastic Concrete mix design to establish the influence of mix design on the corresponding material properties.

Finally, Plastic Concrete specific engineering models were developed to ensure a more accurate and realistic Plastic Concrete cut-off wall design in future and also account for the deviating material behaviour in comparison to standard concrete.

All in all, this dissertation aims to provide new insights into Plastic Concrete material behaviour and address the missing engineering models for Plastic Concrete cut-off wall design.

3 Main Findings

In this chapter, the scientific outputs of this thesis are presented. Since the present thesis is a cumulative dissertation, the main findings can also be found within the published scientific, peer-reviewed papers. The structure followed in the present thesis and the key findings are schematically shown in Figure 3.1.

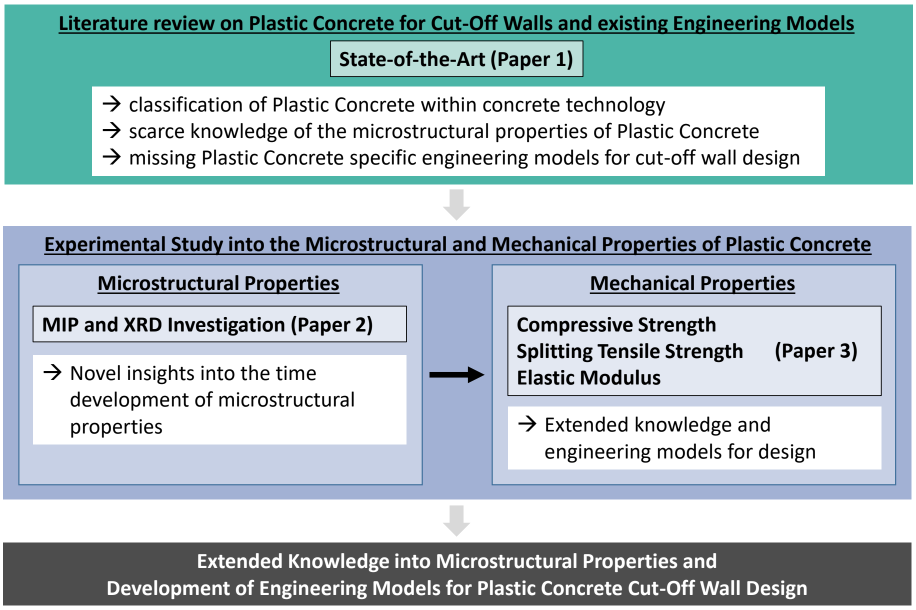

Figure 3.1: Approach and key findings of the present thesis

Firstly, the state-of-the-art on Plastic Concrete for Cut-Off Walls has been extensively reviewed and is summarised in **Paper 1**. Since the existing data provides little insight into the microstructure of Plastic Concrete mixes, an experimental study into the microstructural properties of Plastic Concrete was performed, with the results being reported in **Paper 2**. Finally, the research focus shifted to the mechanical properties of Plastic Concrete with an experimental study providing insights into the compressive strength development over time, the tensile strength and the elastic modulus. Furthermore, corresponding engineering models were developed as shown in **Paper 3**.

In the following sections, the main findings from the corresponding papers are given. The full details can be found within the attached **Paper 1**, **Paper 2** and **Paper 3**.

3.1 State-of-the-art on Plastic Concrete for Cut-Off Walls

The present section is a partial and summarised reprint of **Paper 1**:

Alós Shepherd, D., Kotan, E., Dehn, F.;
Plastic concrete for cut-off walls: A review
Construction and Building Materials **255**, 119248 (2020).
DOI: 10.1016/j.conbuildmat.2020.119248

In **Paper 1**, the first steps are set out for a comprehensive understanding of Plastic Concrete material behaviour. With the acquired knowledge, Plastic Concrete can be used to safely guarantee seepage control inside and below dams with a controlled material behaviour. Furthermore, the existing knowledge gaps are highlighted. All in all, the following considerations may be taken into account for Plastic Concrete cut-off wall design.

3.1.1 Mix Design

Plastic Concrete can be considered to be a low-strength concrete with a low elastic modulus capable of sustaining larger strains than standard concrete. These properties can be achieved through the targeted selection of raw materials and mix design. The key component differentiating Plastic Concrete from ordinary concrete is the far higher w/c-ratio, for which the fresh concrete stability has to be controlled by low amounts of physically water-binding additions. Most commonly, bentonite, a clay rock composed of montmorillonite minerals, is added; however, other additions may also be used. Finally, Plastic Concrete uses regular aggregates with a maximum grain size of 12 mm (due to the segregation risk) as well as including retarding admixtures to delay concrete setting in tremie placement.

Plastic Concrete mix design is similar to that of standard concrete with aggregate contents ranging between 1300 and 1900 kg/m^3 and cement contents lying in the range of 80 to 200 kg/m^3. The w/c-ratios generally range between 2.0 and 5.0, depending on target strength and source materials used. The mixing sequence has also been shown to influence material properties, whereby no standardised mixing sequence currently exists. In Figure 3.2, an overview of representative examples of Plastic Concrete mix designs in comparison to standard concrete and single-phase diaphragm wall materials is given [14, 29, 30, 31].

3.1.2 Mechanical Behaviour

The mechanical behaviour of Plastic Concrete is in line with that which can be expected from concrete technology. It should, however, be noted that much testing is conducted using geotechnical testing standards and not concrete testing standards, which is especially important when testing Plastic Concrete deformability, i.e. elastic modulus.

Generally speaking, it can be ascertained that the compressive strength of Plastic Concrete increases with decreasing w/c-ratio. However, the w/c-ratio does not account for the addition of bentonite and, therefore, does not consider the reduction in free water

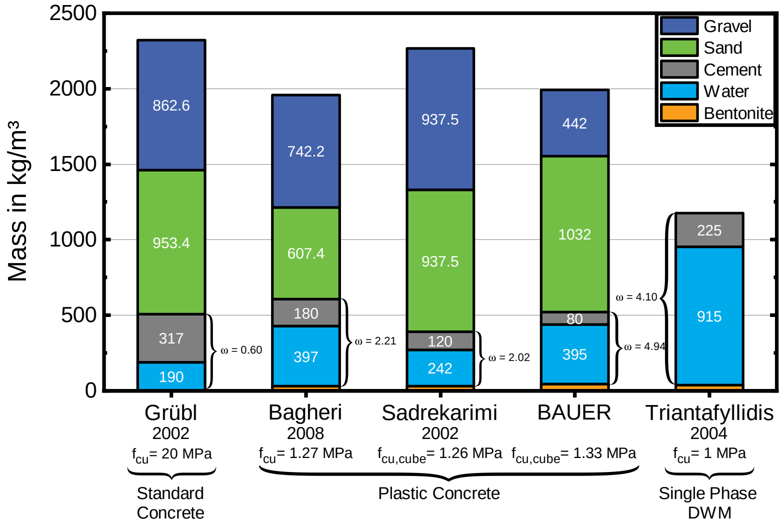

Figure 3.2: Representative examples of Plastic Concrete mix designs [14, 29, 30, 31] and their corresponding compressive strength [**Paper 1**]

available for cement hydration. Plastic Concrete compressive strength normally lies between 0.5 to 2.5 MPa at 28 days, with compressive strength development being very pronounced, far beyond the 28 day mark. It may, therefore, also be expedient to test Plastic Concrete compressive strength at higher ages, e.g. 90 days. Furthermore, the loading rate should be adjusted to account for the low strength of the material and should be tested with a loading speed between 0.02 MPa/s and 0.03 MPa/s. In Figure 3.3, an overview of the unconfined compressive strength development over time [30, 32, 33, 34] in comparison to the *fib* MC 2010 [35] time development model (and similarly applicable for *fib* MC 2020 [36]) is given.

The strain at failure of Plastic Concrete is also far greater than that of standard concrete, where a maximum strain of 1% can be achieved under compression. The tensile-to-compressive strength ratio of Plastic Concrete is also expected to be greater than that of standard concrete, lying in the range of 10% to 20%. Under multi-axial load, the load-bearing capacity clearly increases with axial strains as high as 10%.

The magnitude of the elastic modulus of Plastic Concrete clearly depends on the testing standard used due to differing definitions of elastic modulus and diverging specimen deformation measurement set-ups. The deformation modulus (geotechnical standard) of Plastic Concrete can therefore be estimated to be 100–600 MPa, whilst Young's modulus (concrete standard) should be estimated in the range of 300–1800 MPa. In Figure 3.4, an overview of the elastic modulus as a function of the compressive strength at 28 days is given [31, 32, 33, 37, 38, 39, 40].

Due to the high w/c-ratio of Plastic Concrete, the creep and relaxation properties are more pronounced than those of standard concrete. With this, the final creep coefficient can be expected to be $\varphi_\infty \geq 3.0$. Therefore, the relaxation potential of Plastic Concrete is also notably higher than that of standard concrete. The higher relaxation potential of

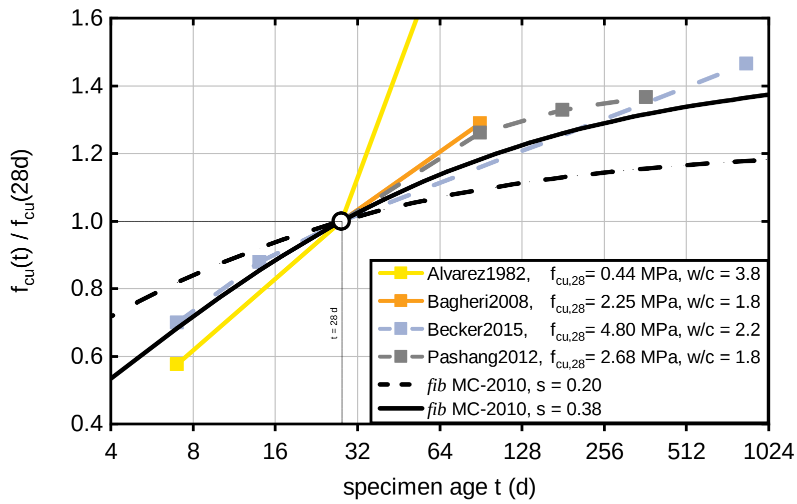

Figure 3.3: Overview of the unconfined compressive strength development as a function of time [30, 32, 33, 34] in comparison to the *fib* MC 2010 [35] [**Paper 1**]

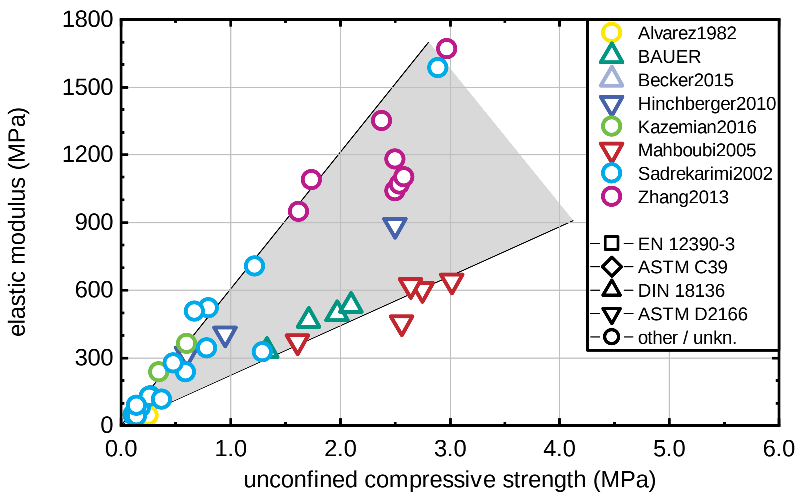

Figure 3.4: Elastic modulus as a function of the compressive strength at 28 days [31, 32, 33, 37, 38, 39, 40] [**Paper 1**]

Plastic Concrete is, in turn, beneficial to prevent material stress peaks during loading and avoid the formation of cracks, which would incur an increase in permeability.

3.1.3 Hydraulic Behaviour

The hydraulic behaviour of Plastic Concrete, and concrete in general, remains a relatively unstudied field, especially for testing under realistic stress conditions. For Plastic Concrete it has been shown that permeability decreases with decreasing w/c-ratio, which is linked to a less porous material structure [30, 33, 41, 42]. The change in Plastic Concrete permeability over time is scarcely reported in the literature; however, a decrease in permeability over time has been shown to exist. It is, therefore, expedient that Plastic Concrete permeability testing is conducted at ages greater than 28 days (e.g. 90 days) to account for the permeability increase with time. Plastic Concrete permeability can therefore be estimated in the range of 10^{-8} m/s to 10^{-9} m/s depending on testing age.

3.2 Key Results on the Microstructural Properties of Plastic Concrete

The present section is a partial and summarised reprint of **Paper 2**:

Alós Shepherd, D., Bogner, A., Bruder, J., Dehn, F.;
Experimental Study into the Time Development of the Microstructural Properties of Plastic Concrete: Material Insights & Experimental Boundaries.
Case Studies in Construction Materials.
Submitted, in Review

Paper 2 aimed to determine the effect of Plastic Concrete mix design, especially bentonite contents and type, on the long-term development of Plastic Concrete's microstructural properties and corresponding compressive strength. In addition, **Paper 2** was designed to systemically use mercury intrusion porosimetry (MIP) and X-ray diffractometry (XRD) for the first time on Plastic Concrete samples, hereby setting out the experimental boundaries of these measurement techniques for Plastic Concrete. Detailed information on the Plastic Concrete mixes tested and the experimental test procedures used can be found in **Paper 2**.

3.2.1 Mercury Intrusion Porosimetry (MIP)

The results of this study show that MIP, despite the technique's inherent limitations, could successfully be applied for the first time to systematically study the pore-structure changes of Plastic Concrete with varying mix designs and sample ages of 7 d, 28 d, 56 d, 91 d and four years. The porosimetry results of Plastic Concrete samples show a bi-modal pore size distribution, with two age-dependent peaks at approximately 10,000–20,000 nm and 100–700 nm, which have not been reported in the literature to date. An overview of the differential mercury intrusion porosimetry results in dependence of mix design and sample age can be found in Figure 3.5. In addition, the experimental boundaries of MIP testing, specifically for Plastic Concrete samples, are set out for the first time, with this study highlighting the key aspects to be considered regarding sample preparation, porosimeter setup and data analysis. Most notably the effect of varying drying temperatures, the porosimeter calibration set-up as well as test result standard deviation were studied (see **Paper 2**).

Furthermore, the obtained data shows a clear pore refinement over time, with the coarse porosity share dropping significantly over four years, with coarse porosity dropping from 26% to 15% over four years, as can be seen in Figure 3.6.

Moreover, the fine porosity is refined substantially over time and positively correlates with a significant increase in compressive strength. In addition, the fine porosity peak clearly relates to the bentonite type and b:c-ratio used, with higher bentonite contents incurring an overall finer porosity. In Figure 3.7, the compressive strength of Plastic Concrete samples is shown over the corresponding pore entry radius of the fine porosity peak.

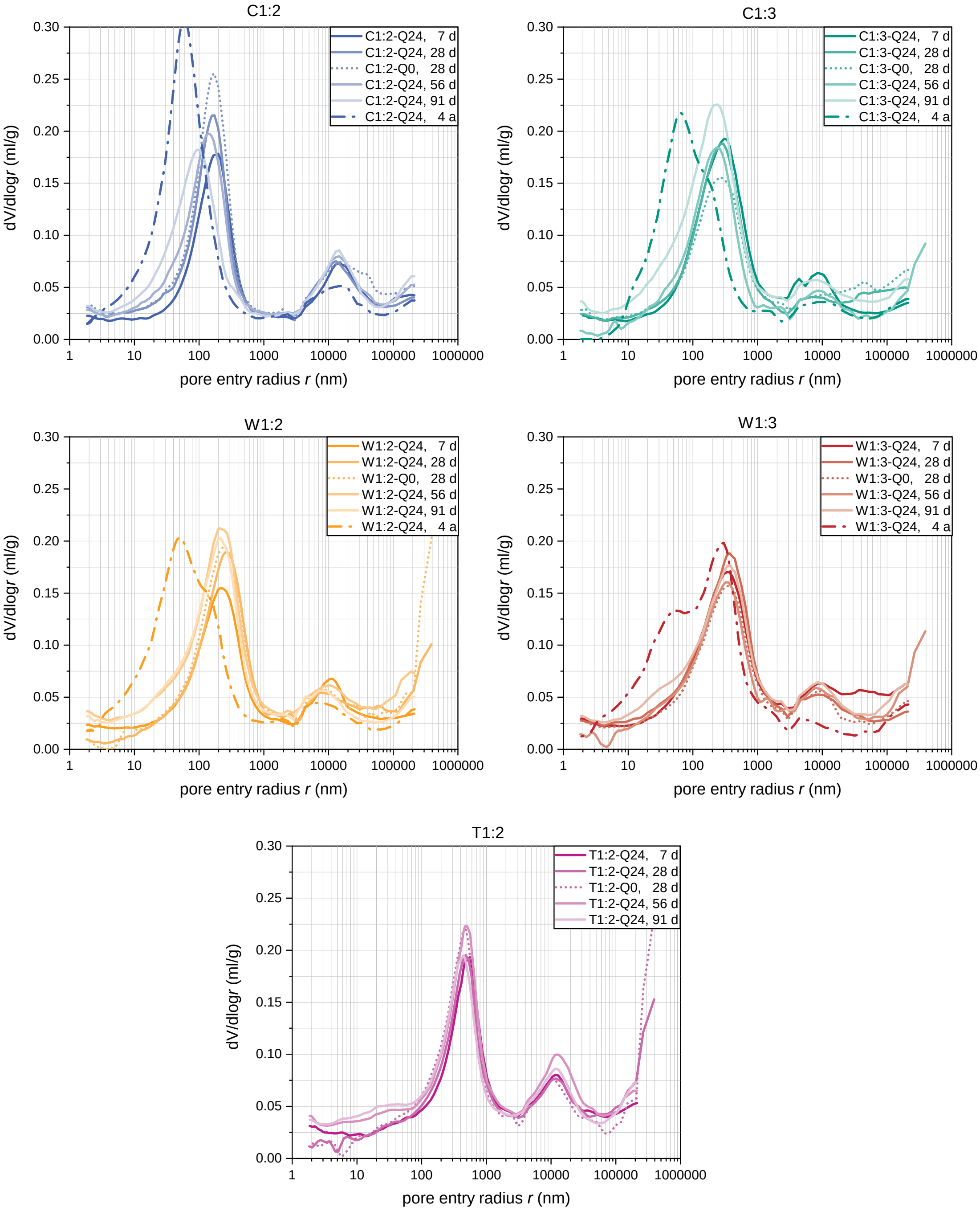

Figure 3.5: Differential mercury intrusion porosimetry results in dependence of mix design and sample age [**Paper 2**]

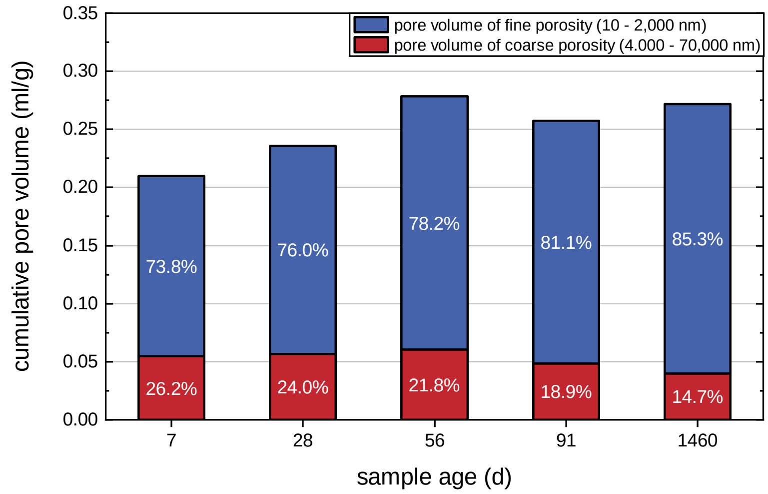

Figure 3.6: Cumulative porosity and percentage share of porosity of the W1:2-Q24 mix over time [**Paper 2**]

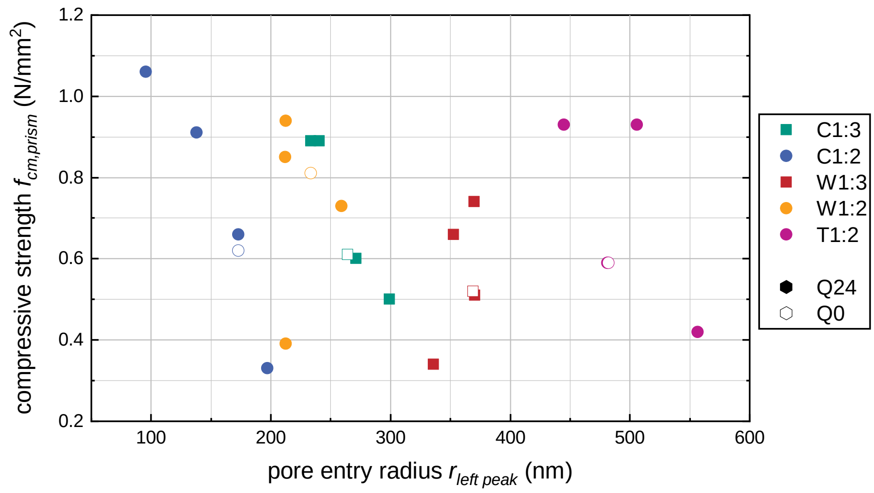

Figure 3.7: Compressive strength of Plastic Concrete samples over corresponding pore entry radius of the left peak, sample age up to 91 days [**Paper 2**]

3.2.2 X-Ray Diffractometry (XRD)

Finally, XRD measurements were also successfully performed on Plastic Concrete samples. In Figure 3.8, the X-ray diffractograms of an illustrative Plastic Concrete mix (C1:3) at different test ages and swelling times are compared. In addition, the diffractograms of the source materials are also shown.

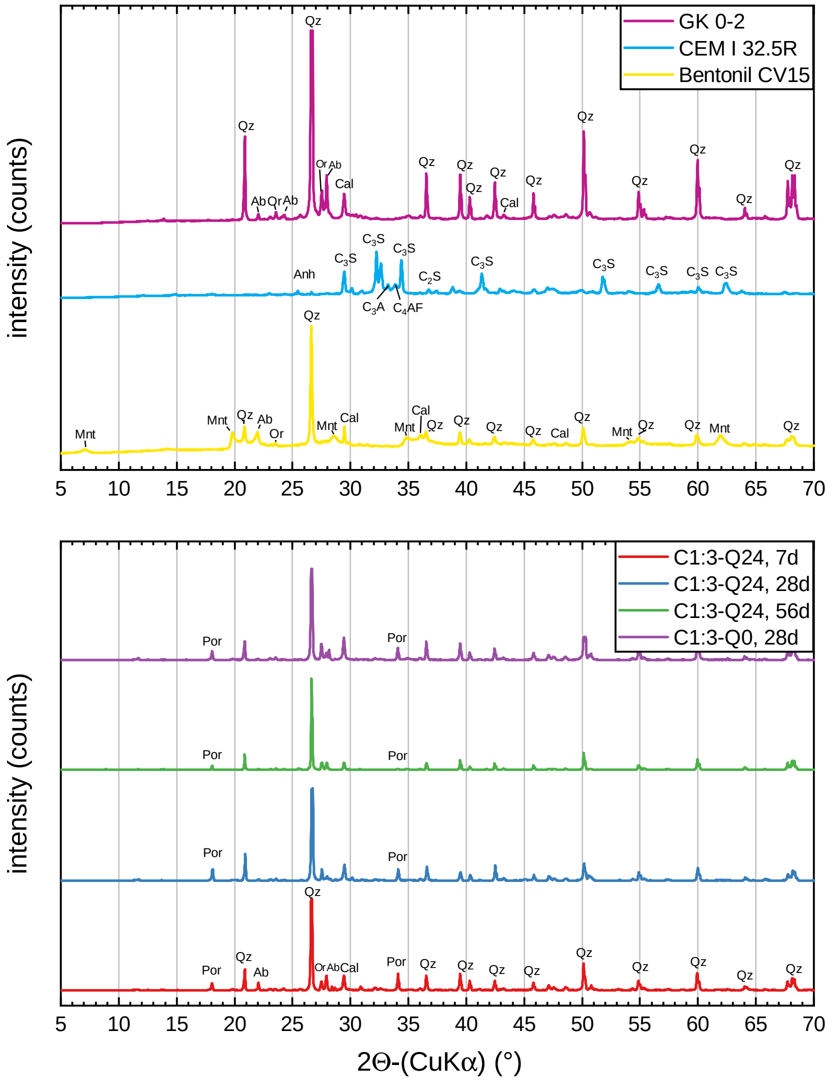

Figure 3.8: XRD diffractograms of an illustrative Plastic Concrete mix (CV15 1:3) over time and corresponding source materials, vertically shifted [**Paper 2**]

It becomes apparent that the results of the Plastic Concrete mixes are almost identical, independent of test age or swelling time. The minimal differences in signal intensity are likely due to sample preparation inhomogeneities. Compared to the source materials, it also becomes clear that the more prominent peaks can be attributed to the aggregates used, especially quartz phases. Bentonite (e.g. montmorillonite) peaks are barely visible in the overall peak intensity of Plastic Concrete samples. Moreover, some bentonite peaks overlap with those of the aggregates. Some minor changes in peak intensity of portlandite ($Ca(OH)_2$) can be seen, which correspond to the typical depletion of portlandite during cement hydration [43].

Despite the possibility of the formation of non-crystalline products, this is rather unlikely. In addition, the results shown here display no evidence to support the theory of any pozzolanic reaction within the tested time frame (91 days). Whether bentonite acts as a nucleation site for calcium silicate hydrates (C-S-H), calcium aluminate hydrates (C-A-H), or calcium aluminate silicate hydrates (C-A-S-H) remains unclear.

3.3 Key Results on the Mechanical Properties of Plastic Concrete

The present section is a partial and summarised reprint of **Paper 3**:

Alós Shepherd, D., Dehn, F.;
Experimental Study into the Mechanical Properties of Plastic Concrete: Compressive Strength Development over Time, Tensile Strength and Elastic Modulus.
Case Studies in Construction Materials **19**, e02521 (2023).
DOI: 10.1016/j.cscm.2023.e02521

Paper 3 aimed to determine the effect of Plastic Concrete mix design on its mechanical properties over time and to develop appropriate models. In addition, **Paper 3** also aimed to model the tensile-to-compressive strength ratio specifically for Plastic Concrete. Finally, the elastic modulus of Plastic Concrete was to be tested for the first time following EN 12390-13 and related to the corresponding compressive strength. Detailed information on the Plastic Concrete mixes tested and the experimental test procedures used can be found in **Paper 3**.

3.3.1 Fresh Concrete Test Correlation

The fresh concrete results show a good correlation between slump and flow table test results. Despite concrete being measured under different conditions (self-weight vs. compaction), both test methods are suitable for testing high workability mixes [44, 16]. In Figure 3.9, the correlation between the flow table and slump tests results for all mixes from **Paper 2** and **Paper 3** is plotted.

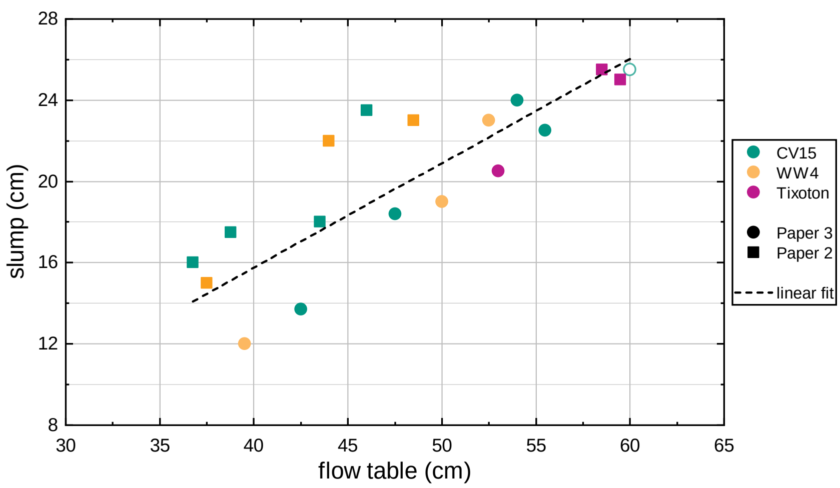

Figure 3.9: Correlation between flow table and slump tests results for all mixes from **Paper 2** and **Paper 3** [**Paper 3**]

It can be seen that, as expected, slump increases with increasing flow table spread, similar to results in standard concrete [45]. In addition, this trend occurs independently of the type of bentonite used. The linear trend of these results can be fitted, and an approximate inclination of 0.52 is obtained, i.e. that an increase in flow table spread of 10 cm incurs a 5.2 cm larger slump, inline with results presented in [16]. The coefficient of determination R^2 is only 0.646 due to the high, expected deviation of the fresh concrete test results. This high deviation is inherent to the applied fresh concrete test, reported to be ± 4 cm for flow table test results [16]. However, the overall trend can be accurately described with the displayed curve. Therefore, an approximation for the calculation of slump s as a function of the flow table results ft can be established within the tested data range displayed in Figure 3.9, as shown in Equation 3.1.

$$s = 0.52 \cdot (ft - 40\ \text{cm}) + 16\ \text{cm} \tag{3.1}$$

3.3.2 Influence of Sample Size on Compressive Strength

Within **Paper 2** and **Paper 3**, compressive strength tests were conducted on cube samples with an edge length of 200 mm due to the low strength properties of Plastic Concrete. In **Paper 2** additionally, $40 \times 40 \times 160\ \text{mm}^3$ prism samples were cast, and the prism halves were also tested in compression. In addition, all samples from both papers were produced using the same batch of cement and bentonite, as well as aggregates from the same deposit, thus reducing the possible material scattering to a minimum. In Figure 3.10, the sample compressive strength is displayed over the corresponding mix design.

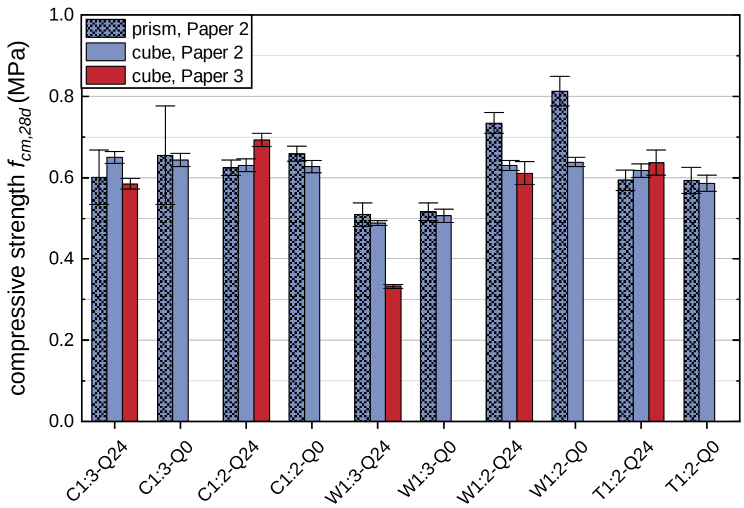

Figure 3.10: Comparison of compressive strength of prism (testing area = $40 \times 40\ \text{mm}^2$) and cube samples (testing area = $200 \times 200\ \text{mm}^2$) from **Paper 2**, with cube samples (testing area = $200 \times 200\ \text{mm}^2$) from **Paper 3**, at 28 days [**Paper 3**]

From this data it becomes apparent that cube samples have an overall repeatability since both studies provide similar compressive strength results for cube samples. In addition, for most mix designs, the compressive strength of prism halve samples is close to that of cube samples, with both results lying within the standard deviation of one another. The data also shows that the standard deviation is approximately three times higher for the prism than cube samples, as would be expected due to the size and failure concentration effect based on the WEIBULL theory [44]. From the results shown in Figure 3.10, an average coefficient of the mean cube strength and prism strength can be calculated ($f_{cm,cube}/f_{cm,prism}$), with cubes strength being on average 0.963× prism strength, in line with the expected theoretical correlation in literature [44].

3.3.3 Compressive Strength Development over Time

As reported in **Paper 1** the compressive strength development of Plastic Concrete has shown to be very pronounced far beyond the 28-day mark. Therefore, in the present study, compressive strength tests with varying mix designs were performed at higher ages up to 4 years. The results from this study show that the strength development over time is far more significant for Plastic Concrete samples than the *fib* MC 2010 [35] predicts. Therefore, in Figure 3.11 the extended time development model according to *fib* MC 2020 [36] at a reference age t_{ref} of 91 days with s_C = 0.50 coefficient is plotted over time against the results from the present thesis.

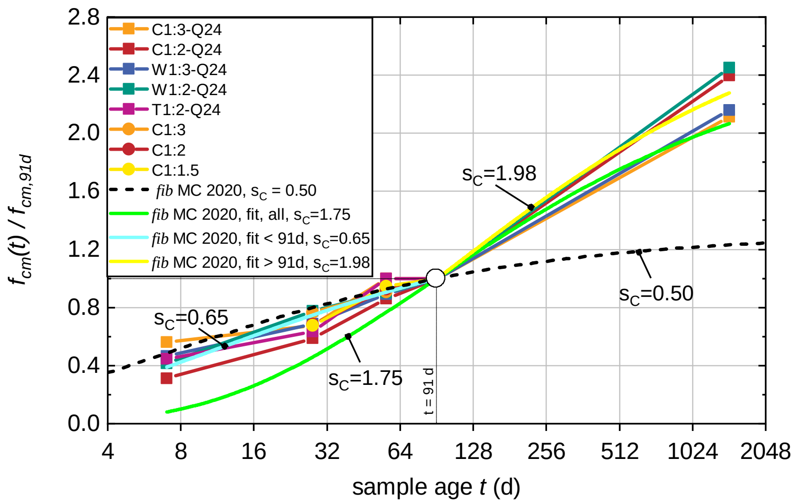

Figure 3.11: Compressive strength of Plastic Concrete samples over time from **Paper 2** and **Paper 3**, as well as *fib* MC 2020 [36] function, with t_{ref} = 91 d [**Paper 3**]

The results show that due to the high w/c-ratio used, the strength development of Plastic Concrete is still significantly slower than the *fib* Model Code 2020 [36] estimates. Therefore, a Plastic Concrete specific best-fit approximation of the s_C coefficient for the data available can be performed. The results show that a best-fit approximation with the *fib* MC 2020 curve for s_C = 1.75 (R^2 = 0.82) incurs in an underestimation of the strength development, most significantly for early age. Therefore, subdividing the approximation into two data sets, before and after 91 days, may be more expedient.

It can be seen that through the split, best-fit approximation, a better correlation with the data can be achieved, with the early age strength development approximated with $s_C = 0.65$ ($R^2 = 0.90$) and the later age strength development approximated with $s_C = 1.98$ ($R^2 = 0.97$) providing a far better correlation to the presented data. With this, the best-fit approximation for the s_C coefficient at $t_{ref} = 91$ days can be achieved as shown in Equation 3.2.

$$s_C = \begin{cases} 0.65 & t < 91 \text{ d} \\ 1.98 & t > 91 \text{ d} \end{cases} \tag{3.2}$$

Although unexpected, such a differentiated compressive strength development can make sense for Plastic Concrete. The initial, somewhat faster, strength development coincides with the initial cement hydration. The long-term, slower compressive strength development is likely caused by another strength development mechanism, possibly through a cement-bentonite interaction. **Paper 2** confirmed that a significant pore refinement and compressive strength increase occurs between 91 days and 4 years; however, no evidence of a further interaction mechanism could be obtained.

Overall, with the results presented here, a better approximation of the long-term strength development can be achieved, ensuring a better and more realistic design of Plastic Concrete cut-off walls.

3.3.4 Tensile to Compressive Strength Ratio

The splitting tensile strength results show that Plastic Concrete has a slightly higher tensile-to-compressive strength ratio than standard concrete despite the overall higher standard deviation of splitting tensile test results [29]. In Figure 3.12, the splitting tensile strength is drawn over the corresponding compressive strength for the literature data [46, 47, 48] as well as the data from this thesis. In addition, best-fit modelling approaches following *fib* MC 2020 [36] / Heilmann [49] are shown, with the corresponding best-fit equation.

The results show a good correlation between splitting tensile strength and compressive strength results for Plastic Concrete samples over a broader range of compressive strength. The data furthermore lies above the expected ratio of 1/10. If a linear fit is applied, the splitting tensile strength ratio can be approximated to Equation 3.3, with a ratio of 0.135. The coefficient of determination R^2 is 0.983, providing an overall excellent accordance for this data.

$$f_{ctm,sp} = 0.135 \cdot f_{cm} \tag{3.3}$$

Alternatively an approximation in line with *fib* MC 2020 [36] / Heilmann [49] can be calculated. The resulting approximation is shown in Equation 3.4. The coefficient of determination R^2 is 0.895, providing an overall good accordance for this data. However, as can be seen in Figure 3.12, the tensile strength would be overestimated for low compressive strengths (0 - 1.5 MPa) and underestimated for higher compressive strengths (4 - 10 MPa) with this model. In addition, the formula would incur a non-steady transition to the *fib* MC

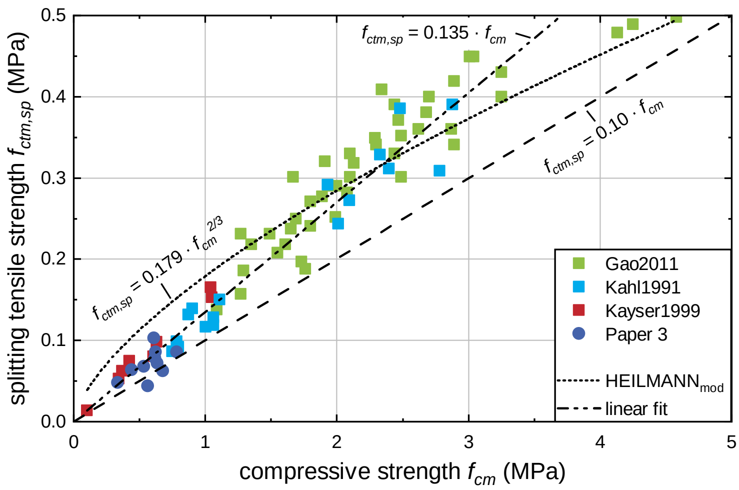

Figure 3.12: Splitting tensile strength over compressive strength from this study and [46, 47, 48] as wells as modelling approximations in accordance with [36, 49]; [**Paper 3**]

2020 [36] estimations for compressive strength classes from C12/15 onwards. However, this is non-crucial for Plastic Concrete since such strengths are not achieved.

$$f_{ctm,sp} = 0.179 \cdot f_{cm}^{2/3} \tag{3.4}$$

In this sense, the linear prediction model (Equation 3.3) currently provides the more accurate results, especially at very low compressive strengths, and should therefore be preferred and used for future Plastic Concrete cut-off wall design within the defined compressive strength range.

3.3.5 Elastic Modulus Test Results

The elastic modulus testing procedure clearly influences the obtained test results, in line with varying definitions of elastic modulus as well as varying deformation measurement techniques underlying the individual testing procedures (see also **Paper 1**). Therefore, in the present study, the stabilised elastic modulus $E_{C,S}$ (hereinafter "stabilised modulus") was tested according to EN 12390-13, procedure B [50]. In addition, during subsequent compressive strength testing, the load-displacement curve was measured using the testing machines' crosshead displacement and further used to analyse sample deformation. Based on the *fib* MC 2020 [36], the initial elastic modulus E_{ci} can be obtained as the maximum tangent slope of the load-displacement-curve (hereinafter "tangent modulus"). In addition, the secant elastic modulus E_{c1} can also be obtained as the secant modulus from the origin to the peak compressive stress (hereinafter "secant modulus"). In Figure 3.13, the results of the present study with the stabilised elastic modulus $E_{C,S}$, the tangent elastic modulus E_{ci} and the secant elastic modulus E_{c1} are shown against the corresponding compressive strength. In addition the available literature data reported in **Paper 1** and based on [31, 33, 37, 39, 38, 32, 40] is shown in grey.

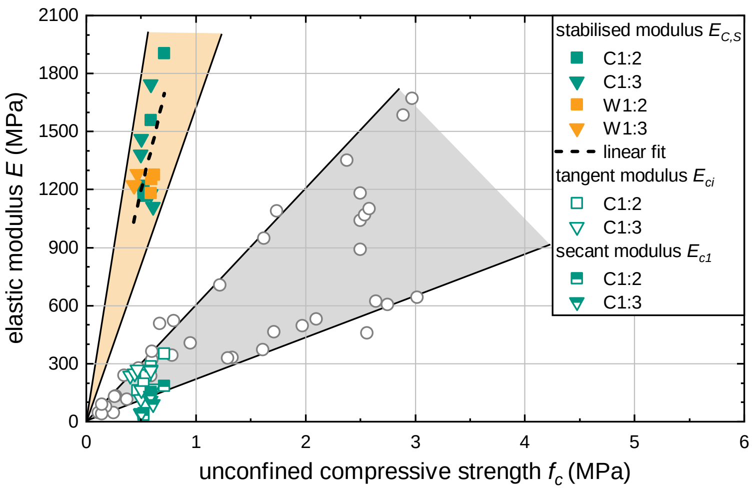

Figure 3.13: Elastic modulus testing results ($E_{C,S}$, E_{ci}, E_{c1}) over corresponding unconfined compressive strength in comparison to literature results (**Paper 1**, in grey) with varying mix design [**Paper 3**]

From the results in Figure 3.13, it becomes clear that the stabilised elastic modulus $E_{C,S}$ lies far above the other elastic moduli due to the direct deformation measurement of the samples and, therefore, also represents the "real" material behaviour. This testing incurs the lowest overall deformation and, thus, the highest elastic modulus, especially since deformation is measured only in the middle third of the sample height. When fitting the results, a linear approximation between the stabilised elastic modulus $E_{C,S}$ and the compressive strength f_c provides the best approximation with a coefficient of determination R^2 of 0.975 and is shown in Equation 3.5.

$$E_{C,S} = 2385 \cdot f_c \tag{3.5}$$

The results also show that the secant modulus $E_{c,i}$ and the tangent modulus E_{c1} provide similar results and are, as expected, in line with the results shown in literature from geotechnical testing standards. The tangent modulus is consistently higher than the secant modulus, which relates to the secant modulus accounting for the higher, plastic deformation of the Plastic Concrete samples.

The present results clearly highlight that, to date, cut-off wall design significantly underestimates Plastic Concrete material stiffness. However, since Plastic Concrete should provide a similar stiffness to the surrounding soil [28], and the soil stiffness is established as the tangent modulus in a load-displacement curve, the tangent modulus E_{ci} may be the most appropriate value for geotechnical cut-off wall design. This is not least because the settlement calculations, and thus the load transfer onto the cut-off wall, use soil stiffness (i.e. tangent modulus) as input parameters. Once the design loads are obtained, these can be used as input for the Plastic Concrete cut-off wall stress analysis and design. The stress analysis can then be performed following available concrete design codes and using this thesis's newly developed mechanical models, including the stabilised elastic modulus $E_{C,S}$.

4 Conclusions and Outlook

4.1 Conclusions

The present thesis sets the first steps for a comprehensive understanding of Plastic Concrete material behaviour. With the acquired knowledge, Plastic Concrete can be used to safely guarantee seepage control inside and below dams with a controlled material behaviour.

Overall, the mix design, especially bentonite contents and type, significantly influences Plastic Concrete's microstructural and mechanical properties which are clearly dependent on sample age, with significant material property changes far beyond the 28-day mark. An extensive literature review provided first insights into the material properties and highlighted the current research gaps on Plastic Concrete's material behaviour. Most importantly, the literature review proved that Plastic Concrete's material behaviour aligns with concrete technology and can therefore be studied using the established concrete investigation procedures.

The microstructural properties investigated through MIP and XRD show a significant pore refinement over an extended study time period of 4 years, correlating with increased material strength. In addition, the pore size distribution clearly depends on the mix design and further correlates to the source materials used. The mineralogical study using XRD confirms the existence of typical crystalline products from cement hydration.

The mechanical properties investigated also clearly correlate to the selected mix design, especially to the water, cement and bentonite contents used. The compressive and tensile strength clearly correlate with the mix design and significantly increase with sample age. This thesis also develops Plastic Concrete specific mechanical property models for the first time. The compressive strength development over time can be estimated for a sample age of up to 4 years as a modification of the *fib* Model Code 2020 [36] time development model. The tensile-to-compressive strength ratio has been established to be best correlated using a linear approximation. Finally, the stabilised elastic modulus $E_{C,S}$ has shown to be closely correlated to the Plastic Concrete mix design and can be estimated from the corresponding compressive strength. This thesis also confirms the major impact elastic modulus test set-up, most importantly sample deformation measurement techniques, has on the obtained elastic modulus.

In addition, some of the results from this thesis are reflected within the draft for the new standard prEN 206-3:2023-09 [51], to which the author contributed in the corresponding working group in CEN/TC 288. For the first time, the draft standard prEN 206-3:2023-09 [51] provides an independent section for the specific requirements of Plastic Concrete mix design. In addition, a new definition of the term Plastic Concrete is established for clear reference in future research and project tendering.

Finally, this thesis' findings are of significant value for future Plastic Concrete cut-off wall design since a more realistic and accurate time-dependent design will be possible in future, addressing the specific material behaviour of Plastic Concrete.

4.2 Outlook and Perspectives

All in all, this thesis has provided novel and more profound insights into the understanding of Plastic Concrete's material properties. The results presented in this thesis provide a solid basis for further research, for which various recommendations can be proposed.

Firstly, Plastic Concrete mix design can be further developed using novel additives and admixtures to enhance Plastic Concrete mechanical behaviour further. Most notably, the use of fibres (e.g. steel fibres or polymer fibres) should be intensively studied since these enhance overall material ductility, especially in the post-peak behaviour [52, 53, 54, 55]. In addition, the use of novel, clay-based admixtures or SCMs [56, 57, 58, 59, 60] can also improve Plastic Concrete's mechanical performance. In addition, concrete durability may also increase through bentonite addition [61, 62].

Future studies should also concentrate on the creep and shrinkage behaviour of Plastic Concrete [63, 64]. The Plastic Concrete creep is expected to be significantly higher than that of standard concrete, further enhancing cut-off wall performance through stress relaxation [37].

Moreover, the strength development mechanisms over time remain unclear, especially at high sample age. Therefore, further studies attempt to identify the underlying mechanisms, e.g. cement-bentonite interaction [65, 63], which incur in material strength increase far beyond 91 days. In addition, the use of cement with lower clinker content, such as CEM III, could be explored [28].

Finally, the hydraulic conductivity of Plastic Concrete should be investigated systematically to ensure the overall permeability requirements from Plastic Concrete cut-off wall design are met during stress conditions [66, 67].

Bibliography

[1] D. A. Bruce, ed. *Specialty construction techniques for dam and levee remediation.* Boca Raton: CRC Press, 2013. ISBN: 978-0-415-78194-7.

[2] US Army Corps of Engineers. *Performance Evaluation of the New Orleans and Southeast Louisiana Hurricane Protection System: Final Report of the Interagency Performance Evaluation Task Force: Volume I – Executive Summary and Overview.* 2009. URL: `https://lccn.loc.gov/2006618548`.

[3] American Society of Civil Engineers. *The New Orleans hurricane protection system: What went wrong and why ; a report.* Reston, Va., 2007. ISBN: 978-0-7844-0893-3.

[4] US Army Corps of Engineers. *National Inventory of Dams (NID).* 2023. URL: `nid.sec.usace.army.mil` (visited on 09/12/2023).

[5] S. Mohr et al. "A multi-disciplinary analysis of the exceptional flood event of July 2021 in central Europe – Part 1: Event description and analysis". In: *Natural Hazards and Earth System Sciences* 23.2 (2023), pp. 525–551. ISSN: 1561-8633. DOI: `10.5194/nhess-23-525-2023`.

[6] P. Ludwig et al. "A multi-disciplinary analysis of the exceptional flood event of July 2021 in central Europe – Part 2: Historical context and relation to climate change". In: *Natural Hazards and Earth System Sciences* 23.4 (2023), pp. 1287–1311. ISSN: 1561-8633. DOI: `10.5194/nhess-23-1287-2023`.

[7] S. Cusack. "A long record of European windstorm losses and its comparison to standard climate indices". In: *Natural Hazards and Earth System Sciences* 23.8 (2023), pp. 2841–2856. ISSN: 1561-8633. DOI: `10.5194/nhess-23-2841-2023`.

[8] T. H. Raupach et al. "The effects of climate change on hailstorms". In: *Nature Reviews Earth & Environment* 2.3 (2021), pp. 213–226. ISSN: 2662-138X. DOI: `10.1038/s43017-020-00133-9`.

[9] R. Fell et al. *Geotechnical engineering of dams.* 2nd. Boca Raton, FL: CRC Press, 2015. ISBN: 978-1-138-00008-7.

[10] U.S. Bureau of Reclamation. *Design Standards No. 13: Embankment Dam, Chapter 16: Cutoff Walls, Revision 14.* 2014/07. URL: `https://www.usbr.gov/tsc/techreferences/designstandards-datacollectionguides/designstandards.html`.

[11] D. Alós Shepherd, E. Kotan, and F. Dehn. "Plastic concrete for cut-off walls: A review". In: *Construction and Building Materials* 255 (2020), p. 119248. ISSN: 0950-0618. DOI: `10.1016/j.conbuildmat.2020.119248`.

[12] P. P. Xanthakos. *Slurry walls.* New York: McGraw-Hill, 1979. ISBN: 978-0-070-72215-6.

[13] S.-H. Chen. *Hydraulic Structures.* Berlin, Heidelberg: Springer, 2015. ISBN: 978-3-662-47330-6.

[14] T. Triantafyllidis. *Schlitzwand- und Dichtwandtechnik.* Vol. 1. Planung und Bauausführung im Spezialtiefbau. Berlin: Ernst & Sohn, 2004. ISBN: 978-3-433-02859-1.

[15] European Federation of Foundation Contractors and Deep Foundations Institute. *Guide to Support Fluids for Deep Foundations, 1st Edition.* 2019. URL: `https://www.effc.org/media_corner/effc-dfi-guide-to-support-fluids-for-deep-foundations-edition-1/`.

[16] European Federation of Foundation Contractors and Deep Foundations Institute. *Guide to Tremie Concrete for Deep Foundations, 2nd Edition.* 2018. URL: `https://www.effc.org/media_corner/effc-dfi-guide-to-tremie-concrete-for-deep-foundations-2nd-edition/`.

[17] K. Beckhaus et al. "Design concept for sustainable cut-off walls made of highly deformable filling materials". In: *Proceedings of the 12th ICOLD European Club Symposium 2023 (ECS 2023, Interlaken, Switzerland, 5-8 September 2023).* Ed. by R. Boes, P. Droz, and R. Leroy. Milton: CRC Press, 2023, pp. 641–650. ISBN: 978-1-032-57668-8. DOI: `10.1201/9781003440420-72`.

[18] A. Lobbestael and A. Athanasopoulos-Zekkos. "The Effect of Input Frequency on Dynamic Soil-Structure Interaction of Levees with Cutoff Walls". In: *Geo-Congress 2013.* Ed. by C. L. Meehan et al. Reston: American Society of Civil Engineers, March 2013, pp. 1260–1269. ISBN: 978-0-784-41278-7. DOI: `10.1061/9780784412787.127`.

[19] M. Ghazavi, Z. Safarzadeh, and H. Hashemolhoseini. "Response Of Plastic Concrete Cut-Off Walls In Earth Dams To Seismic Loading Using Finite Element Methods". In: *Proceedings of the 13th World Conference on Earthquake Engineering.* Ed. by Canadian Association for Earthquake Engineering. Vancouver, 2004.

[20] S. Klima and K. Beckhaus. "Dichtwand im Sylvensteindamm". In: *Vorträge zum 10. Hans Lorenz Symposium.* Ed. by S. A. Savidis and F. Remspecher. Veröffentlichungen des Grundbauinstitutes der Technischen Universität Berlin. Aachen: Shaker, 2014, pp. 235–243. ISBN: 978-3-844-02988-5.

[21] P. Banzhaf. "Erfahrungen bei der Herstellung der Zweiphasen-Dichtwand Hinze-Damm, Australien". In: *Vorträge zum 17. Darmstädter Geotechnik-Kolloquium.* Ed. by C. Bergmann. Mitteilungen des Institutes und der Versuchsanstalt für Geotechnik der Technischen Universität Darmstadt. Darmstadt, 2010, pp. 39–48. ISBN: 978-3-931-39694-7.

[22] P. Banzhaf. "Dichtwandherstellung für den Bagatelle-Damm auf Mauritius". In: *bbr Leitungsbau, Brunnenbau, Geothermie* 67.8 (2016), pp. 36–41. ISSN: 1611-1478.

[23] M. Baltruschat and K. Beckhaus. "Dammabdichtung im Paradies - dauerhafte Untergrundabdichtung im Basalt". In: *Wasserwirtschaft* 109.5 (2019), pp. 182–185. ISSN: 0043-0978.

[24] I. Faridmehr et al. “Construction and Monitoring of Cement/Bentonite Cutoff Walls: Case Study of Karkheh Dam, Iran”. In: *Studia Geotechnica et Mechanica* 41.4 (2019), pp. 184–199. ISSN: 0137-6365. DOI: 10.2478/sgem-2019-0019.

[25] Comité Européen de Normalisation. *EN 206:2017-01 - Concrete - Specification, performance, production and conformity (German version).*

[26] Comité Européen de Normalisation. *EN 1538:2015-10 - Execution of special geotechnical work — Diaphragm walls (German version).*

[27] Deutsche Vereinigung für Wasserwirtschaft, Abwasser und Abfall e.V. *Merkblatt 512-1 - Dichtungssysteme im Wasserbau - Teil 1: Erdbauwerke (in German).* 2012/02.

[28] International Commission On Large Dams. *Filling materials for watertight cut off walls, Bulletin 51.* Paris, 1985.

[29] P. Grübl, H. Weigler, and S. Karl. *Beton: Arten, Herstellung und Eigenschaften (in German).* 2nd. Handbuch fur Beton-, Stahlbeton- und Spannbetonbau. Berlin: Ernst & Sohn, 2001. ISBN: 978-3-433-01340-3.

[30] A. R. Bagheri, M. Alibabaie, and M. Babaie. “Reduction in the permeability of plastic concrete for cut-off walls through utilization of silica fume”. In: *Construction and Building Materials* 22.6 (2008), pp. 1247–1252. ISSN: 0950-0618. DOI: 10.1016/j.conbuildmat.2007.01.024.

[31] J. Sadrekarimi. “Plastic Concrete Mechanical Behaviour”. In: *Journal of the Institution of Engineers. India. Civil Engineering Division* 82.FEV (2002), pp. 201–207. ISSN: 0020-336X.

[32] L. Alvarez et al. “Characteristics of the Plastic Concrete of the Diaphragm Wall of Convento Viejo Dam”. In: *14th International Congress on Large Dams in Rio de Janeiro, Brazil.* Ed. by International Commission On Large Dams. Vol. IV. 1982, pp. 371–389.

[33] A. Becker and C. Vrettos. “Laboruntersuchungen zum Materialverhalten von Tonbeton (in German)”. In: *Bautechnik* 92.2 (2015), pp. 152–160. ISSN: 1437-0999. DOI: 10.1002/bate.201400064.

[34] Y. Pashang Pisheh and S. M. Mir Mohammad Hosseini. “Stress-strain behavior of plastic concrete using monotonic triaxial compression tests”. In: *Journal of Central South University* 19.4 (2012), pp. 1125–1131. ISSN: 2095-2899. DOI: 10.1007/s11771-012-1118-y.

[35] International Federation for Structural Concrete, ed. *fib Model Code for Concrete Structures 2010.* 1st. Berlin: Ernst & Sohn, 2013. ISBN: 978-3-433-03061-5.

[36] International Federation for Structural Concrete, ed. *fib Model Code for Concrete Structures 2020: Final Draft, May 2023.* Unpublished. Lausanne, 2023/05.

[37] S. Hinchberger, J. Weck, and T. Newson. “Mechanical and hydraulic characterization of plastic concrete for seepage cut-off walls”. In: *Canadian Geotechnical Journal* 47.4 (2010), pp. 461–471. ISSN: 0008-3674. DOI: 10.1139/T09-103.

[38] S. Kazemian, S. Ghareh, and L. Torkanloo. “To Investigation of Plastic Concrete Bentonite Changes on it’s Physical Properties”. In: *Procedia Engineering* 145 (2016), pp. 1080–1087. ISSN: 1877-7058. DOI: 10.1016/j.proeng.2016.04.140.

[39] A. Mahboubi and A. Ajorloo. "Experimental study of the mechanical behavior of plastic concrete in triaxial compression". In: *Cement and Concrete Research* 35.2 (2005), pp. 412–419. ISSN: 0008-8846. DOI: 10.1016/j.cemconres.2004.09.011.

[40] P. Zhang, Q. Guan, and Q. Li. "Mechanical Properties of Plastic Concrete Containing Bentonite". In: *Research Journal of Applied Sciences, Engineering and Technology* 5.4 (2013), pp. 1317–1322. ISSN: 2040-7459.

[41] J. C. Evans, E. D. Stahl, and E. Drooff. "Plastic Concrete Cutoff Walls". In: *Geotechnical practice for waste disposal 1987*. Ed. by R. D. Woods. Geotechnical Special Publications. New York: ASCE, 1987, pp. 462–472. ISBN: 978-0-872-62604-1.

[42] S. Z. Cheng et al. "Experimental Study on Mix Design of Plastic Concret with Lower Elastic Modulus and Higher Impervious Coefficient". In: *Advanced Materials Research* 535-537 (2012), pp. 1936–1939. ISSN: 1022-6680. DOI: 10.4028/www.scientific.net/AMR.535-537.1936.

[43] R. Snellings. "X-ray powder diffraction applied to cement (Chapter 4)". In: *A practical guide to microstructural analysis of cementitious materials*. Ed. by K. Scrivener, R. Snellings, and B. Lothenbach. Boca Raton, Florida: CRC Press, 2016. ISBN: 978-1-4987-3867-5.

[44] A. M. Neville. *Properties of concrete*. 5th. Harlow: Pearson, 2011. ISBN: 978-8-131-79107-3.

[45] G. A. Smith and S. W. Benham. "A Study Of the Flow-Table And The Slump Test". In: *ACI Journal Proceedings* 27.1 (1931), pp. 420–438. ISSN: 0002-8061. DOI: 10.14359/8194.

[46] D. Y. Gao, S. Q. Song, and L. M. Hu. "Relationships of Strengths and Dimensional Effect of Plastic Concrete". In: *Advanced Materials Research* 306-307 (2011), pp. 1029–1037. ISSN: 1662-8985. DOI: 10.4028/www.scientific.net/AMR.306-307.1029.

[47] T. W. Kahl, J. L. Kauschinger, and E. B. Perry. *Plastic Concrete Cut-Off Walls for Earth Dams, Technical Report REMR-GT-15*. Vicksburg, MS: USACE, 1991. URL: https://apps.dtic.mil/sti/citations/ADA234566.

[48] J. Kayser and T. Schulz. "Spannungs-Verformungs-Verhalten erhärteter Bentonit-Zement-Suspensionen (in German)". In: *Bautechnik* 76.9 (1999), pp. 747–756. ISSN: 1437-0999. DOI: 10.1002/bate.199904870.

[49] H. G. Heilmann. "Relations between tensile and compressive strength of concrete (in German)". In: *Beton* 19.2 (1969), pp. 68–70. ISSN: 0005-9846.

[50] Comité Européen de Normalisation. *EN 12390-13:2014-06 - Testing hardened concrete - Part 13: Determination of secant modulus of elasticity in compression (German version)*.

[51] Comité Européen de Normalisation. *prEN 206-3:2023-09 - Concrete — Specification, performance, production and conformity — Part 3: Additional requirements for specification and conformity of concrete for special geotechnical works (Internal Document)*.

[52] S.-K. Razavi, M. Hajialilue-Bonab, and A. Pak. "Design of a Plastic Concrete Cutoff Wall as a Remediation Plan for an Earth-Fill Dam Subjected to an Internal Erosion". In: *International Journal of Geomechanics* 21.5 (2021), p. 04021061. ISSN: 1532-3641. DOI: 10.1061/(ASCE)GM.1943-5622.0001991.

[53] M. G. Alberti et al. "Using Polyolefin Fibers with Moderate-Strength Concrete Matrix to Improve Ductility". In: *Journal of Materials in Civil Engineering* 31.9 (2019). ISSN: 0899-1561. DOI: 10.1061/(ASCE)MT.1943-5533.0002775.

[54] M. Bahrami and Mir Mohammad Hosseini, Seyed Majdeddin. "A new incorporative element to modify plastic concrete mechanical characteristics for cut-off wall construction in very soft soil media: Identification of tensile galvanized open-mesh distributer (TGOD) element". In: *Construction and Building Materials* 350 (2022), p. 128884. ISSN: 0950-0618. DOI: 10.1016/j.conbuildmat.2022.128884.

[55] A. Ostovarzijerdi, A. Ghanbari, and M. Karkon. "Investigating the Behavior of the Plastic Concrete Made with Different Types of Fibers with an Approach to the Mixing Plans of Plastic Concrete". In: *Civil Engineering Journal* 5.1 (2019), p. 227. ISSN: 2476-3055. DOI: 10.28991/cej-2019-03091240.

[56] R. Snellings, P. Suraneni, and J. Skibsted. "Future and emerging supplementary cementitious materials". In: *Cement and Concrete Research* 171 (2023), p. 107199. ISSN: 0008-8846. DOI: 10.1016/j.cemconres.2023.107199.

[57] Y. Shi et al. "Micro–macro properties of plastic concrete anti-seepage wall materials mixed with low-liquid limit clay". In: *Advances in Mechanical Engineering* 11.5 (2019), p. 168781401984973. ISSN: 1687-8140. DOI: 10.1177/1687814019849736.

[58] B. Cao, J. Chen, and A. Al-Tabbaa. "Crack-resistant cement–bentonite cut-off wall materials incorporating superabsorbent polymers". In: *Canadian Geotechnical Journal* 58.6 (2021), pp. 800–810. ISSN: 0008-3674. DOI: 10.1139/cgj-2020-0181.

[59] B. Cao et al. "The first microcapsule-based self-healing cement–bentonite cut-off wall materials". In: *Géotechnique* 73.2 (2023), pp. 105–114. ISSN: 0016-8505. DOI: 10.1680/jgeot.19.P.316.

[60] M. L. Nehdi. "Clay in cement-based materials: Critical overview of state-of-the-art". In: *Construction and Building Materials* 51 (2014), pp. 372–382. ISSN: 0950-0618. DOI: 10.1016/j.conbuildmat.2013.10.059.

[61] C. Andrade et al. "Reduced Carbonation, Sulfate and Chloride Ingress Due to the Substitution of Cement by 10% Non-Precalcined Bentonite". In: *Materials* 14.5 (2021). ISSN: 1996-1944. DOI: 10.3390/ma14051300.

[62] K. Joshi et al. "Laboratory and In Situ Tests for Long-Term Hydraulic Conductivity of a Cement-Bentonite Cutoff Wall". In: *Journal of Geotechnical and Geoenvironmental Engineering* 136.4 (2010), pp. 562–572. ISSN: 1090-0241. DOI: 10.1061/(ASCE)GT.1943-5606.0000248.

[63] H. Zhao et al. "Effect of clay content on shrinkage of cementitious materials". In: *Construction and Building Materials* 322 (2022), p. 125959. ISSN: 0950-0618. DOI: 10.1016/j.conbuildmat.2021.125959.

[64] J. K. Norvell et al. "Influence of Clays and Clay-Sized Particles on Concrete Performance". In: *Journal of Materials in Civil Engineering* 19.12 (2007), pp. 1053–1059. ISSN: 0899-1561. DOI: 10.1061/(ASCE)0899-1561(2007)19:12(1053).

[65] K.-H. Ohrdorf et al. "The unusual behavior of a Milos bentonite in cement suspensions". In: *Applied Clay Science* 54.3-4 (2011), pp. 189–195. ISSN: 0169-1317. DOI: 10.1016/j.clay.2011.08.001.

[66] F. Solomon and S. O. Ekolu. "Comparison of Various Permeability Methods Applied upon Clay Concretes–Statistical Evaluation". In: *Journal of Testing and Evaluation* 48.4 (2020), p. 20160546. ISSN: 0090-3973. DOI: 10.1520/JTE20160546.

[67] A. Basha and W. Mansour. "Variation of the Hydraulic Conductivity and the Mechanical Characteristics of Plastic Concrete with Time". In: *International Journal of Concrete Structures and Materials* 17.1 (2023). ISSN: 1976-0485. DOI: 10.1186/s40069-023-00589-1.

Paper 1

Plastic concrete for cut-off walls: A review

Publisher's version

Published in *Construction and Building Materials*

Volume 255, 2020, pp. 119248

DOI: 10.1016/j.conbuildmat.2020.119248

Authors: **David Alós Shepherd**, Engin Kotan, Frank Dehn

Construction and Building Materials 255 (2020) 119248

Contents lists available at ScienceDirect

Construction and Building Materials

journal homepage: www.elsevier.com/locate/conbuildmat

Review

Plastic concrete for cut-off walls: A review

David Alós Shepherd [a,*], Engin Kotan [b], Frank Dehn [a,b]

[a] *Materials Testing and Research Institute Karlsruhe (MPA Karlsruhe), Gotthard-Franz-Str. 2/3, 76131 Karlsruhe, Germany*
[b] *Institute of Concrete Structures and Building Materials (IMB), Gotthard-Franz-Str. 3, Bldg. 50.31, 76131 Karlsruhe, Germany*

HIGHLIGHTS

- Low strength, low elastic modulus concrete capable of sustaining larger strains.
- Mix design with high w/c-ratio with water-binding additions e.g. bentonite.
- Mechanical behaviour in line with concrete technology; challenging sample testing.
- Compressive strength 0.5–2.5 MPa, elastic modulus 300–1800 MPa at 28 days.
- Permeability correlates with strength; range between 1 10^{-8} m/s and 1 10^{-9} m/s.

ARTICLE INFO

Article history:
Received 12 September 2019
Received in revised form 14 March 2020
Accepted 16 April 2020
Available online 30 April 2020

Keywords:
Plastic concrete
Cut-off wall
Design
Review
Dam remediation

ABSTRACT

The remediation of earthen dams is of growing interest worldwide. Plastic Concrete cut-off walls hereby provide an effective method to control dam seepage. However, Plastic Concrete material behaviour is not yet thoroughly understood. The review presented here confirms that Plastic Concrete may be consiered to be a low-strength, low-stiffness impervious concrete with high deformation capacity under load, but also supports the need for further investigations into the mechanical and hydraulic material properties. This review provides an important opportunity to advance in the understanding of the material behaviour of Plastic Concrete and make a contribution towards a more realistic design of Plastic Concrete cut-off walls.

Contents

* Corresponding author.
E-mail address: david.alosshepherd@kit.edu (D. Alós Shepherd).
URL: http://www.betoninstitut.eu (D. Alós Shepherd).

https://doi.org/10.1016/j.conbuildmat.2020.119248
0950-0618/

1. Introduction

1.1. Background

The worldwide ageing infrastructure is a reason for concern in many countries. Unfortunately, only when a catastrophic failure of some infrastructure occurs, this topic obtains public awareness. A key example for the systematic, catastrophic failure of embankment dams and levees occurred in 2005 during the Katrina and Rita Hurricanes in the North-American Gulf Shore area [1].

Various failure modes are possible for earthen dams, ranging from dam over-topping and inadequate maintenance to foundation defects and slope instability. The latter generally occurs through water seepage below the dam body causing a reduction in internal friction and causing the dam to slip. Therefore, major concern has been raised regarding dam safety and various dam repair and remediation programs have been initiated worldwide. A common solution to counter dam seepage is the design and construction of cut-off walls. The planned cut-off wall is hereby extended into an underlying impervious stratum, e.g. rock [2], see Fig. 1. The most effective cut-off walls for seepage control can be constructed with excavated slurry-trench walls, especially for greater depths [3].

In a first step a slurry wall trench is excavated using clamshell excavators or hydromill trench cutters (see Fig. 2, left). The trench is hereby filled with a support fluid in order to stop the excavated trench from collapsing. Most commonly bentonite or polymer support fluids are used. Before the backfill material can be placed, the support fluid used during excavation has to be replaced by a clean support fluid with defined material properties [4] (see Fig. 2, centre). The backfill material is thereafter placed using the tremie method. The backfill material is hereby placed through the so-called tremie pipe, whereby the lower end of the tremie pipe always remains below the concrete surface (see Fig. 2, right). As backfill materials a wide range of possibilities exist, however, a growing interest has arisen in Plastic Concrete due to the materials' suitable characteristics.

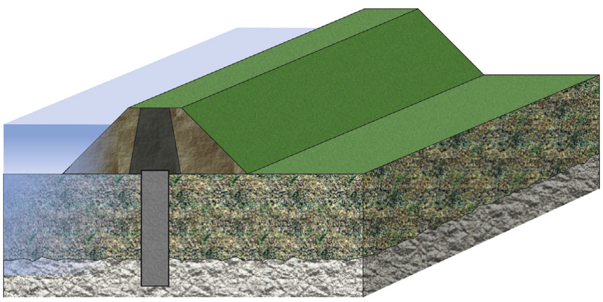

Fig. 1. Schematic overview of a cut-off wall below an earthen dam.

Plastic Concrete is hereby characterised through a high deformation capacity under load, which is of great advantage when ductile walls are needed when significant bending strains are expected due to unequal deformations of the cut-off wall, large annual reservoir fluctuations or significant seismic events [1,2]. Especially the latter has lately been of strong research interest, since few backfill materials can withstand these high deformation [5,6]. The high deformation capacity of Plastic Concrete in turn decreases both rupture probability and crack opening width, which would incur in material permeability increase [1,6]. An example of cut-off wall deformation due to reservoir fluctuation and dam consolidation can be seen in Fig. 3. Plastic Concrete has therefore been widely used worldwide in dam remediation for many years, with projects like the Sylvenstein Dam (Germany) [7], Hinze Dam (Australia) [8], Bagatalle Dam (Mauritius) [9] or Karkheh Dam (Iran) [10].

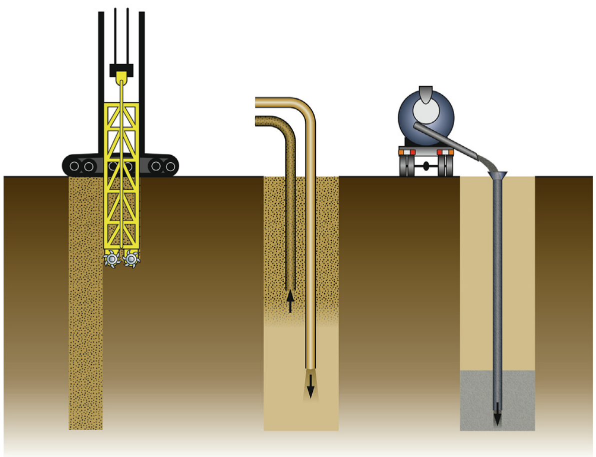

Fig. 2. Overview of the construction of a slurry trench wall using a hydromill trench cutter (left) support fluid replacement (centre) and concrete placement using the tremie method (right).

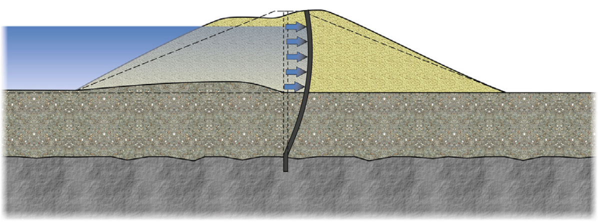

Fig. 3. Schematic overview of cut-off wall deformation after dam consolidation and reservoir fluctuation, as well as original state (dashed lines).

1.2. Problem

Despite its indisputably beneficial material properties, Plastic Concrete has not yet been thoroughly studied. To date, the design of cut-off walls considers Plastic Concrete to be a linear-elastic material. Its undoubtedly existing ductile and plastic behaviour in the ultimate limit state as well as its clearly viscous behaviour during serviceability are neglected not least due to the lack of appropriate constitutive laws and substantiated scientific investigations. Few studies have been large enough to provide reliable estimates of material behaviour under load during a prolonged period of time and therefore have failed to systematically develop a constitutive law for Plastic Concrete.

1.3. Focus & research questions

This paper therefore aims to critically review the existing literature in Plastic Concrete and proposes general statements and reference values with which the design of Plastic Concrete can be enhanced to reflect material behaviour more realistically. Qualitative content analysis was used for this purpose.

This paper begins by describing the mix design of Plastic Concrete including the materials used as well as the variations in mixture composition and their influence on the fresh properties of Plastic Concrete. The third chapter discusses the significant findings regarding the mechanical behaviour of Plastic Concrete, most notably its material strength, elastic modulus, creep and relaxation properties. The hydraulic behaviour of Plastic Concrete is covered in chapter four. The final chapter draws together the key findings of this paper and aims to establish reference values which may be used for Plastic Concrete cut-off wall design.

2. Mix design

2.1. Source materials

Contemporary standard concrete is considered a five-phase construction material composed of cement, water, aggregate, additions (e.g. supplementary cementitious materials) and admixtures. Plastic Concrete can also be considered a five-phase construction material, however, in differing proportions to those usually mixed with standard concretes and containing bentonite as an additional constituent to obtain a highly ductile and impermeable material. However, the composition of Plastic Concrete is not limited to the aforementioned components and could be produced using other supplementary cementitious materials or other physically water-binding additions.

2.1.1. Cement

For Plastic Concrete two main choices exist. The International Commission on Large Dams (ICOLD) recommends within its Bulletin 51 [11] the use of blast-furnace (BLF) or pozzolan (POZ) cement since these types of cement have a stronger resistance against chemically aggressive water, as is also common knowledge within concrete technology [12–14]. In concrete construction it is also known, that through the use of BLF cement, concrete strength development at early age is much slower than with ordinary Portland cement [1,12,13,15]. With this, when the secondary slurry-trench element is cut between two previously tremie-placed primary elements, while the tremie concrete is still of low strength. In addition, the regional availability of BLF or POZ cements may also be a limiting factor in cement type selection.

2.1.2. Bentonite

Bentonite is a weathered rock composed of clay-like minerals which was first discovered in 1898 in Fort Benton, MT (U.S.A.) and is an alteration product of volcanic ash [16]. Although the bentonite discovered in Fort Benton is mainly composed of montmorillonite minerals ($\geqslant$80 wt.%), the term bentonite is however now well established and encompasses any clay-rock composed of smectite minerals, which in turn dominate the physical properties of the rock [16].

Smectite minerals form platelets composed of three layers. The most common smectite mineral, montmorillonite, consists of two SiO_4-tetrahedron on opposite sides of an AlO_6-octahedron [17,18]. Due to the partial, isomorphic substitution of some cations a layer charge is generated, which is in turn counter-balanced by other cations within the interlayer space. Most commonly the interlayer cations are Ca^{2+}, Mg^{2+} or Na^{+} which neutralise the negative surface charge, and account for the two main bentonite groups Na-bentonite and Ca-bentonite (which commonly includes magnesium-bentonites) [19,20,18]. Furthermore, the weak layer charge permits the interlayer cations to adsorb and retain water molecules [19,21]. The water adsorption capacity of sodium and calcium bentonite is however disparate, with Ca-bentonite adsorbing 200–300% water, while Na-bentonite can adsorb up to 600–700% of water [18,22]. This water adsorption phenomena causes the clay minerals, especially montmorillonite to significantly increase in volume, multiplying its starting volume manifold. More recent research has also found that other physically water-binding additions (e.g. sepiolite, silty clay, etc.) can be used to effectively produce Plastic Concrete, although with some limitations [23,24]. Bentonite has however remained of utmost importance in recent years, since bentonite's heavy metal absorption capacity has lead to growing interest in the application of bentonite for containment barriers for waste water or radioactive waste [25,26,23].

2.1.3. Aggregates and admixtures

The most important criteria for the choice of aggregates in Plastic Concrete is the maximum grain size, due to the high segregation risk of fresh Plastic Concrete. This is caused by the relatively high w/c-ratio and the need to use bentonite as a stabilising agent (see Section 2.2). Therefore, aggregates are generally limited to sands and fine to medium gravels. Most specifications have limited maximum grain size to $d_{max} \leqslant 22mm$ [2,27] and practical applications predominantly limit maximum grain size to $d_{max} \leqslant 12mm$.

Furthermore, the fine particle content is also partially regulated to guarantee the necessary flowability [27]. It should however be noted that it is often difficult to meet specific grading demands at building sites in some countries. Furthermore, rounded aggregate is preferred as this type of aggregate further enhances the flowability of tremie concrete [28]. Moreover, the type of aggregate used is regulated by the exposure to any aggressive contaminant, with quartz based aggregate being the preferred aggregate type [28].

Various types of admixtures are also used in Plastic Concrete mix designs. Most often, retarding admixtures are used to slow down concrete setting and prevent premature concrete stiffening during tremie placement [2]. With this, a longer workability window is achieved and longer slurry trench elements can be produced, for which concrete placement with the tremie method can be safely finalised. Depending on Plastic Concrete mixture composition varying amounts of retarding admixtures may be added normally ranging from 1 wt.% to 2.5 wt.% of cement content, with special care being necessary when constructing long slurry-trench elements [8].

In some cases superplasticizing admixtures are also used to ensure better and more controlled workability of the Plastic Concrete mixture. It should however be noted that the effectiveness of modern polycarboxylate ether-based superplasticizers (PCEs) is negatively affected by the presence of clay minerals, especially montmorillonite [29].

In most instances, tap water is generally suitable for Plastic Concrete production. However, untreated water or water with high ion concentrations may affect bentonite dispersion or hydration process and should therefore be tested in trial mixtures if required [30].

2.2. Mixture composition

As mentioned previously, Plastic Concrete is composed of cement, bentonite, aggregates, admixtures and water. In contrast to standard concrete, the w/c-ratio of Plastic Concrete is much higher, with values ranging from 3.3 to 10 [11]. The cement content is also significantly lower than that of standard concrete, rarely surpassing the 200 kg/m^3 mark and even being as low as 80 kg/m^3.

In Fig. 4 five different concrete mixtures are shown, of which three correspond to Plastic Concrete mixtures. The concrete example from [12] represents a standard concrete with 20 MPa compressive strength at 28 days. The middle three mixtures are examples for Plastic Concrete with an approximate compressive strength of 1.30 MPa at 28 days [31,32]. Finally, a mixture composition by [33] of a single-phase diaphragm wall material with 1 MPa compressive strength at 28 days is given for comparison.

As can be seen, the Plastic Concrete mix design is a combination of standard concrete and single-phase diaphragm wall material. The use of aggregates (most notably sand and fine gravel) in somewhat reduced quantities compares to the composition of standard concrete. The density of Plastic Concrete is also similar to that of concrete ranging from 1.9 g/cm^3 to 2.3 g/cm^3 and enough to effectively displace the bentonite slurry within the slurry trench element without mixing during tremie placement. The w/c-ratio on the other hand compares to that of single-phase diaphragm wall materials, exceeding by far 1.0, implying the existence of a far coarser micro-structure. Also, the use of bentonite as a stabilising admixture is comparable to that of single-phase diaphragm wall materials.

It should be emphasised however, that the in situ composition of the backfill material is also dependent on the adjacent soil properties and especially on the casting method used. However, when Plastic Concrete is correctly placed using the tremie method (see Section 1.1) the best material properties can be obtained, which are closest to the target properties.

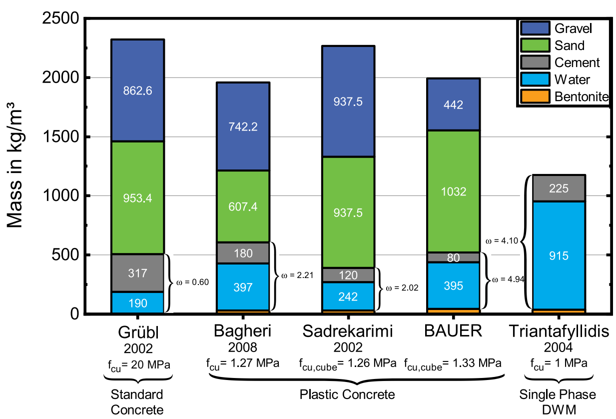

Fig. 4. Representative examples of Plastic Concrete mix designs and their corresponding compressive strength.

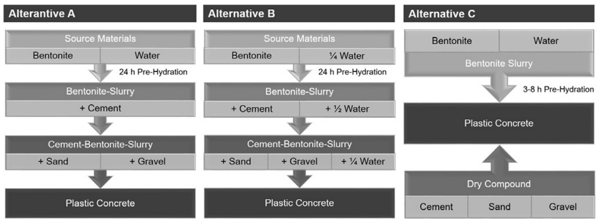

Fig. 5. Representative examples of Plastic Concrete mixing sequences.

2.3. Mixing sequence

Across the literature the Plastic Concrete mixing procedure is not consistent. Various options are presented, which are schematically shown in Fig. 5.

Alternative A is the most commonly described variant in literature [31,32,34–39]. In this, bentonite and water are gradually mixed together and then let to hydrate for up to 24 h. After this, cement is added to the bentonite-suspension and thereafter the aggregates are added. Alternative B [23] has a similar mixing sequence to alternative A, however the addition of water is hereby split into three separate stages. The bentonite slurry is also hydrated for up to 24 h, before cement, sand, gravel and the remaining water are added in two separate stages. Finally, alternative C is an often used mixing sequence in practical application, whereby cement and aggregate are mixed to a dry compound, whilst bentonite and water are mixed into a slurry [7]. The bentonite slurry is then mixed with the dry compound to obtain the Plastic Concrete mixture, whereby the bentonite slurry is hydrated from 0 h to 8 h before use. It should be noted however, that due to the differing mixing sequence and hydration time, varying results can be expected in terms of mechanical properties and permeability values. This is most likely the fact, as the bentonite hydration phase is different for the three aforementioned alternatives, which in turn affects the void filling in the hardened cement paste. In addition, the hydration of bentonite is however not only dependant on the aforementioned differences between bentonite types (see Section 2.1.2) but also on the type of mixer and thus the induced shear rate $\dot{\gamma}$. For any given mixer it can be seen that the higher the maximum achievable shear rate $\dot{\gamma}$ is, the shorter the hydration time required for bentonite samples will be [40].

However, to date, only Fadaie et al. have studied the effect of dry and saturated bentonite on the mechanical properties of Plastic Concrete [41]. In their study, the authors found that the mechanical properties are nearly identical for samples were bentonite was added in a dry state and those where bentonite was hydrated for 24 h. Furthermore the difference in mechanical properties is further decreased with increasing sample age [41]. Due to scarce scientific evidence in literature of the influence of the mixing sequence on Plastic Concrete properties, this topic should therefore be systematically studied in future research.

2.4. Fresh properties

To ensure the correct placement of concrete, which in turn enhances hardened concrete quality, the fresh properties of Plastic Concrete mixtures have to be controlled, especially concrete flowability (often referred to as "slump") during the whole casting process. Therefore, the fresh properties must be controlled not only during initial placement, but also measure the thixotropic and flow retention characteristics of the concrete over time [42]. Despite the complexity and relevance of concrete rheology it is still not uncommon for simple concrete testing procedures (e.g. slump test, flow table test, etc.) to be used to determine the fresh properties of concrete [42]. It should be noted that many problems in diaphragm walls may be attributed to the use of inadequate concrete mixes resulting from poor concrete specifications due to deficient or simplistic testing procedures [42,43].

For Plastic Concrete placed with the tremie method various guidelines and standards exist, which require specific values of concrete fresh properties. Concrete flowability is generally controlled through the water content and superplasticizing agent content, however the stability of the Plastic Concrete has to be closely monitored. For more detailed information regarding the various fresh concrete testing methods applicable for the tremie method (e.g. slump test, flow-table test, etc.) reference is made to the EFFC/DFI Guide to Tremie Concrete for Deep Foundations [43]. Scientific fundamentals on concrete rheology can be found in [44].

3. Mechanical behaviour

3.1. Plastic concrete strength

The mechanical behaviour of concrete samples is most commonly related to the samples' compressive strength. However for cut-off wall design the knowledge of Plastic Concrete's tensile strength as well as multi-axial strength is also of utmost importance.

3.1.1. Unconfined compressive strength

General The strength of Plastic Concrete can be characterised with various parameters, most commonly however the unconfined compressive strength (UCS) is therefore used. In concrete technology, the w/c-ratio is the most commonly used parameter affecting concrete strength, whereby a lower w/c-ratio incurs in higher concrete strength [12,13]. Various studies have tested the UCS of Plastic Concrete with varying mix design and is summarised in Fig. 6 [31,32,34–38,45,46]. The experimental data plotted in Fig. 6 corresponds to cylindrical Plastic Concrete specimens with a height-to-diameter ratio of 2.0 (with varying size) produced with common mixture compositions and tested at 28 days of age. The data shape indicates which testing standard was used and is depicted in the graph legend.

The graph shows that, as would be expected, there is a gradual decline in Plastic Concrete strength with increasing w/c-ratio, closely describing an exponential trend. In addition, some authors [32,35] use a high w/c-ratio far exceeding commonly used w/c-ratios. However, due to the presence of bentonite the effective w/c-ratio is smaller, since the bentonite absorbs water into its structure reducing the readily available water for cement hydration. Although the water binding capacity of bentonite is different for Na-based and Ca-based bentonites, as described in Section 2.1, the existing literature fails to analyse the contending behaviour of cement and bentonite for the available water and the likely interaction between these. In more recent studies, first steps have been made to predict the compressive strength of Plastic Concrete using computational methods (e.g. artificial neural networks [47,25]), however further research into this field is needed.

In concrete technology and design, standard concrete normally achieves a fracture strain of approximately 0.2%–0.3% when tested under standardised unconfined compression conditions [12]. It is furthermore of common knowledge that the fracture strain increases with increasing concrete strength, however the post-cracking behaviour is far more brittle the higher the concrete strength is [12]. Plastic Concrete is therefore expected to have a higher fracture strain than ordinary concrete and a far more ductile post-peak behaviour. This behaviour has been corroborated by various studies, which identify an achievable strain at failure for Plastic Concrete between 0.5% and 1.0% in unconfined compression

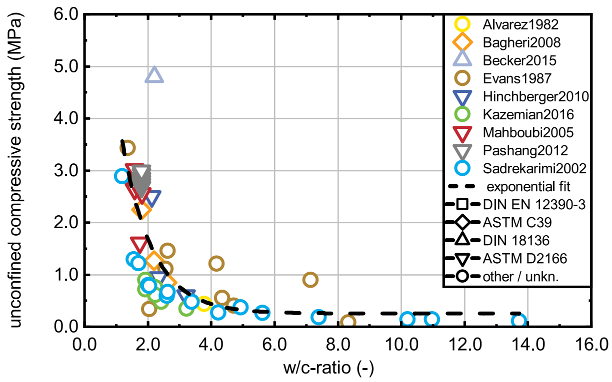

Fig. 6. Overview of the UCS of Plastic Concrete at 28 days as a function of w/c-ratio.

tests [46,34,48]. However, the aforementioned guide values are also dependant on loading speed, since concrete is a crack sensitive material [15].

Loading Rate Since Plastic Concrete is commonly placed as a cut-off wall material below earthen dams, the material is subject to lateral forces induced through reservoir fluctuation, dam consolidation and seismic events. On the one hand reservoir fluctuation and dam consolidation happen at a very slow speed, whilst seismic events induce high loading rates on the cut-off wall. It is therefore important to comprehend the material behaviour in both cases.

With increasing loading speed, the measured concrete strength increases as the possibility of crack propagation around aggregate particles is reduced favouring particle rupture [15,49]. At very high rates of loading additional inertial effects may further occur [15]. At very low loading speeds, creep deformation may also occur in addition to elastic deformation, causing concrete testing to determine lower compressive strength [15,12,49].

Therefore the standards referring to compressive strength testing of concrete all define a specific loading speed. In EN 12390-3 [50] the loading speed for concrete specimens is set to 0.6 ± 0.2MPa/s, ensuring specimen failure to take place after 60 to 90 s. According to the German National Annex the loading speed may also be adjusted for specimens with a compressive strength above 80 MPa or below 20 MPa. ASTMC39/C39M [51] establishes that a rate of movement corresponding to a specimen stress rate of 0.25 ± 0.05 MPa/s should be applied. On the other hand, geotechnical testing standards for soil such as DIN 18136 [52] and ASTMD2166/D2166M [53] use strain rate as the defining loading speed, which should be 1% and 0.5% - 2% of the sample height per minute, respectively.

Kazemian et al. [45] found that the stress-strain behaviour of Plastic Concrete differs from that of ordinary concrete (not linear between 0% and 40%) and, as expected, the standard loading speed is generally too high to measure stress-strain. Hinchberger et al.'s study [36] with strain controlled experiments also showed that Plastic Concrete is sensitive to varying compression rates, whereby higher compression rates (0.01 mm/min $>$ 0.001 mm/min) result in higher compressive stress values [36].

Therefore, it is expedient to adjust the standard loading speed of concrete testing standards for Plastic Concrete specimens to achieve measurable and precise data. With Plastic Concrete compressive strength at 28 days ranging between 1 and 3 MPa, samples should be tested with a lower loading speed between 0.02 MPa/s and 0.03 MPa/s. For example, in DIN 4093 [54], which regulates the design of strengthened soil using jet grouting, deep mixing or grouting techniques, the loading speed is reduced to 0.05 MPa/s for samples with an expected compressive strength $f_{cyl,m} \leqslant 4$ MPa. This loading speed would also be in line with Plastic Concrete requirements and achieve failure after approximately 20 s.

Strength Development Although most reference testing is carried out at 28 days it is known that concrete strength continues to increase after 28 days. Concrete curing hereby mainly depends on the cement strength class, cement type and w/c-ratio used [12]. Blast furnace cement (e.g. CEM III) develops initial strength far slower than ordinary Portland cement (e.g. CEM I), however increases steadily far beyond the 28 day mark due to the latent hydraulic properties of blast furnace slag [13,12]. Furthermore, the cement strength class also influences concrete strength development, with higher cement strength classes causing a more rapid strength development due to their higher fineness [13,12]. For strength development of standard concrete, the *fib* Model Code 2010 [55] gives an approximation for the time function of the concrete strength development β_{cc} as a function of a cement-strength-class-dependant coefficient s and concrete age t, as shown in Eq. 1.

$$\beta_{cc}(t) = \exp(s \cdot [1 - (28/t)^{0.5}]) \tag{1}$$

In line with these considerations, it can therefore expected that Plastic Concrete has a very low hydration rate due to the use of a low cement strength class, a high w/c-ratio and partially through the use of blastfurnace cement. Various studies have examined the long-term strength of Plastic Concrete mixtures, for which an overview is given in Fig. 7 [46,31,34,38,39].

As can be seen, the strength development of Plastic Concrete is not finalised after 28 days, instead increasing steadily after 28 days. The studies also show that due to the high w/c-ratio used the strength development of Plastic Concrete, at any given cement strength class, is slower than the *fib* Model Code 2010 estimates. It is also apparent that Plastic Concrete strength increases far beyond the 28 day mark and increases slowly before this date. However, from the literature review, it remains unclear how Plastic Concrete strength development affects the strain at failure of samples, since contradictory results can be found [39,34,48,46,37]. Against the background of concrete technology it should however be expected that strain at failure increases with increasing Plastic Concrete strength [12].

The knowledge of the long term strength development of Plastic Concrete is of utmost importance, since cut-off walls are constructed for design periods far exceeding 25 years. It is therefore not essential to test characteristic compressive strengths of Plastic Concrete samples at 28 days and can instead be tested at a higher age. Caution is hereby advised, since a very low strength development may also compromise the construction operation efficiency due to the alternating sequence of primary and secondary panel construction and should therefore be considered during the design phase.

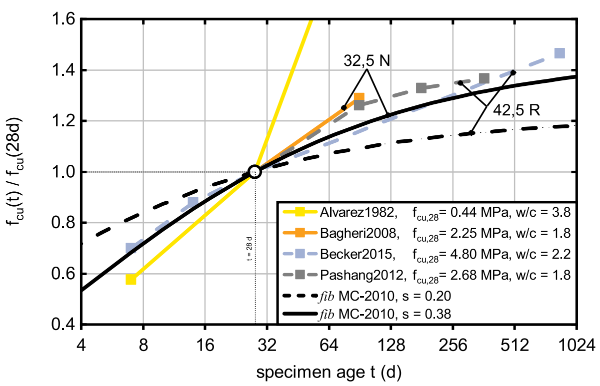

Fig. 7. Overview of the UCS devleopment as a function of time.

3.1.2. Tensile strength

Next to the unconfined compressive strength the uniaxial tensile strength (f_{ct}) is an important parameter for the design of concrete structures. For standard concrete the uniaxial tensile strength averages 10% of unconfined compressive strength f_{cu} [13]. This f_{ct}/f_{cu}-ratio is however not constant and e.g. decreases with increasing time and compressive strength f_{cu} [13]. Furthermore, the ratio is affected by the type of aggregate, aggregate grading, as well as curing conditions.

The *fib* Model Code 2010 suggests that the mean tensile strength f_{ctm} can be estimated from the characteristic compressive strength f_{ck} following Eq. 2 for concrete grades ⩽C50 [55].

$$f_{ctm} = 0.3 \cdot (f_{ck})^{2/3} \tag{2}$$

For a Plastic Concrete sample with a characteristic compressive strength f_{ck} of 2.0 MPa this would incur in a mean tensile strength f_{ctm} of 0.48 MPa, suggesting a f_{ct}/f_{cu}-ratio of 0.24.

It should be however noted that the mean tensile strength f_{ctm} refers to uniaxial conditions, whilst tensile strength testing of concrete specimens most commonly occurs with the splitting tensile strength $f_{ct,sp}$ test, whereby the conversion between both values has not been finally resolved in literature. For Plastic Concrete solely the USACE REMR-GT-15 report also tests the splitting tensile strength of concrete, with splitting tensile strength $f_{ctm,sp}$ averaging 13% of the ultimate compressive strength f_u of the samples tested [56].

The exact tensile strength to compressive strength relationship f_{ct}/f_{cu} for Plastic Concrete remains however unclear and should therefore be an important part of further investigation. It may seem expedient, against the background of concrete technology, to estimate Plastic Concrete tensile strength to be 10%–20% of compressive strength.

3.1.3. Multi-axial load-bearing capacity

In cut-off walls Plastic Concrete is intrinsically submitted to a multi-axial stress state. It is therefore of utmost importance to also understand the multi-axial behaviour of Plastic Concrete.

Firstly, it is expedient to remember that standard concrete failure under a uni-axial compressive force occurs through the inherent development of a transversal tensile stress and the exceedance of the concrete tensile strength [15]. The concrete specimen hereby fails through the development of cracks parallel to the direction of main loading exhibiting a brittle behaviour [13]. This lateral strain may however be hindered through the application of a compressive force perpendicular to the direction of main loading, hereby increasing the overall compressive load-bearing capacity of a concrete specimen [15]. Similarly therefore if a triaxial compression is applied with high lateral stresses, the concrete load-bearing capacity increases manifold [13]. This increase is also known to be more pronounced the lower the ultimate compressive strength of concrete is [12]. The failure however no longer occurs through the exceedance of tensile strength but instead through crushing, incurring in a change in failure towards a more ductile behaviour [13]. An overview of the failure mode change depending on the stress applied can be found in [57].

For Plastic Concrete a similar behaviour to standard concrete can be expected. Since the uniaxial compressive strength is low, the multi-axial load-bearing capacity increase can be expected to be more pronounced. However, this increase is likely limited due to the high water and moisture content of Plastic Concrete samples. Various studies have also confirmed the change in failure mode with increasing confining pressure for Plastic Concrete samples [39,34,36–38]. The specimens tested at higher confining pressures not only exhibit a higher compressive load-bearing capacity and elastic modulus [39], but also a more ductile behaviour and an

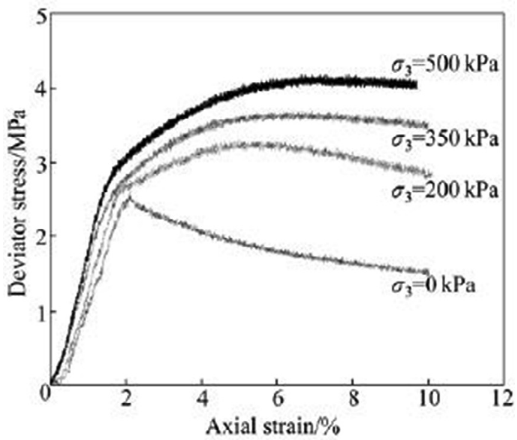

Fig. 8. Variation of deviator stress versus axial strain for unconfined and triaxial compression tests [38].

overall higher strain at failure [34,37–39]. An example of this change in behaviour with increasing confining pressure can be seen in Fig. 8 [38].

3.2. Elastic modulus

The elastic modulus E of concrete is primarily determined by the elastic moduli of its components cement paste and aggregate, as well as the volumetric proportions of the materials in the mix, and may be estimated through composite theory [15]. Therefore, generally speaking, an increase in water content or a decrease in cement content causes the elastic modulus of concrete to decrease [15]. Furthermore, with increasing degree of hydration the elastic modulus increases, whereby the elastic modulus increase precedes the compressive strength increase [12]. In Fig. 9 the elastic modulus of Plastic Concrete is plotted over the corresponding compressive strength [46,34,36,45,37,32,58].

Similarly to ordinary concrete, the elastic modulus of Plastic Concrete increases with increasing compressive strength. However, it hereby becomes apparent that the testing procedure used clearly influences the obtained elastic modulus, in-line with varying definitions of elastic modulus underlying the individual testing procedures. The "elastic modulus" determined with concrete testing standards (Zhang et al. [58]) is higher than that obtained from geotechnical testing standards (e.g. Mahboubi et al. [37]). This is most likely due to the deformation measurement techniques used, since concrete standards measure specimen deformation in situ (e.g. strain gauges) while geotechnical standards generally use the machine displacement to obtain specimen deformation. Based on the literature review, and as shown in Fig. 9, the elastic modulus of Plastic Concrete can be assumed to be in the range of 300–1500 MPa dependant on the testing standard used.

Since the elastic modulus of concrete directly relates to it's compressive strength, it is important to note that the requirement of a characteristic compressive strength f_{ck} (defined statistically as the 5-percentile value) is not expedient since this automatically relates to an increase in the elastic modulus [7]. It is therefore purposive to define a mean compressive strength f_{cm} which is required for the proposed cut-off wall and hereby also establish the targeted elastic modulus. This further substantiates the fact, that the testing conditions should therefore be specified during planning and tendering of projects.

In addition, the target elastic modulus of Plastic Concrete should be similar to that of the surrounding soil and should not

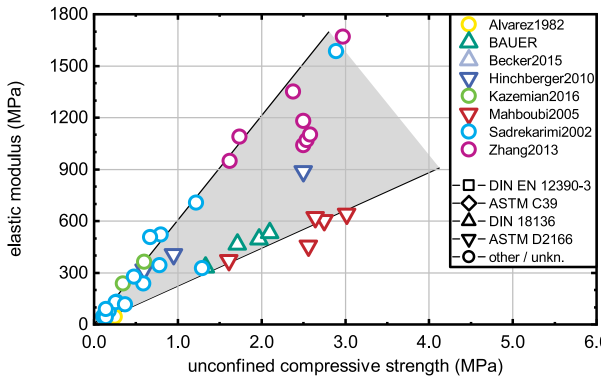

Fig. 9. Elastic modulus as a function of the compressive strength at 28 days.

exceed five times the latter [11]. This has also been confirmed by some numerical studies into the deformation of cut-off walls due to high overburden or seismic load, which show that a higher elastic modulus of the backfill material causes higher strain and stress within the cut-off wall, which in turn may incur in cut-off wall seepage or even failure [6,59].

3.3. Creep and relaxation

When concrete is subjected to a load, concrete firstly reacts elastically. However, besides elastic strain components, concrete also presents a non-linear stress-strain behaviour when subjected to sustained loading. Strain hereby increases gradually with time due to concrete creep. The creep coefficient φ is hereby the most common engineering approach to estimate concrete creep and is defined according to *fib* Model Code 2010 as the quotient of the concrete creep strain ε_{cc} and the concrete elastic strain ε_{ci} following Equation 3 [55,15].

$$\varphi(t,t_0) = \frac{\varepsilon_{cc}(t,t_0)}{\varepsilon_{ci}(t_0)} \tag{3}$$

Various parameters affect the creep behaviour of concrete. With an increasing cement content and increasing water content, concrete creep increases as it is the cement paste phase which undergoes creep [13]. Concrete creep is also dependant on the age at loading, with creep increasing disproportionally the younger the concrete is at loading [60]. Therefore, depending on the conditions present the final creep coefficient φ_∞ may vary greatly, normally ranging between $1 < \varphi_\infty < 3$ for standard concrete [15].

On the contrary, if a stressed concrete specimen is subjected to a constant strain, the specimen stress will gradually decrease with time, known as relaxation. Both creep and relaxation are based on the same molecular mechanisms and therefore all influences affecting concrete creep also affect concrete relaxation [12].

Taking into account the aforementioned influencing parameters, it should be expected that Plastic Concrete has a greater creep and relaxation behaviour than standard concrete, with various studies having confirmed these expectations [36,61,48]. Firstly, the very high w/c-ratio likely incurs in high water loss and specimen deformation. In addition, due to the very slow strength development of Plastic Concrete mixtures the specimen loading will likely occur at a low degree of hydration furthering concrete creep. Beckhaus et al. suggest a final creep coefficient $\varphi_\infty \geqslant 2$ for Plastic Concrete samples, which was derived from results on soil samples solidified with the jet grouting technique [61]. It can be expected however that Plastic Concrete mixtures may have even higher creep coefficients (e.g. $\varphi_\infty > 3$). Hinchberger et al. [36] studied the effect of constant axial strain on the stress behaviour of Plastic

Concrete and found that Plastic Concrete shows significant stress relaxation effects with the measured stress reducing approximately 30% after an 8 h period, with the reduction having not yet stabilised up until this point. All in all, Plastic Concrete is expected to have a stronger relaxation behaviour than standard concrete and therefore a time-dependant constitutive model is required for Plastic Concrete [36].

4. Hydraulic behaviour

Since seepage control of earth dams is the main purpose of a cut-off wall, the hydraulic conductivity of Plastic Concrete is one of the most important parameters to be tested. Despite this, no specific testing standard exists for the measurement of Plastic Concrete permeability. Therefore, standard test methods from geotechnical engineering as well as concrete technology are used.

The hydraulic conductivity testing of concrete specimens can be foremost divided into two main testing groups, namely those under loaded and unloaded conditions, whereby in concrete technology material hydraulic permeability is normally tested without simultaneous loading, as reviewed by Hoseini et al. [62]. Despite most data reviewed corresponding to testing methods where permeability was measured after loading, in various practical applications (including Plastic Concrete) concrete is submitted to compressive or flexural forces while simultaneously being permeated through. Few testing methods exist for this purpouse, however geotechnical triaxial cells may be used for this purpose, with which the hydraulic conductivity *k* can be determined [63].

In addition, due to its low strength, degree of water-tightness and composition, Plastic Concrete is commonly tested following geotechnical testing standards and not structural concrete penetration tests. An overview of some test results of hydraulic conductivity *k* without confining pressure is given in Fig. 10 [31,35,34,64,65].

It can be seen that, similarly to standard concrete, the hydraulic conductivity of Plastic Concrete specimens decreases with increasing compressive strength. This may be ascribed to a reduced particle-cross linking and an increased air void content with increasing w/c-ratio i.e. decreasing compressive strength.

Moreover, it should be noted that current design procedure for Plastic Concrete does not account for the highly ductile behaviour of this material, whereby a high relaxation and creep potential have been shown to exist (see Section 3.3). This behaviour is beneficial for Plastic Concrete hydraulic permeability, since it can prevent material stress peaks during loading and avoid the formation of cracks, which would incur in an increase in permeability. Some initial studies have shown that with deformation of approximately 70% of strain at failure, no significant increase in hydraulic conductivity occurs [48]. By contrast, crack onset in concrete generally occurs at approximately 20% of strain [48].

Only few studies also refer to the time-development of Plastic Concrete hydraulic conductivity, whereby a decrease in hydraulic conductivity over time is reported [34,66]. This is in line with the strength development behaviour of Plastic Concrete (see Section 3.1.1) and is likely caused by the progress of hydration and the consolidation of concrete microstructure [67]. In addition, crack self-healing and crack obstruction with the transported particles, amongst others, are also known to cause the permeability of concrete to further decrease over time [68]. Nonetheless, this aspect has not yet been finally clarified in literature.

Due to the time-development of Plastic Concrete permeability, some specifications allow for permeability tests at higher ages (e.g. 90 days), to achieve the required design permeability values [30,27]. It may however also be contractually expedient to set 28-day control values, not as the design permeability but as a demonstration of design value achievement, to shorten the acceptance period of the construction services provided [30].

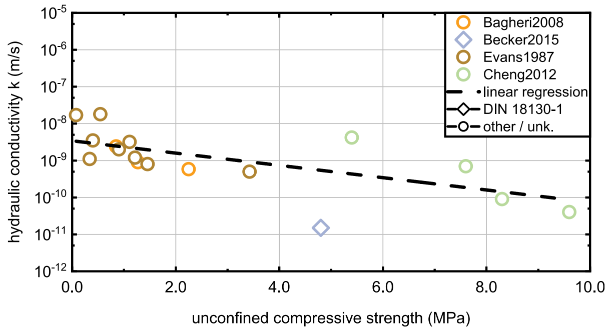

Fig. 10. Hydraulic conductivity of Plastic Concrete over unconfined compressive strength.

5. Conclusions

5.1. Summary

With the present article first steps are set out for a comprehensive understanding of Plastic Concrete material behaviour. With the acquired knowledge Plastic Concrete can be used to safely guarantee seepage control inside and below dams with a controlled material behaviour. All in all, the following considerations may be taken into account for Plastic Concrete cut-off wall design. More detailed information can be found in [69].

Plastic Concrete can be considered to be a low strength concrete with a low elastic modulus capable of sustaining larger strains than normal concrete. These properties can be achieved through the targeted selection of raw materials and mix design. The key component differentiating Plastic Concrete from ordinary concrete is the far higher w/c-ratio, for which the fresh concrete stability has to be controlled by low amounts of physically water-binding additions. Most commonly bentonite, a clay-rock composed of montmorillonite minerals, is added, however other additions may also be used. Finally, Plastic Concrete uses regular aggregate with a maximum grain size of 12 mm (due to the segregation risk) as well as including retarding admixtures to delay concrete setting in tremie placement.

Plastic Concrete mix design is similar to that of standard concrete with aggregate content ranging between 1300 and 1900 kg/m^3 and cement content lying in the range of 80–200 kg/m^3. The w/c-ratio generally ranges between 2.0 and 5.0, depending on target strength and source materials used. The mixing sequence has also been shown to influence material properties, whereby currently no standardised mixing sequence exists.

The mechanical behaviour of Plastic Concrete is in line with that which can be expected from concrete technology. It should however be noted that much testing is conducted using geotechnical testing standards and not concrete testing standards, which is especially important when testing Plastic Concrete deformability i.e. elastic modulus.

Generally speaking, it can be ascertained that the compressive strength of Plastic Concrete increases with decreasing w/c-ratio. However, the w/c-ratio does not account for the addition of bentonite and therefore not consider the reduction in free water available for cement hydration. Plastic Concrete compressive strength normally lies between 0.5 and 2.5 MPa at 28 days, with compressive strength development being very pronounced, far beyond the 28 day mark. It may therefore also be expedient to test Plastic

Concrete compressive strength at higher ages, e.g. 90 days. Furthermore, the loading rate should be adjusted to account for the low strength of the material and should be tested with a loading speed between 0.02 MPa/s and 0.03 MPa/s.

The strain at failure of Plastic Concrete is also far greater than that of standard concrete, where under compression a maximum strain of 1% can be achieved. The tensile to compressive strength ratio of Plastic Concrete is also expected to be greater than that of standard concrete, lying in the range of 10%–20%. Under multiaxial load, the load bearing capacity clearly increases with axial strains as high as 10%.

The magnitude of the elastic modulus of Plastic Concrete clearly depends on the testing standard used, due to differing definitions of elastic modulus and diverging specimen deformation measurement set-ups. The deformation modulus (geotechnical standard) of Plastic Concrete can therefore be estimated to 100–600 MPa, whilst Young's modulus (concrete standard) should be estimated in the range of 300–1800 MPa.

Due to the high w/c-ratio of Plastic Concrete, the creep and relaxation properties are more pronounced than those of standard concrete. With this, the final creep coefficient can be expected to be $\varphi_\infty \geqslant 3.0$. Therefore, the relaxation potential of Plastic Concrete is also notably higher than that of standard concrete. The higher relaxation potential of Plastic Concrete is in turn beneficial to prevent material stress peaks during loading and avoid the formation of cracks, which would incur in an increase in permeability.

The hydraulic behaviour of Plastic Concrete, and concrete in general, remains a relatively unstudied field, especially for testing under realistic stress conditions. For Plastic Concrete it has been shown that permeability decreases with decreasing w/c-ratio which is linked to a less porous material structure. The change in Plastic Concrete permeability over time is scarcely reported in literature, however a decrease in permeability over time has been shown to exist. It is therefore expedient that Plastic Concrete permeability testing is conducted at ages greater than 28 days (e.g. 90 days) to account for the permeability increase with time. Plastic Concrete permeability can therefore be estimated in the range of 10^{-8} to 10^{-9} m/s depending on testing age.

5.2. Unresolved questions

Despite these promising results, questions remain which should be the purpose of further studies. Firstly, further research is required to examine the effects of the mixing procedure on Plastic Concrete hardened behaviour. The focus of these studies should be placed at understanding the interaction of water, bentonite and cement and to what extent the varying mixing procedures may alter the availability of water during cement hydration. Most notably reliable analytical methods must be studied to comprehensively characterise bentonite raw materials as this may shed light on the mechanism underlying Plastic Concrete behaviour and establish bentonite requirements. The understanding of these mechanisms is also of utmost importance to establish their influence on compressive and tensile strength of Plastic Concrete as well as creep behaviour. Furthermore, the creep and relaxation potential of Plastic Concrete should be intensively studied, since these have a significant impact on the material stress and in turn strongly affects cut-off wall design and dimensioning. On the other hand, the permeability changes in Plastic Concrete should be the subject of further studies. A greater focus on the determination of Plastic Concrete permeability under simultaneous loading could produce important findings that account for a more realistic design of Plastic Concrete cut-off walls. For this, the development of a new testing method may also be necessary.

All in all, it may be summarised that the findings of this study have a number of important implications for future best practice. However, continued efforts are needed to further understand Plastic Concrete behaviour and ensure its correct application in cut-off wall design.

Declaration of Competing Interest

The authors declare that they have no known competing financial interests or personal relationships that could have appeared to influence the work reported in this paper.

Acknowledgements

This work was supported by the BAUER Forschungsgemeinschaft under Grant No. BFG 041.

References

[1] D.A. Bruce (Ed.), Specialty Construction Techniques for Dam and Levee Remediation, CRC Press, Boca Raton, 2013.
[2] U.S. Bureau of Reclamation, Design Standards No. 13: Embankment Dam, Chapter 16: Cutoff Walls, Revision 14 (2014/07).
[3] P.P. Xanthakos, Slurry Walls, McGraw-Hill, New York, 1979.
[4] European Federation of Foundation Contractors, Deep Foundations Institute, Guide to Support Fluids for Deep Foundations, first ed., 2019.
[5] A. Lobbestael, A. Athanasopoulos-Zekkos, The Effect of Input Frequency on Dynamic Soil-Structure Interaction of Levees with Cutoff Walls, in: C.L. Meehan, D. Prade, M.A. Pando, J.F. Labuz (Eds.), Geo-Congress 2013, American Society of Civil Engineers, Reston, March 2013, pp. 1260–1269. https://doi.org/10.1061/9780784412787.127.
[6] M. Ghazavi, Z. Safarzadeh, H. Hashemolhoseini, Response of plastic concrete cut-off walls in earth dams to seismic loading using finite element methods, in: Canadian Association for Earthquake Engineering (Ed.), Proceedings of the 13th World Conference on Earthquake Engineering Vancouver, 2004.
[7] S. Klima, K. Beckhaus, Dichtwand im Sylvensteindamm, in: S.A. Savidis, F. Remspecher (Eds.), Vorträge zum 10. Hans Lorenz Symposium, Veröffentlichungen des Grundbauinstitutes der Technischen Universität Berlin, Shaker, Aachen, 2014, pp. 235–243 (in German).
[8] P. Banzhaf, Erfahrungen bei der Herstellung der Zweiphasen-Dichtwand Hinze-Damm, Australien, in: C. Bergmann (Ed.), Vorträge zum 17. Darmstädter Geotechnik-Kolloquium, Mitteilungen des Institutes und der Versuchsanstalt für Geotechnik der Technischen Universität Darmstadt, Darmstadt, 2010, pp. 39–48 (in German).
[9] P. Banzhaf, Dichtwandherstellung für den Bagatelle-Damm auf Mauritius, bbr Leitungsbau, Brunnenbau, Geothermie 67 (8) (2016) 36–41 (in German).
[10] I. Faridmehr, M.R. YazdaniPour, M.J. Jokar, T. Ozbakkaloglu, Construction and Monitoring of Cement/Bentonite Cutoff Walls: Case Study of Karkheh Dam, Iran, Studia Geotechnica et Mechanica 41 (4) (2019) 184–199, https://doi.org/10.2478/sgem-2019-0019.
[11] International Commission On Large Dams, Filling materials for watertight cut off walls, Bulletin 51, 1985.
[12] P. Grübl, H. Weigler, S. Karl, Beton: Arten, Herstellung und Eigenschaften, 2nd Edition, Handbuch fur Beton-, Stahlbeton- und Spannbetonbau, Ernst & Sohn, Berlin, 2001 (in German).
[13] A.M. Neville, Properties of concrete, fifth ed., Pearson, Harlow, 2011.
[14] R. Weber, P. Bilgeri, H. Kollo, H.-W. Vißmann (Eds.), Hochofenzement – Eigenschaften und Anwendungen im Beton, second ed., Verl. Bau+Technik, Düsseldorf, 1998 (in German).
[15] H.-W. Reinhardt, Ingenieurbaustoffe, second ed., Ernst & Sohn, Berlin, 2010 (in German).
[16] R.E. Grim, N. Güven, Bentonites: geology, mineralogy, properties and uses, Developments in sedimentology, vol. 24, Elsevier, Amsterdam, 1978.
[17] P. von Soos, J. Engel, Eigenschaften von Boden und Fels – ihre Ermittlung im Labor, in: K.J. Witt (Ed.), Grundbau-Taschenbuch, Teil 1: Geotechnische Grundlagen, Ernst & Sohn, Berlin, 2008, pp. 123–218 (in German).
[18] S. Praetorius, B. Schößer, Bentonithandbuch: Ringspaltschmierung für den Rohrvortrieb, Bauingenieur-Praxis, Ernst & Sohn, Berlin, 2016 (in German).
[19] D. Koch, Eigenschaften und Einsatzmöglichkeiten von Bentonit/Zement-Mischungen im Spezialtiefbau, in: K. Eichler (Ed.), Spezialtiefbau, Expert Verlag, Renningen, Kontakt & Studium, 2015, pp. 170–189 (in German).
[20] K. Jasmund, G. Lagaly (Eds.), Tonminerale und Tone: Struktur, Eigenschaften, Anwendungen und Einsatz in Industrie und Umwelt, Steinkopff, Darmstadt, 1993. https://doi.org/10.1007/978-3-642-72488-6 (in German).
[21] IBECO Bentonit-Technologie GmbH, Bentonit im Tiefbau: Ein Handbuch für die Baupraxis, 1st Edition, Mannheim, 1998 (in German).
[22] M. Geil, Untersuchungen der physikalischen und chemischen Eigenschaften von Bentonit-Zement-Suspensionen im frischen und erhärteten Zustand, Dissertation, Technische Universität Braunschweig, Braunschweig, 1989 (in German).
[23] H. Abbaslou, A.R. Ghanizadeh, A.T. Amlashi, The compatibility of bentonite/sepiolite plastic concrete cut-off wall material, Constr. Build. Mater. 124 (2016) 1165–1173, https://doi.org/10.1016/j.conbuildmat.2016.08.116.

[24] L.M. Hu, X.L. Lv, D.Y. Gao, K.B. Yan, S.Q. Song, Analysis of the influence of clay dosage and curing age on the strength of plastic concrete, Adv. Mater. Res. 936 (2014) 1433–1437, https://doi.org/10.4028/www.scientific.net/AMR.936.1433.
[25] A.T. Amlashi, S.M. Abdollahi, S. Goodarzi, A.R. Ghanizadeh, Soft computing based formulations for slump, compressive strength, and elastic modulus of bentonite plastic concrete, J. Cleaner Prod. 230 (2019) 1197–1216, https://doi.org/10.1016/j.jclepro.2019.05.168.
[26] O. Nasir, T.S. Nguyen, J.D. Barnichon, A. Millard, Simulation of hydromechanical behaviour of bentonite seals for containment of radioactive wastes, Can. Geotech. J. 54 (8) (2017) 1055–1070, https://doi.org/10.1139/cgj-2016-0102.
[27] Österreichisches Normungsinstitut, ÖNORM B 4452 - Erd- und Grundbau - Dichtwände im Untergrund (1998/12) (in German).
[28] A. Weinmann, Vertical barriers with plastic concrete for containment of landfills and contaminated land, in: 3rd International Symposium and Exhibition on Environmental Contamination in Central and Eastern Europe, Warsaw, 1996.
[29] J. Plank, Einfluss von Tonmineralien auf die Wirkung von PCE-Fließmitteln, Beton 66 (7+8) (2016) 288–290 (in German).
[30] Institution of Civil Engineers, Construction Industry Research and Information Association, Building Research Establishment, Specification for the construction of slurry trench cut-off walls: as barriers to pollution migration, 1999.
[31] A.R. Bagheri, M. Alibabaie, M. Babaie, Reduction in the permeability of plastic concrete for cut-off walls through utilization of silica fume, Constr. Build. Mater. 22 (6) (2008) 1247–1252, https://doi.org/10.1016/j.conbuildmat.2007.01.024.
[32] J. Sadrekarimi, Plastic concrete mechanical behaviour, J. Inst. Engineers India Civil Eng. Division 82 (FEV) (2002) 201–207.
[33] T. Triantafyllidis, Schlitzwand- und Dichtwandtechnik, Planung und Bauausführung im Spezialtiefbau, vol. 1, Ernst & Sohn, Berlin, 2004.
[34] A. Becker, C. Vrettos, Laboruntersuchungen zum Materialverhalten von Tonbeton, Bautechnik 92 (2) (2015) 152–160, https://doi.org/10.1002/bate.201400064 (in German).
[35] J.C. Evans, E.D. Stahl, E. Drooff, Plastic concrete cutoff walls, in: R.D. Woods (Ed.), Geotechnical practice for waste disposal '87, Geotechnical Special Publications, ASCE, New York, 1987, pp. 462–472.
[36] S. Hinchberger, J. Weck, T. Newson, Mechanical and hydraulic characterization of plastic concrete for seepage cut-off walls, Can. Geotech. J. 47 (4) (2010) 461–471, https://doi.org/10.1139/T09-103.
[37] A. Mahboubi, A. Ajorloo, Experimental study of the mechanical behavior of plastic concrete in triaxial compression, Cem. Concr. Res. 35 (2) (2005) 412–419, https://doi.org/10.1016/j.cemconres.2004.09.011.
[38] Y. Pashang Pisheh, S.M. Mir Mohammad Hosseini, Stress-strain behavior of plastic concrete using monotonic triaxial compression tests, J. Central South Univ. 19 (4) (2012) 1125–1131, https://doi.org/10.1007/s11771-012-1118-y.
[39] F. Jafarzadeh, S.H. Mousavi, Effect of specimen's age on mechanical properties of plastic concrete walls in dam foundations, Electron. J. Geotechnical Eng. 17 (D) (2012) 473–482. URL: http://www.ejge.com/2012/Abs12.042.htm.
[40] J. de Vries, Afdichtingswanden van cement-bentoniet, rapport BSW 91–13, Bouwdienst Rijkswaterstaat, Utrecht, 1992 (in Dutch).
[41] M.A. Fadaie, M. Nekooei, P. Javadi, Effect of dry and saturated bentonite on plastic concrete, KSCE J. Civil Eng. 23 (8) (2019) 3431–3442, https://doi.org/10.1007/s12205-019-0835-2.
[42] T. Kränkel, D. Lowke, C. Gehlen, Rheology Testing of Deep Foundation Concrete, in: W. Kusterle, O. Teubert, M. Greim (Eds.), Rheologische Messungen an Baustoffen 2016, tredition, Hamburg, 2016, pp. 211–223 (in German).
[43] European Federation of Foundation Contractors, Deep Foundations Institute, Guide to Tremie Concrete for Deep Foundations, second ed., 2018.
[44] N. Roussel (Ed.), Understanding the Rheology of Concrete, Woodhead Publishing, Cambridge and Philadelphia, PA, 2012.
[45] S. Kazemian, S. Ghareh, L. Torkanloo, To investigation of plastic concrete bentonite changes on it's physical properties, Proc. Eng. 145 (2016) 1080–1087, https://doi.org/10.1016/j.proeng.2016.04.140.
[46] L. Alvarez, J. Larenas, A. Bernal, J.A. Marin, Characteristics of the Plastic Concrete of the Diaphragm Wall of Convento Viejo Dam, in: International Commission On Large Dams (Ed.), 14th International Congress on Large Dams in Rio de Janeiro, Brazil, Vol. IV, 1982, pp. 371–389.
[47] A.R. Ghanizadeh, H. Abbaslou, A.T. Amlashi, P. Alidoust, Modeling of bentonite/sepiolite plastic concrete compressive strength using artificial neural network and support vector machine, Front. Struct. Civil Eng. 13 (1) (2019) 215–239, https://doi.org/10.1007/s11709-018-0489-z.
[48] P. Lappenküper, Untersuchungen zur Wasserdurchlässigkeit von Erdbetondichtwänden unter Biegescherbeanspruchung, Technische Universität Hamburg-Harburg, Masterarbeit, 2016 (in German).
[49] C. Ozyildirim, N.J. Carino, Concrete Strength Testing, in: J.F. Lamond, J.H. Pielert (Eds.), Significance of Tests and Properties of Concrete and Concrete-Making Materials – STP 169D, ASTM International, West Conshohocken, PA, 2006, pp. 125–140.
[50] Comité Européen de Normalisation, EN 12390-3:2009-07 – Prüfung von Festbeton – Teil 3: Druckfestigkeit von Probekörpern (German version).
[51] ASTM International, ASTM C39/C39M-17 - Test Method for Compressive Strength of Cylindrical Concrete Specimens. doi:10.1520/C0039_C0039M-17.
[52] Deutsches Institut für Normung, DIN 18136:2003-11 - Baugrund, Untersuchung von Bodenproben – Einaxialer Druckversuch (in German).
[53] ASTM International, ASTM D2166/D2166M-16 - Test Method for Unconfined Compressive Strength of Cohesive Soil.https://doi.org/10.1520/D2166_D2166M-16.
[54] Deutsches Institut für Normung, DIN 4093:2015-11 - Bemessung von verfestigten Bodenkörpern – Hergestellt mit Düsenstrahl-, Deep-Mixing- oder Injektions-Verfahren (in German).
[55] International Federation for Structural Concrete (Ed.), fib Model Code for Concrete Structures 2010, first ed., Ernst & Sohn, Berlin, 2013.https://doi.org/10.1002/9783433604090.
[56] T.W. Kahl, J.L. Kauschinger, E.B. Perry, Plastic Concrete Cut-Off Walls for Earth Dams, Technical Report REMR-GT-15, USACE, Vicksburg, MS, 1991. URL: http://wri.usace.army.mil/remr/technical_reports/.
[57] K. Speck, M. Curbach, Ein einheitliches dreiaxiales Bruchkriterium für alle Betone, Beton- und Stahlbetonbau 105 (4) (2010) 233–243, https://doi.org/10.1002/best.200900077 (in German).
[58] P. Zhang, Q. Guan, Q. Li, Mechanical properties of plastic concrete containing bentonite, Res. J. Appl. Sci., Eng. Technol. 5 (4) (2013) 1317–1322.
[59] S.-H. Liu, L.-J. Wang, Z.-J. Wang, E. Bauer, Numerical stress-deformation analysis of cut-off wall in clay-core rockfill dam on thick overburden, Water Sci. Eng. 9 (3) (2016) 219–226, https://doi.org/10.1016/j.wse.2016.11.002.
[60] I. Anders, Stoffgesetz zur Beschreibung des Kriech- und Relaxationsverhaltens junger normal- und hochfester Betone: Dissertation, Vol. 73 of Karlsruher Reihe Massivbau, Baustofftechnologie, Materialprüfung, KIT Scientific Publishing, Karlsruhe, 2013.https://doi.org/10.5445/KSP/1000035242 (in German).
[61] K. Beckhaus, H. Lesemann, P. Banzhaf, C. Högl, Welches Stoffmodell für hochverformbaren Dichtwandbeton ist geeignet für die geotechnische Bemessung im Dammbau?, in: Österr. Ingenieur- und Architekten-Verein (Ed.), Tagungsbeiträge zur 10. Österreichischen Geotechniktagung, Wien, 2015, pp. 211–222 (in German).
[62] M. Hoseini, V. Bindiganavile, N. Banthia, The effect of mechanical stress on permeability of concrete: a review, Cem. Concr. Compos. 31 (4) (2009) 213–220, https://doi.org/10.1016/j.cemconcomp.2009.02.003.
[63] C. Scholz, M. Rosenberg, J. Dietrich, A. Märten, Durchlässigkeitsbestimmung von Einphasen-Dichtwandmassen - was ist theoretisch möglich und was ist praktisch notwendig?, in: M. Rosenberg (Ed.), Qualitätssicherung und Innovation, Mitteilung des Instituts für Grundbau und Bodenmechanik, Technische Universität Braunschweig, vol. 69, Braunschweig, 2002, pp. 241–263 (in German).
[64] S.Z. Cheng, S.J. Xu, R. Cong, K.L. Wang, Experimental study on mix design of plastic concrete with lower elastic modulus and higher impervious coefficient, Adv. Mater. Res. 535–537 (2012) 1936–1939, https://doi.org/10.4028/www.scientific.net/AMR.535-537.1936.
[65] Deutsches Institut für Normung, DIN 18130-1:1998-05 - Baugrund, Untersuchung von Bodenproben – Bestimmung des Wasserdurchlässigkeitsbeiwerts. Teil 1: Laborversuche (in German).
[66] B.L. Kilpatrick, S.J. Garner, Use of cement-bentonite for cutoff wall construction, in: R.H. Borden, R.D. Holtz, I. Juran (Eds.), Proceedings of the 1992 American Society of Civil Engineers; Specialty Conference on Grouting, Soil Improvement and Geosynthetics, Geotechnical Special Publication No. 30, ASME, New York, 1992, pp. 803–815.
[67] S. Hoshino, T. Yamaguchi, T. Maeda, M. Mukai, T. Tanaka, S. Nakayama, Mineralogical Changes of Cement and Bentonite Accompanied With Their Interactions, in: B.E. Burakov, A.S. Aloy (Eds.), Proceedings of the 2009 MRS Meeting – Scientific Basis for Nuclear Waste Management XXXIII, Materials Research Society, Warrendale, PA, 2009, pp. 445–452.
[68] C.K. Edvardsen, Wasserdurchlässigkeit und Selbstheilung von Trennrissen in Beton, Deutscher Ausschuß für Stahlbeton, vol. 455, Beuth, Berlin, 1996.
[69] D. Alós-Shepherd, E. Kotan, F. Dehn, State-of-the-Art-Report on Plastic Concrete for Cut-Off Walls.https://doi.org/10.5445/IR/1000085901.

Paper 2

Experimental Study into the Time Development of the Microstructural Properties of Plastic Concrete: Material Insights & Experimental Boundaries

Preprint version

Submitted to *Case Studies in Construction Materials*

Authors: **David Alós Shepherd**, Andreas Bogner, Julia Bruder, Frank Dehn

Experimental Study into the Time Development of the Microstructural Properties of Plastic Concrete: Material Insights & Experimental Boundaries

David Alós Shepherd [a,b,*], Andreas Bogner[a,b], Julia Bruder[b], Frank Dehn[a,b]

[a] *Materials Testing and Research Institute Karlsruhe (MPA Karlsruhe), Gotthard-Franz-Str. 2/3, 76131 Karlsruhe, Germany*
[b] *Institute of Concrete Structures and Building Materials (IMB), Gotthard-Franz-Str. 3, Bldg. 50.31, 76131 Karlsruhe, Germany*

Abstract

Plastic Concrete is a low-strength ($f_{cm,28d} \leq 1.0$ MPa), low-stiffness impervious concrete used for cut-off walls in earthen dams worldwide. These properties are achieved through a very high w/c-ratio (w/c ≥ 3.0) and water-binding additions (e.g. bentonite). To date, the effect of mix design, especially w/c-ratio, as well as bentonite content and type, on the long-term time development of the microstructural properties and corresponding compressive strength of Plastic Concrete has yet to be systematically studied. Furthermore, in literature, Mercury Intrusion Porosimetry (MIP) and X-Ray Diffractometry (XRD) have yet to be applied systematically to Plastic Concrete for this purpose. The present study closes this gap. Ten Plastic Concrete mixes with two bentonite-cement ratios, three types of sodium bentonite and two swelling times were produced. MIP and XRD measurements and compressive strength tests were performed at sample ages of 7 d, 28 d, 56 d, 91 d and four years. The results show that both MIP and XRD can be successfully used; however, meticulous sample preparation and data analysis must be considered. The porosimetry results show a bi-modal pore size distribution, with two age-dependent peaks at approximately 10,000–20,000 nm and 100–700 nm. The results also exhibit a clear pore refinement over time, with coarse porosity dropping from 26% to 15% over four years. In addition, the fine porosity peak is significantly refined over time and positively correlates with the significant increase in compressive strength. The XRD results show no unexpected crystalline phases over the same period. Overall, this study links MIP and corresponding compressive strength data specifically for Plastic Concrete for the first time, confirming the key role the mix design of Plastic Concrete plays on the long-term microstructural and mechanical properties and ensuring a more realistic cut-off wall design in future. In addition, the experimental boundaries for MIP testing on Plastic Concrete are set out for

*Corresponding author
Email address: `david.alosshepherd@kit.edu` (David Alós Shepherd)
URL: `www.betoninstitut.eu` (David Alós Shepherd)

Preprint submitted to Case Studies in Construction Materials *October 10, 2023*

the first time, enabling future research in this field.

Keywords: Plastic Concrete, microstructure, time development, MIP, porosity, compressive strength

Research Highlights

- Plastic Concrete microstructural properties successfully studied using MIP
- Experimental boundaries of MIP for Plastic Concrete must be considered carefully
- Porostiy refinement of Plastic Concrete over time visible with MIP
- Positive correlation between porosity and compressive strength over time
- XRD displays no unexpected crystalline phases from cement bentonite interaction

1. Introduction

1.1. Background

The most common solution for the remediation of earthen dams and levees is the design and construction of cut-off walls [1, 2]. The planned cut-off wall is generally constructed as a slurry-trench wall [3] and extended into an underlying impervious stratum [4]. The excavated trench is filled with a support fluid to stop the excavated trench from collapsing and then backfilled using the tremie method [1, 2]. As backfill materials, a wide range of possibilities exist, with growing interest in Plastic Concrete due to the materials' suitable characteristics [1].

Plastic Concrete is a low strength, low elastic modulus concrete characterised by a high deformation capacity under load, which in turn decreases both rupture probability and crack opening width, which would incur in material permeability increase [1, 2, 5]. The key component differentiating Plastic Concrete from ordinary concrete is the very high w/c-ratio (w/c $\geq$ 3.0) used and the addition of water-binding additions (e.g. bentonite) to ensure fresh concrete stability and obtain a highly ductile and impermeable material [1]. Furthermore, Plastic Concrete has a low cement content ($\leq$ 200 kg/m^3) and uses regular aggregate with a maximum grain size of 12 mm (due to the segregation risk) [1]. With this, Plastic Concrete compressive strength typically ranges between 0.5 MPa and 2.5 MPa at 28 days [1].

In general terms, bentonite encompasses any clay rock composed of smectite minerals, which in turn dominate the physical properties [6]. Smectite minerals form platelets composed of three layers, with montmorillonite being the most typical representative, consisting of two SiO_4-tetrahedron on opposite sides of an AlO_6-octahedron [7, 8]. Due to the partial, isomorphic substitution of some cations, a layer charge is generated, which is in turn counter-balanced by other cations within the interlayer space such as Ca^{2+}, Mg^{2+} or Na^{+} [8, 9, 10]. Furthermore, the weak layer charge permits the interlayer cations to adsorb and retain water molecules [9, 11]. This water adsorption phenomenon causes the clay minerals, especially montmorillonite, to significantly increase in volume, multiplying its starting volume manifold [9, 11].

Despite its indisputably beneficial material properties, Plastic Concrete has not yet been thoroughly studied. To date, the design of cut-off walls considers Plastic Concrete to be a linear-elastic material with a defined compressive strength at 28 days [12], since close to no studies provide reliable estimates of material behaviour over time [1]. The lack of a realistic constitutive law for Plastic Concrete is not least because most previous studies do not establish to which extent the mix design and microstructural properties (especially porosity) influence Plastic Concrete's mechanical and hydraulic behaviour over an extended period of time.

The most common method to investigate the pore structure of cementitious materials is mercury intrusion porosimetry (MIP), as it covers a wide range of pore sizes present in hardened cement paste and is a relatively fast measurement technique. The measurement principle is based on applying an increasing pressure to force the intrusion of the non-wetting fluid mercury into pores while measuring the intruded volume for each pressure [13]. The higher the applied pressure, the smaller the sample pores that can be intruded, as described by the Washburn equation [14]. MIP requires a unique sample preparation (e.g. direct drying) to evacuate all water in cementitious samples prior to sample testing [13]. The difficulty herein lies in removing as much free water from the pore space as possible and, at the same time avoiding damaging the pore structure by capillary hydrostatic stresses due to receding water menisci during drying and by removing chemically bound water [13]. Despite criticism on the validity and accuracy of MIP for the quantitative determination of sample porosity due to sample preparation techniques [13, 15, 16, 17, 18], MIP is still a valid measuring technique to comparatively study the pore-structure changes of cement-based materials [19, 20], e.g. with varying mix design or sample age.

Whilst some research has been carried out on the influence of clay additions on the microstructural and mechanical properties of standard concrete [21, 22, 23, 24, 25, 26] (within typical w/c-ratios ≤ 1.0), there have been few experimental investigations into the microstructural properties of very high w/c-ratio mixes (w/c ≥ 3.0) such as Plastic Concrete. Norvell et al. [23] established that the addition of clay, especially montmorillonite, clearly affects the properties of fresh and hardened standard-strength concrete, whilst clay-sized particles have a lesser effect. This is related to the clear water binding capacity of smectite minerals, and its intensity can be correlated to the cation-exchange capacity (CEC) [23]. Furthermore, as reported by Fam and Santamarina [27], the addition of cement to a bentonite slurry, with the accompanying high pH during cement hydration, favours the solubility of SiO_2 and Al_2O_3, which interact with the Ca^{2+} ions from cement hydration. This increased concentration of Ca^{2+} causes cation exchange in the interlayer of Na-bentonite, causing shrinkage of the double layer and possible flocculation [27]. SHI ET AL. [28] reported a decrease in coarse porosity (> 200 nm) over time in Plastic Concrete, as measured with MIP, which the authors ascribe to progressing cement hydration; however, the results are based on minimal data. YANG ET AL. [26] studied the effect of bentonite addition on cement mortar microstructure and established that bentonite addition causes a pore refinement due to the reduction in free water during the initial stages of hardening and subsequently densifies the paste matrix. Furthermore, various studies have suggested that bentonite particles may cause a pozzolanic reaction with the $Ca(OH)_2$ present after cement hydration [29, 30, 31]. It has also been suggested that bentonite may have a nucleation effect on cement phase hydration [26, 30] and could incur in a chemical reaction forming new crystalline phases [21]. However, despite various studies having aimed to study these effects using X-Ray diffractometry (XRD) or scanning electron microscopy (SEM), there is still no general agreement [21, 28, 31, 32, 33, 34]. This is not least due to the explicit dependency of Plastic Concrete properties on the selected mix design and the hereby chosen proportions of cement, bentonite and water, which dominate material performance, especially at high w/c-ratios [35].

1.2. Focus & Research Questions

In conclusion, the existing literature does not systematically study the effect of mix design, especially w/c-ratio, bentonite content and type, on the long-term time development of the microstructural properties and corresponding compressive strength specifically for Plastic Concrete. Furthermore, the possible interaction between bentonite and cement remains unclear, especially in high w/c-ratio mixes (w/c $\geq$ 3.0) such as Plastic Concrete. In addition, in literature, MIP has yet to be applied systematically to Plastic Concrete at varying sample ages, with current Plastic Concrete studies failing to study the microstructural properties of the material beyond the 28 day mark. The successful application of MIP on low-strength concrete ($f_{cm,28d} \leq 1.0$ MPa), such as Plastic Concrete, also remains to be proven.

This paper, therefore, aims to critically study the effect of Plastic Concrete mix design, especially bentonite content and type, on its microstructural properties. The focus hereby also lies on the long-term (up to 4 years) time development of microstructural properties of Plastic Concrete and a possible correlation to the materials' compressive strength. The study presented here is the first investigation to use MIP and XRD specifically on Plastic Concrete samples systematically and, therefore, also aims to set out the experimental boundaries of these measurement techniques for high water content, low strength concrete samples such as Plastic Concrete and enable future studies in this field. The findings should also contribute to the understanding of Plastic Concrete's microstructure development over an extended period of time (here up to 4 years) and correlate these to the corresponding compressive strength development, further enhancing the accuracy and specifications of cut-off wall design.

2. Materials and Methods

2.1. Materials

2.1.1. Cement and Bentonite

In the present study, a German OPC cement CEM I 32.5 R according to EN 197-1 [36] was used. Three activated sodium bentonites from different European deposits were used to study the corresponding effect on Plastic Concrete performance. Herefore, Bentonil CV15, Bentonil WW4 and Tixoton, all produced and provided by CLARIANT Deutschland GmbH, were used. No further SCMs were added.

The chemical composition of the source materials, as determined through X-ray fluorescence analysis (XRF), is given in Table 1. The physical characteristics of the source materials are given in Table 2. In Table 3, the mineralogical composition, as determined by XRD, as well as the cation exchange capacity (CEC), as determined through Cu-trien method according to [37, 38], of the bentonites used are shown.

Table 1: Chemical composition of the cement and bentonites used, corrected by LoI

		CaO	SiO_2	Al_2O_3	MgO	Fe_2O_3	Others	LoI
CEM I	(wt.-%)	61.8	22.2	5.2	2.9	2.4	3.6	2.7
CV15	(wt.-%)	2.3	59.8	12.0	1.9	2.2	3.4	15.7
WW4	(wt.-%)	4.0	50.6	16.7	3.1	3.8	4.1	17.8
Tixoton	(wt.-%)	3.9	49.2	17.5	2.5	5.3	5.4	18.2

Table 2: Physical characteristics of the cement and bentonite source materials used

	PSD* (µm)			density (g/cm^3)			specific surface Blaine (cm^2/g)
	$d_{10\%}$	$d_{50\%}$	$d_{90\%}$	no-dry	60 °C	105 °C	
CEM I	1.52	17.20	55.30	3.10	-	-	3 477
CV15	1.20	7.13	38.34	2.40	2.72	2.79	-
WW4	0.93	4.75	39.90	2.54	2.72	2.86	-
Tixoton	1.97	16.78	57.19	2.57	2.72	2.78	-

* Determination in water with $Na_4P_2O_7$ by laser granulometry

2.1.2. Aggregates and Water

The aggregates used were local Rhine sand and gravel from Graben-Neudorf, Germany. The maximum aggregate size was $d_{max} = 8$ mm, in line with considerations from literature [1]. The particle size distribution is shown in Table 4 and lies between control sieve curve A8 and B8 according to DIN 1045-2 [39].

Table 3: Mineralogical composition determined by XRD and CEC of the bentonites used.

	CV15	WW4	Tixoton
Quartz	X	X	X
Carbonate (mainly calcite)	X	X	X
Illite / Mica (di)			X
Montmorillonite	X	X	X
Plagioclase	X	X	X
K-feldspar		X	X
CEC (cmol$^+$/kg)	61	88	65

"X" marks where the minerals are present

Table 4: Particle size distribution of aggregates used

Sieve size	(mm)	0.125	0.25	0.5	1	2	4	8
Sieve passing	(wt.-%)	0.1	6.6	22.5	31.9	38.0	64.6	98.9

The mixing water used was tap water from Karlsruhe, previously tempered to 20 °C, and in line with the requirements according to DIN EN 1008 [40]. No admixtures were used since currently available PCE-based admixtures interact (negatively) with clay, rendering these ineffective [41].

2.2. Methods

2.2.1. Experimental Setup and Mix Design

As mentioned in section 1, the correlation between porosity and strength for Plastic Concrete has not yet been studied in detail. Traditionally, mercury intrusion porosimetry (MIP) is used to investigate the porosity of cementitious materials. Furthermore, it is common knowledge that the porosity of cementitious materials changes over time due to the hydration of cement phases. Therefore, this study investigated Plastic Concrete's porosity change over time using MIP, with tests performed at 7, 28, 56 and 91 days. In addition, some samples were also tested after four years to account for long-term material behaviour. In addition, X-Ray diffractometry (XRD) was performed at the same ages to detect any changes in mineralogical composition over time. Compressive strength tests were also performed at the aforementioned ages to correlate material porosity with Plastic Concrete strength. A timeline of the experimental tests is shown in Figure 1. Some tests were performed with a 24 h swelling process of the bentonite slurry, some at 0 h, as noted by the indexes (see also subsubsection 2.2.2).

To further understand the changes in Plastic Concrete porosity, the bentonite type, as well as the bentonite content, were varied. Three activated sodium bentonites were used (see section subsubsection 2.1.1), and the bentonite to cement ratio (b:c-ratio) was varied between 1:3 and 1:2, in line with established

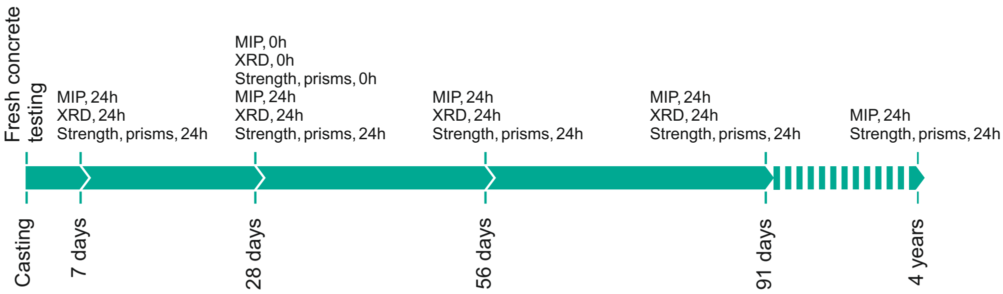

Figure 1: Timeline of the experimental testing carried out in this study, (index = swelling time)

proportions in literature [1]. Furthermore, two swelling times (24 h and 0 h) were used to investigate the possible influence of the bentonite slurry properties on Plastic Concrete porosity. An overview of the varying mix design factors and the corresponding designation of the mixes used is given in Table 5.

Table 5: Overview of the varying mix design factors and corresponding designation of the mix designs used

b:c-ratio	Swelling Time	Bentonite Type		
		Bentonil CV15	Bentonil WW4	Tixoton
1:3	24 h	C1:3-Q24	W1:3-Q24	-
	0 h	C1:3-Q0	W1:3-Q0	-
1:2	24 h	C1:2-Q24	W1:2-Q24	T1:2-Q24
	0 h	C1:2-Q0	W1:2-Q0	T1:2-Q0

It is well established in the literature that the bentonite to cement ratio (b:c-ratio), as well as the w/c-ratio, have a crucial influence on the material strength obtained for a Plastic Concrete mix [1]. A Plastic Concrete mix with 100 kg/m^3 of cement and a w/c-ratio of 4.0 was used to obtain a target compressive strength between 0.5 and 2.5 MPa at 28 days [1]. The mix designs of Plastic Concrete used in this study are shown in Table 6.

2.2.2. Concrete Batching and Fresh Concrete Testing

Based on the experimental setup developed in subsubsection 2.2.1, and following considerations in [1], the Plastic Concrete mixes in this study were produced by combining the dry components (cement and aggregate) with the (prehydrated) bentonite slurry. Since no standardised batching procedure exists for Plastic Concrete, this process is described in more detail.

The bentonite slurry was produced in a batch suspension mixer type SC-20-K from MAT Mischanlagentechnik GmbH (Immenstadt, Germany). This mixer reaches a rotational speed of approx. 3000 rpm (50 Hz) and has a nominal power of 5.5 kW. The capacity of the mixer is approximately 20 litres, with which the

Table 6: Mix design of Plastic Concrete

	Mix I (kg/m^3)	Mix II (kg/m^3)
CEM I 32.5 R	100.0	100.0
Water	400.0	400.0
Bentonite	33.3	50.0
Sand (0-2) mm	542.3	536.3
Gravel (2-8) mm	920.3	910.1
b:c-ratio	1:3	1:2

bentonite slurry could be produced in one batch. The batch suspension mixer was filled with 20 litres of water (pre-tempered to 20 °C), bentonite powder was added evenly to avoid clump formation [42] and subsequently mixed in the mixer for 6 minutes to achieve a homogeneous bentonite slurry [1, 43]. The slurry was then filled into buckets through a discharge pipe on the mixer. The 24-hour swelling process and storage required for some mix designs also took place in these buckets, which were placed in a climate-controlled room with an air temperature of 20 °C and a relative humidity of 65%.

The fresh Plastic Concrete was mixed using a Zyklos ZZ 75 EH concrete mixer from Pemat Mischtechnik GmbH (Freisbach, Germany). This mixer has a nominal power of 3.3 kW, a rotational speed of approximately 70 rpm and a capacity of 75 litres. Based on the required sample quantity, 40 to 50 litres of Plastic Concrete were mixed, requiring only one batch per mix design. The ambient temperature in the laboratory was approximately 20 °C.

First, sand, gravel and cement were placed in the mixer drum and premixed for 1 minute. After that, the bentonite slurry (with a prior 0 h or 24 h swelling time) was added to the mixer drum. The Plastic Concrete was then mixed for 5 minutes until a homogeneous concrete mix was obtained. This is in line with the most common mixing procedure for Plastic Concrete [1].

The finalised fresh concrete is then tested, with slump test according to DIN EN 12350-2 [44] and flow table test according to DIN EN 12350-5 [45] being performed immediately after mixing. Following on, fresh concrete density according to DIN EN 12350-6 [46] and air content according to DIN EN 12350-7 [47] were measured.

Thereafter part of the concrete was cast into standard $40 \times 40 \times 160$ mm^3 steel prism moulds according to DIN EN 196-1 [48] and vibrated on a shaking table with a 40 Hz frequency for 15 s. All samples were then stored in the moulds for 72 h (due to the low early age strength) at 20 °C under plastic foil and wet jute to avoid desiccation of samples following DIN EN 12390-2 [49]. The demoulded samples were then cured under water at 20 °C for the entirety of the sample storage duration.

2.2.3. Mercury Intrusion Porosimetry (MIP)

To ensure comparability of all MIP measurements, it is vital that sample preparation and testing are carried out identically [20]. Therefore, the cast and stored prisms were removed from the water bath and surface dried. After that, a centre piece of the prism was extracted with a chisel and a hammer. The obtained granulate was then oven dried at 60 °C for 24 hours achieving mass constance (see also subsubsection 3.3.3).

Mercury Intrusion Porosimetry was conducted according to DIN EN 15901-1 [50], using two different devices. The main part of the measurements was carried out in the laboratories of the Institute of Concrete Structures and Building Materials (IMB) using a Micrometrics Autopore V porosimeter. The other measurements were carried out at the Institute of Applied Geosciences (AGW) using a Micrometrics Autopore IV porosimeter. In both cases, the mercury pressure increase was applied stepwise in 142 steps. The measurement was performed in two regimes, with a low-pressure regime from approximately 0.004 MPa to 0.2 MPa and a high-pressure regime from approximately 0.2 MPa to 406 MPa. These correspond to pore entry radii of approximately 210,300 nm to 3,700 nm and approximately 3,700 nm to 1.9 nm, respectively. The contact angle was set to 141.3°, as no cement-bentonite specific contact angle is available in literature [51]. Due to different penetrometers used, the sample mass at IMB was approximately 2.5 g and at AGW approximately 1.0 g. However, it was ensured that the STEM volume (percentage of the maximum intrusion volume utilised in each station) was within the manufacturer's recommendations (between 25% and 90%) for all measurements at both institutes. For every point in time and selected mix at least two separate samples were tested.

2.2.4. X-Ray powder Diffractometery (XRD)

Similarly to the MIP testing, a part of the granulate obtained from the centre piece of the stored prisms was oven dried at 60 °C for 24 hours and then ground using a mortar. The obtained powder is then sieved through a 10 µm sieve and loaded into a preparation holder from the back side to ensure a low preferential orientation [52].

X-Ray powder Diffractometery was conducted according to DIN EN 13925 [53, 52, 54]. The XRD device used was a D8 Advance diffractometer from Bruker AXS GmbH (Karlsruhe, Germany). A CuKα-radiation was used with the angular range 2θ between 5 ° and 70 °.

2.2.5. Compressive Strength Testing

Since the Plastic Concrete studied here has a maximum aggregate size d_{max} of 8 mm, prisms could be used for compressive strength determination. Three prisms were cast following DIN EN 196-1 [48] for any given age and mix. The cast prisms were removed from the water bath curing and surface dried using a cloth towel. Thereafter the prisms were halved and subsequently used for compressive strength testing (testing cross-section 40×40 mm^2). The compressive strength was not tested according to DIN EN 196-1 [48] but according to

DIN EN 1015-11 [55] since the loading speed could be changed in line with the low strength requirements of Plastic Concrete. The loading speed was set to 0.005 kN/s for testing up to 91 days, as similarly described in DIN 4093 [56] for the testing of strengthened soil samples. For the 4-year-old samples, the loading speed was set to 0.025 kN/s to account for the expected higher strength of these samples.

3. Results

3.1. Fresh Concrete Results

As mentioned in subsubsection 2.2.2, fresh concrete tests were performed on the concrete batches produced. Figure 2 provides an overview of the fresh concrete test results.

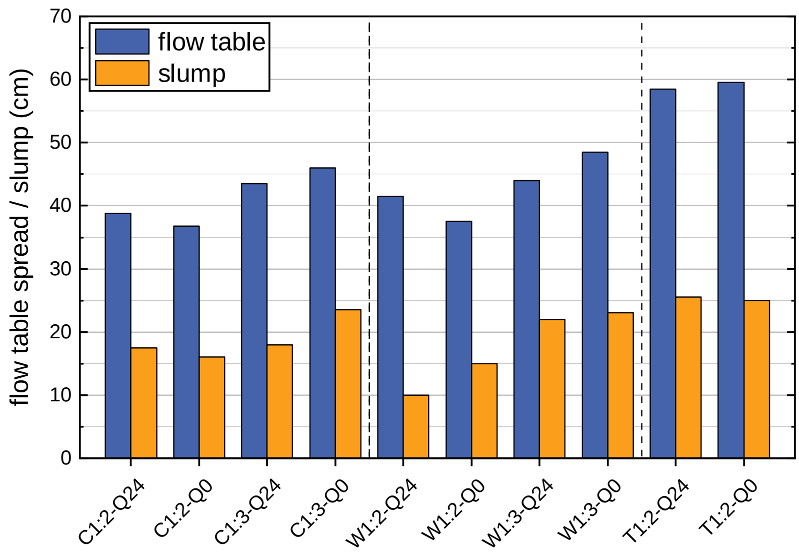

Figure 2: Fresh concrete tests results of all mixes

The graph shows that at a constant b:c-ratio, the bentonite type used clearly affects the concrete workability, with mixes produced with Tixoton displaying the highest workability overall. This is likely due to the varying water binding capacity of the different bentonites used in the presence of cement particles, also affecting the stability of the concrete mixes. The results also show that, as expected, for one constant bentonite type, a higher b:c-ratio incurs lower concrete workability due to the water-binding capacity of bentonite. The results are in agreement with other research where a similar workability loss with increasing bentonite content has been reported [23, 24, 25, 34]. On the other hand, no significant difference between the two swelling times (0 h and 24 h) is evident for identical mix compositions. Finally, the results display a good correlation between the flow table and slump test results for Plastic Concrete fresh concrete testing, as expected for concrete within this consistency range. However, further fresh concrete testing should be conducted to ensure the reproducibility of these test results. Therefore, a further study by the authors addresses this issue and analyses the correlation between both test methods [57].

3.2. Compressive Strength Results

As mentioned in subsubsection 2.2.5, the compressive strength was tested according to DIN EN 1015-11 [55]. For every point in time and selected mix, three prisms were split under tension; subsequently, six prism halves (testing cross-section 40×40 mm^2) were tested on compression. In Figure 3, the results from compressive strength testing are shown over time, whereby each point represents the mean value of six results.

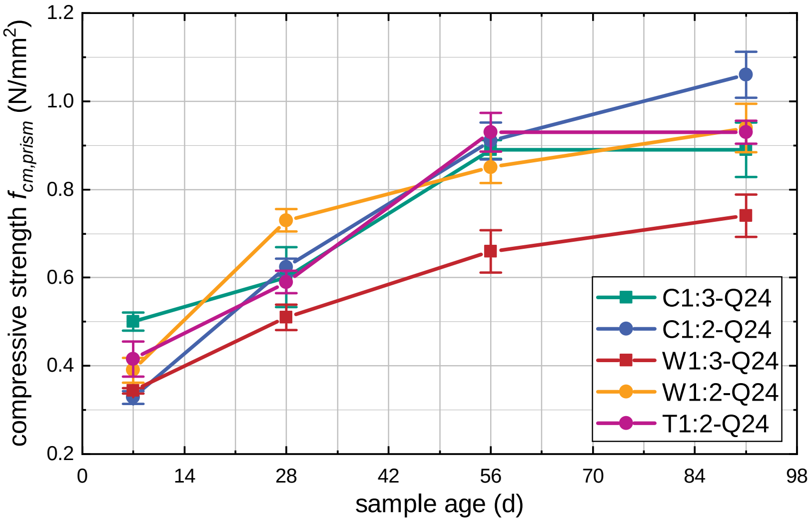

Figure 3: Mean compressive strength (and standard deviation) of six prism halves (40×40 mm^2) over time in dependence of Plastic Concrete mix design

Figure 3 shows that the compressive strength increases steadily from 7 days onwards. The compressive strength at 28 days lies between 0.50 MPa and 0.75 MPa, consistent with the results expected in literature for the chosen mix [1, 35]. In addition, the strength increase beyond 28 days is far greater than that of standard concrete, likely due to Plastic Concrete's far higher w/c-ratio. Moreover, these results are consistent with literature findings that suggest retardation of cement hydration through the addition of bentonite [27, 33, 58]. The compressive strength of Plastic Concrete samples tested here increases by approximately 50 % to 80 % between 28 days and 91 days.

Moreover, the results show a clear correlation between compressive strength and the b:c-ratio used since, for a given bentonite type, the compressive strength of mixes with a 1:2 ratio (circles) lies above that of 1:3 mixes (squares). This is consistent with the assumption that the higher bentonite content incurs in a lower effective w/c-ratio, allowing for a more dense cementitious matrix, thus increasing the compressive strength [33, 58]. The overall strength is, however, also dependent on the bentonite type used, for which literature currently does not provide any apparent cause.

Plastic Concrete's compressive strength development over time is very significant and is therefore investigated in more detail in a further study by the authors [57].

3.3. Porosity using Mercury Intrusion Porosimetry (MIP)

In Figure 4, the differential mercury intrusion porosimetry results of all tests performed on samples with 24 hours swelling time (Q24) at all ages are shown. Standard concrete results from [17] and from internal research results from the authors' institute at a sample age of 28 days with similar drying techniques are shown for comparison purposes.

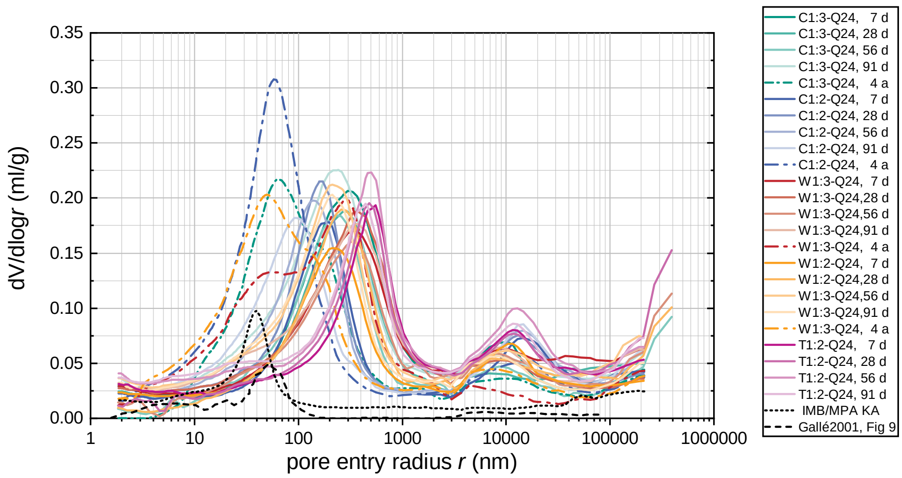

Figure 4: Overview of all differential mercury intrusion porosimetry results for Q24 at all time steps, and two standard concretes as comparison

Firstly, it can be seen that Plastic Concrete samples have a far greater overall porosity than standard concrete, shown by far higher mercury intrusion volume. In addition, Plastic Concrete samples compellingly show a bi-modal porosity distribution not present in standard concrete. However, it is common knowledge that differing sample preparation techniques and porosimeter settings may affect the results obtained from testing [17, 20, 51]. As mentioned in chapter one, no systematic MIP tests on Plastic Concrete have been reported in the literature to date. Therefore, no precedent Plastic Concrete specific settings can be used, relying on general concrete settings. Thus a more detailed investigation into the porosimeter settings and sample preparation techniques was conducted within this study. In the following, various aspects are highlighted, which detail the sample preparation, data interpretation and data validation efforts taken into account in this paper.

3.3.1. Influence of Porosimeter Settings

As mentioned in subsubsection 2.2.3, two separate mercury intrusion porosimeters were used, with both performing tests applying a low-pressure regime and a high-pressure regime.

In addition, for the reliable evaluation of sample porosity, the following changes during the measurement have to be compensated: the compressibility of mercury and oil, the change in dielectric constants and the change in sample vessel (penetrometer) volume. At the Institute of Concrete Structures and Building Materials (IMB), this was done by performing a blank measurement (without any sample) for each sample vessel with the same conditions as the samples and subtracting this baseline (hereinafter "blank measurement calibration"). However, at the Institute of Applied Geosciences (AGW), another possible procedure was used; for each measurement, the same stored formula provided by Micromeritics and based upon averages of large numbers of different blank measurements of various materials was applied (hereinafter "formula calibration"). A comparative example of mercury intrusion porosimetry test results is given in Figure 5.

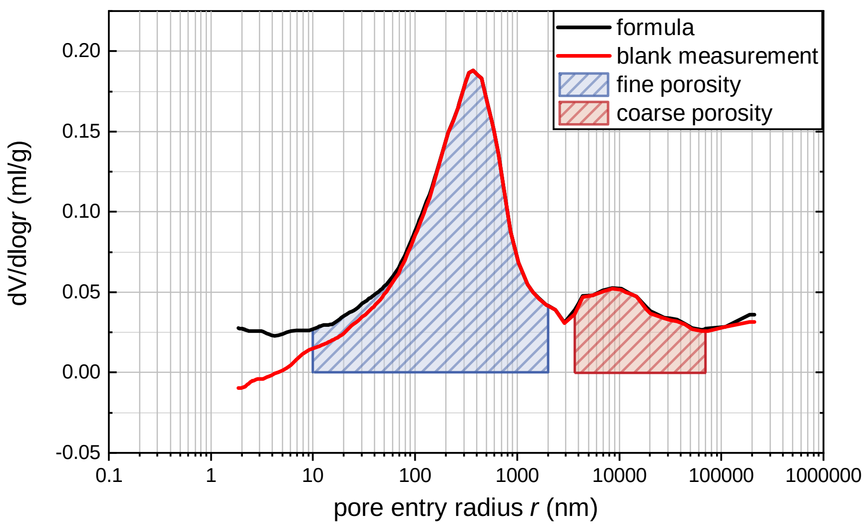

Figure 5: Exemplary comparison of a differential mercury intrusion porosimetry result using blank measurement calibration or formula calibration provided by Micrometrics

It becomes apparent from Figure 5 that the two calibrating methods provide similar results for a wide pore entry radius range between 70,000 nm and 100 nm. For very small pore entry radius, especially those smaller than 10 nm, there is a clear diverging trend between both methods. The formula calibration displays an unexpectedly high porosity below the 10 nm mark, clearly overestimating this porosity range. On the other hand, the blank measurement calibration exhibits negative porosity for a pore entry radius smaller than 4 nm, which is also technically impossible. However, since no blank measurement runs were conducted at AGW, all test results from both porosimeters were recalibrated using the formula calibration to ensure overall data comparability. To ensure correct data validation, the porosity for a pore entry radius smaller than 10 nm is therefore excluded from further analysis.

For very large pore entry radius above 70,000 nm, the porosity increases unexpectedly. This behaviour can be attributed to two effects; on the one hand, the tested Plastic Concrete samples contain aggregates which incur gaps between the individual sand grains in this order of magnitude. On the other hand, MIP can reach its experimental limitations since very large pore entry radius correspond to very low-pressure regimes, close to the atmospheric pressure, and cause unreliable measurements. To ensure correct data validation, the porosity for a pore entry radius greater than 70,000 nm is therefore excluded from further analysis.

Furthermore, all test results (as also shown in Figure 4) display a drop in mercury intrusion at a pore entry radius of approximately 3,000 nm. This radius corresponds to the radius at which the samples must be moved from the low-pressure to the high-pressure testing apparatus within the mercury intrusion porosimeter (see also subsubsection 2.2.3). Therefore, the drop in porosity should be ascribed to the test setup and not material behaviour. Thus, the porosity for a pore entry radius between 4,000 nm and 2,000 nm is excluded in further analysis.

Taking into account all aforementioned influencing parameters, it seems reasonable to only evaluate the overall porosity in two separate segments defined as coarse porosity (with a pore entry radius of 70,000 nm to 4,000 nm) and fine porosity (with a pore entry radius of 2,000 nm to 10 nm), marked in Figure 5. The fine and coarse porosity results will be discussed in section 4.

3.3.2. Influence of Multiple Measurements

To ensure the repeatability of measurements, preliminary testing was conducted. Three Plastic Concrete samples were prepared from one prism, and a triple measurement was performed. Figure 6 displays the average porosity of the three samples and the associated standard deviation.

This data shows that the standard deviation is overall relatively low and most pronounced at the fine (left) porosity peak and for large pore entry radius above 70,000 nm. Since the most pronounced standard deviation in the left peak is limited to a short pore entry radius range, its effect is minor on the cumulative porosity. The larger standard deviation for pore entry radius above 70,000 nm does furthermore not affect the following data interpretation since this porosity has already been discarded (see subsubsection 3.3.1). Due to the results mentioned above from the preliminary study, all following mercury intrusion porosimetry tests were performed solely with a double measurement.

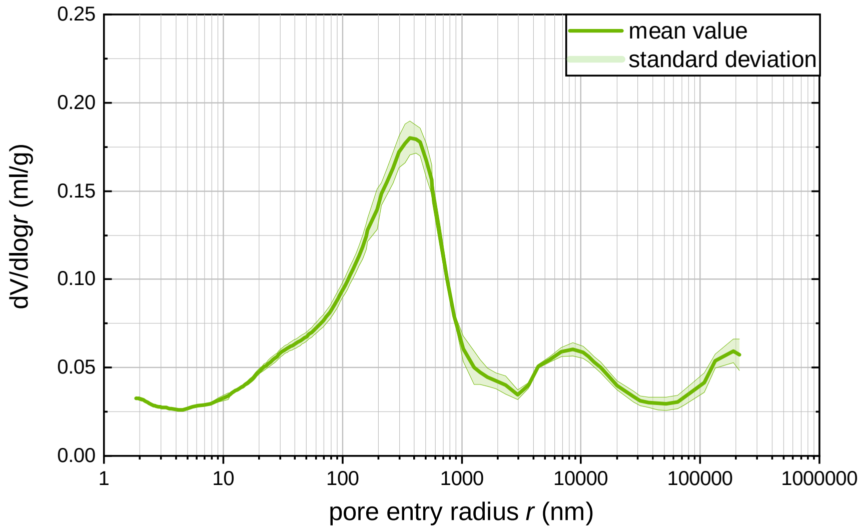

Figure 6: Differential mercury intrusion porosimetry results from a triple measurement and corresponding standard deviation

3.3.3. Influence of Drying Temperature

It is common knowledge in the literature that the drying temperature influences the measured porosity of the samples [13, 17, 18]. Especially too high drying temperatures may cause the pore structure to collapse, increasing the amount of large pores. Therefore, to establish the influence of the drying temperature specifically on Plastic Concrete samples, a preliminary study was performed with one Plastic Concrete mix by varying the drying temperature of the prepared granulate before testing. Three granulate samples were hereby oven dried at 40 ˚C, 60 ˚C and 100 ˚C for 24 hours, respectively, achieving mass constance. The samples were then tested using an identical MIP test setup. The mercury intrusion porosimetry results are shown in Figure 7.

The results indicate that, within the valid data range between 70,000 nm to 10 nm, some differences in porosity exist with different drying temperatures. As reported in [13], it could be expected that higher drying temperatures incur a shift of the left peak towards a larger radius, which cannot be observed here. Nonetheless, sample direct drying temperature of 100 ˚C exhibits a higher porosity between 10 nm and 100 nm and an apparent shift towards smaller pore entry radius, as seen in Figure 7. On the other hand, coarse porosity between 10,000 nm and 70,000 nm is slightly reduced, and an apparent shift towards larger pore entry radius is visible. It can therefore be confirmed that direct drying at 105 ˚C leads to a slight overestimation of total porosity, as described by [17]. No significant differences can be observed between direct drying at 40 ˚C or 60 ˚C. In line with these results, the drying temperature for all following experiments was therefore set to 60 ˚C to ensure sufficient, fast drying of specimens with the lowest possible structure damage.

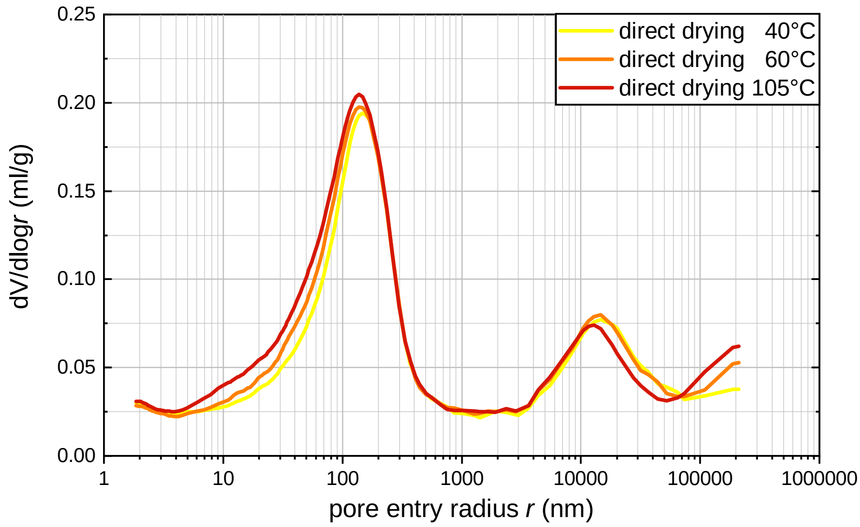

Figure 7: Differential mercury intrusion porosimetry results in dependence of sample drying temperature

3.4. X-Ray Powder Diffractometery (XRD)

As described in subsection 2.2, all Plastic Concrete samples up to the age of 91 days were also tested using X-ray powder diffractometry (XRD). In Figure 8, the X-ray diffractograms of the mixture C1:3, illustrative for all other diffractometery results, at different test ages and swelling times are compared. In addition, the diffractograms of the source materials are also shown.

It becomes apparent that the results of the Plastic Concrete mixes are almost identical, independent of test age or swelling time. The minimal differences in signal intensity are likely due to sample preparation inhomogeneities. Compared to the source materials, it also becomes clear that the more prominent peaks can be attributed to the aggregates used, especially quartz phases. Bentonite (e.g. montmorillonite) peaks are barely visible in the overall peak intensity of Plastic Concrete samples. Moreover, some bentonite peaks overlap with those of the aggregates. Some minor changes in peak intensity of portlandite ($Ca(OH)_2$) can be seen, which correspond to the typical depletion of portlandite during cement hydration [60]. These results reflect those found in the literature, where no additional, unexpected mineral phases can be observed [34, 28, 32]. Despite the possibility of the formation of non-crystalline products [34], this is rather unlikely. In addition, the results shown here display no evidence to support the theory of any pozzolanic reaction within the tested time frame (91 days), confirming some findings found in the literature [34, 32]. Whether bentonite acts as a nucleation site for calcium silicate hydrates (C-S-H) [26, 29], calcium aluminate hydrates (C-A-H) or calcium aluminate silicate hydrates (C-A-S-H) [30, 61] remains unclear. The results of other mixes (with a different bentonite type or bentonite content) display similar results (not shown here).

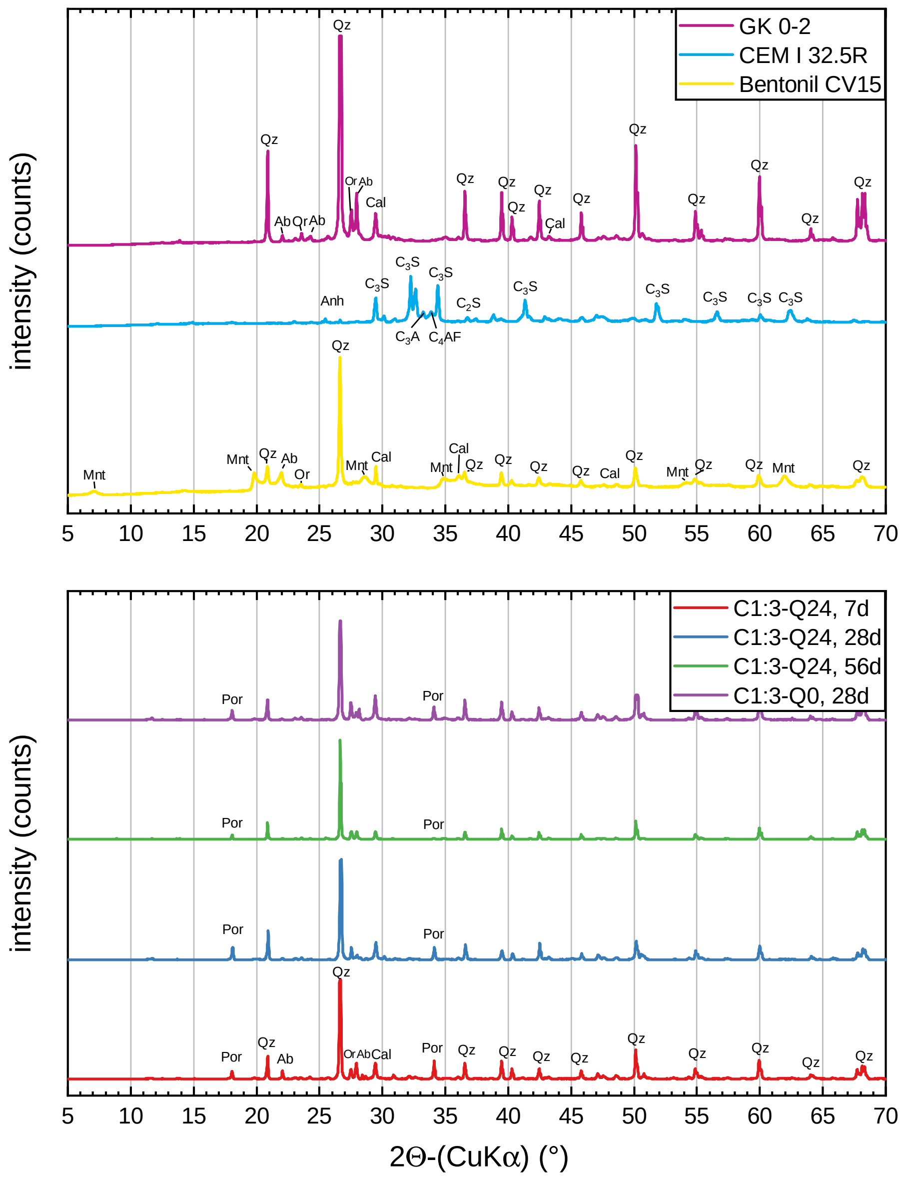

Figure 8: XRD diffractogramms of Plastic Concrete mix CV15 1:3 over time and corresponding source materials, vertically shifted. Phase identification with nomenclature according to [59]

All in all, the XRD results do not show significant changes in mineralogical composition over time, therefore suggesting that the effect of bentonite on Plastic Concrete strength and microstructural properties is probably caused by physical mechanisms, such as the water-binding capacity of bentonite affecting the effective w/c-ratio [34].

4. Discussion

4.1. Analysis of Bimodal Porosity Distribution

The results in Figure 4 show that Plastic Concrete samples display a bimodal porosity distribution. In addition, the porosity of Plastic Concrete samples is far greater, in a significantly wider porosity range, than that of standard concrete samples. Especially the displayed coarse porosity (with a pore entry radius of 70,000 nm to 4,000 nm) and its corresponding peak should be analysed in more detail.

It is possible to hypothesise that the coarse porosity peak, at approximately 10,000 nm to 20,000 nm, might occur due to shrinkage processes in the cement-bentonite paste, primarily due to the high water content in the Plastic Concrete paste matrix. To follow up on this theory, some of the aforementioned prism samples were taken out of the water bath, split and subsequently studied using light microscopic imagery with a Keyence VHX-2000 microscope at a magnification of 1200×. In addition, the same sample was then dried at 60 °C for 24 h and subsequently placed under the microscope in the identical position. The comparative microscopic imagery results of one sample are shown in Figure 9.

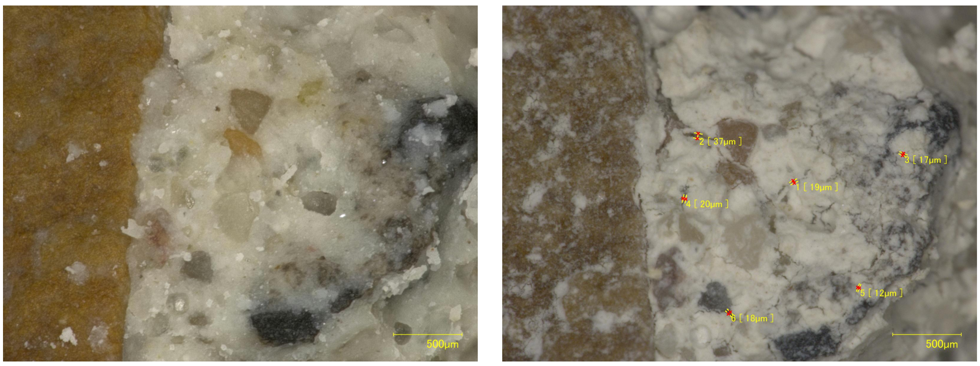

(a) Before drying (b) After 60 °C drying for 24 h

Figure 9: Light microscopic imagery of a prism sample before and after 60 °C drying for 24 hours, at a magnification of 1200×

As seen in Figure 9a, the cement-bentonite paste (white) is evenly distributed around the aggregate particles, and no cracking can be seen. After a 24 h drying process at 60 °C, it becomes apparent, as shown in Figure 9b, that the drying process incurs in microscopic, shrinkage-related cracking, concurring in cracks with varying widths ranging here from 12 µm to 37 µm. These cracks may also occur in standard cement paste (without bentonite), ascribed to irreversible shrinkage during sample drying and must be considered as part of MIP limitations during data analysis [62]. However, for Plastic Concrete, it remains unclear whether shrinkage during sample preparation may be, at least partially, reversible due to the rehydration of bentonite particles in contact with water [26, 33]. In addition, it can be expected that due to a (likely) rehydration of bentonite, the pore entry radius of Plastic Concrete samples in non-dried conditions will decrease, thus, reducing overall sample porosity and decreasing sample permeability. Furthermore, the mentioned cracks are of the same order of magnitude as the right peak of the mercury intrusion porosimetry differential curves as shown in Figure 4 and Figure 7 and would explain this secondary rise in porosity. Moreover, and as shown in subsubsection 3.3.3, the occurrence of these cracks is unavoidable independently of the selected drying temperature, due in part also to the high w/c-ratio used in Plastic Concrete. Furthermore, the vacuum applied during mercury intrusion porosimetry measurements could further increase crack width. Additionally, sample preparation through crushing can further coarsen the measured pore structure, especially in the range of large pores, further enhancing these results [20]. This undesired micro-cracking of Plastic Concrete mortar samples, however, could also reduce the "ink-bottle" effect of MIP measurements [16], enhancing the accessibility to the internal porosity and providing better comparative results for all tested mixes.

Despite the results of coarse porosity being influenced by sample preparation, the magnitude of this influence is also likely dependent on sample age due to an expected pore refinement over time, as described in the following section. This further supports the use of MIP in the present research since the study focuses on comparing similar samples with identical sample preparation.

4.2. Microstructural Change over Time

As shown in subsection 3.2 and subsection 3.3, an increase in Plastic Concrete compressive strength as well as a change in porosity can be observed. In concrete technology, a decrease in porosity has been shown to incur higher compressive strength; thus, it can be hypothesised that this behaviour also exists for Plastic Concrete. Due to the difficulties present in Plastic Concrete MIP data interpretation described in subsubsection 3.3.2 and subsubsection 3.3.1, the cumulative porosity can not be used to establish this correlation. Therefore the cumulative porosity of the two segments, coarse porosity (70,000 nm to 4,000 nm) and fine porosity (2,000 nm to 10 nm), were calculated for all Plastic Concrete mixes and ages.

In Figure 10, the porosity of the W1:2-Q24 mix, representatively for all mixes, is shown in detail. The cumulative pore volume of the two segments is hereby laid out against sample age. In addition, the percentage share of the porosity is shown within the individual columns.

It becomes apparent that the coarse porosity share decreases and the fine porosity share increases over time. This likely relates to a pore refinement due to continuous cement hydration within the samples. However, the unexpected increase in cumulative fine porosity is likely to be attributed to data calculation

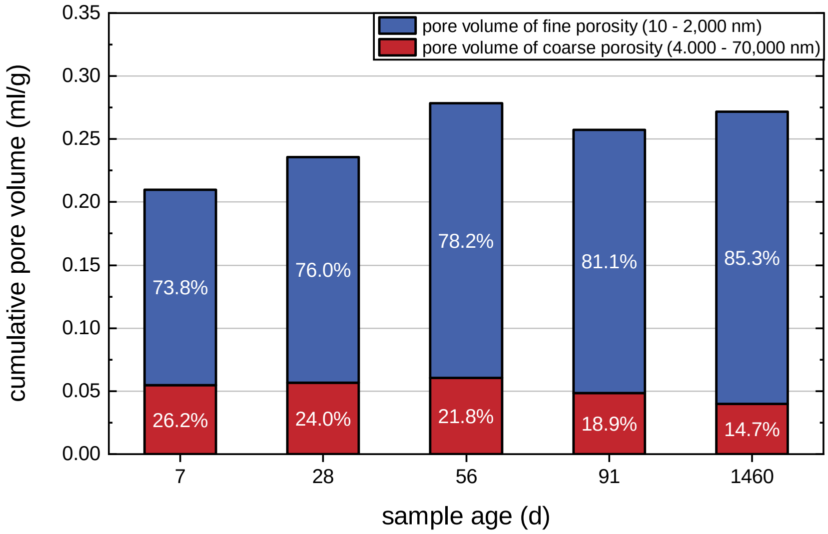

Figure 10: Cumulative porosity and percentage share of porosity of the W1:2-Q24 mix over time

errors since the porosity between 4,000 nm and 2,000 nm is not considered for calculation. Due to pore refinement over time, some porosity in this middle segment shifts towards finer porosity and is then recorded within the fine porosity segment, thus increasing overall porosity. Furthermore, with increasing sample age, the total coarse porosity (4,000 nm to 70,000 nm) decreases, as also shown by [28]. The decreasing porosity is likely due to an increase in C-S-H and concurrent pore refinement over a long period of time, thus increasing sample strength at a microscopic scale and hereby reducing the influence of sample preparation (see subsection 4.1). The significant increase in fine porosity between 91 days and 4 years further confirms the very slow cement hydration rate in Plastic Concrete, concomitant to the high w/c-ratio and the use of bentonite [35, 58].

The representatively shown effects on porosity over time of mix W1:2-Q24 (as demonstrated in Figure 10) also apply to all other mixes. In Figure 11, an overview of the differential mercury intrusion porosimetry results of all mixes over time in dependence of mix design is given.

As can be seen in Figure 11 the pore entry radius of the left peak shifts slightly towards smaller pores with increasing sample age in the first 91 days with all tested mixes. In addition, as mentioned previously, the coarse porosity (described by the right peak) also decreases for all samples over time, thus confirming the results shown in Figure 10. Furthermore, no systematic correlation between the bentonite content and the overall porosity can be seen, confirming results from previous studies [28]. The samples tested at 28 days with different swelling times (0h/24h) also do not show significant differences. However, comparing the results of mixes of identical bentonite type but differing bentonite content (e.g. C1:2 vs. C1:3), it becomes apparent that the pore entry radius of

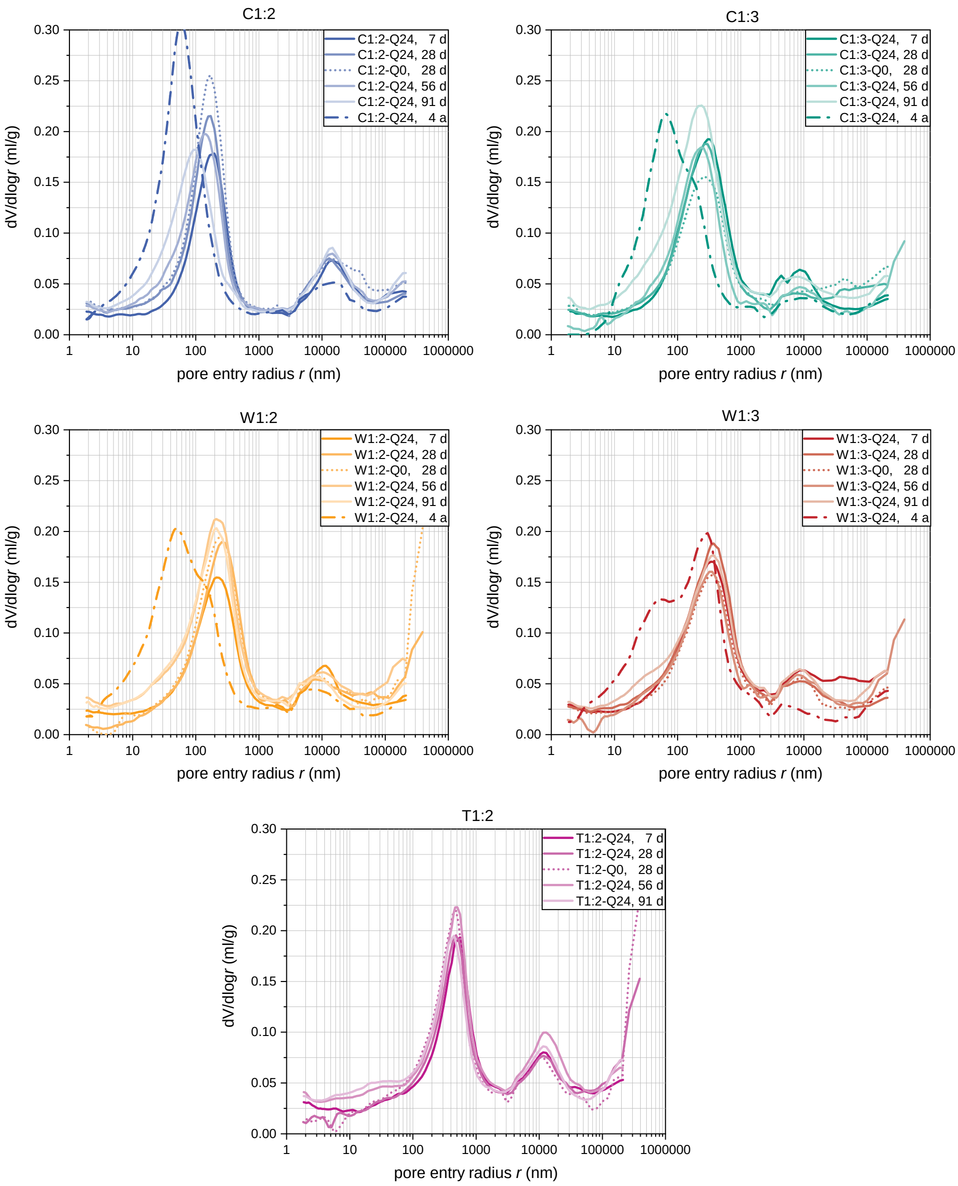

Figure 11: Differential mercury intrusion porosimetry results in dependence of mix design and sample age

the left peak decreases with increasing bentonite content, suggesting a slight pore refinement due to a reduced w/c-ratio. The results in Figure 11 also show that there is a significant change in both fine porosity (left peak) and coarse porosity (right peak) between 91 days and 4 years, further confirming the pore refinement over time. In addition, this effect is more predominant with mixes with a higher bentonite content (b:c-ratio = 1:2) ascribed to the lower effective w/c-ratio.

Finally, the literature often suggests using two parameters to characterise MIP results: threshold pore entry radius and critical pore entry radius [20, 51]. However, the bimodal porosity distribution in this study's results makes it impossible to determine these parameters since the cumulative intrusion curve displays more than one inflexion point. Alternatively, a simple approach can be used where the pore diameter at which the cumulative porosity equals 5% of the total intrudable porosity [20]. However, for the present results, the 5% will always lie within the coarse porosity peak and can, therefore, not be used to describe the overall sample porosity.

4.3. Porosity and Compressive Strength Correlation

Based on the proven pore refinement of Plastic Concrete samples over time, it can be expected that this positively correlates with the increasing compressive strength. To further analyse this correlation, the pore entry radius at the maximum of the fine porosity peak in the differential MIP results (shown in Figure 4) was extracted and plotted against the compressive strength of the same sample. The results are shown in Figure 12.

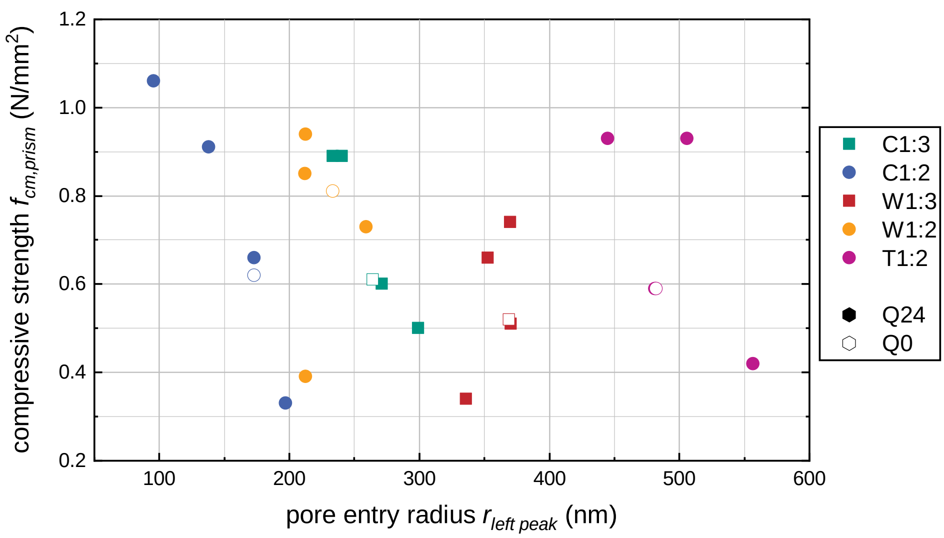

Figure 12: Compressive strength of Plastic Concrete samples over corresponding pore entry radius of the left peak, up to 91 days

From this graph, it can be seen that no direct correlation between an absolute compressive strength value and pore entry radius of the left peak exists. However, the pore entry radius range is clearly associated with a selected mix design, e.g. the pore entry radius of the left peak for C1:2 mixes lie between 95 nm and 197 nm, while those of T1:2 lie between a different range of 444 nm and 556 nm. In addition, for one given bentonite type, the pore entry radius of the left peak decreases with increasing bentonite content, further confirming the reduction in the effective w/c-ratio. The swelling time has a minor effect on pore entry radius or compressive strength (solid vs. open symbols). The pore entry radius of the left peak can therefore be used to identify a specific mix used. Moreover, for a given mix, the pore entry radius mostly decreases with increasing compressive strength, and thus increasing time, further confirming a porosity refinement of the samples and a positive correlation with its compressive strength. These results can further be verified with the results of the 4-year-old samples (not shown here, see Figure 4). Furthermore, the pore entry radius of the left peak correlates closer to the porosity refinement than the cumulative porosity since it is less affected by the standard deviation of sample testing (see subsubsection 3.3.2) as well as the shrinkage cracking (see subsection 4.1).

Overall these results indicate that pore refinement over time also exists for Plastic Concrete, correlating to an increase in compressive strength independent of the selected mix design.

5. Conclusions

5.1. Summary

The present study aimed to determine the effect of Plastic Concrete mix design, especially bentonite content and type, on the long-term development of Plastic Concrete's microstructural properties and corresponding compressive strength. In addition, this paper was designed to systemically use mercury intrusion porosimetry (MIP) and X-Ray diffractometry (XRD) for the first time on Plastic Concrete samples, hereby setting out the experimental boundaries of these measurement techniques for high water content, low-strength concrete mixes such as Plastic Concrete.

Firstly, the results show that the fresh Plastic Concrete properties are clearly dependent on the bentonite type and b:c-ratio used. These parameters also influence the achievable compressive strength. The Plastic Concrete compressive strength increase over time, especially beyond the 28-day mark, is significantly higher than that of standard concrete.

The results of this study also show that MIP, despite the technique's inherent limitations, could successfully be applied for the first time to systematically study the pore-structure changes of Plastic Concrete with varying mix designs and sample ages. The porosimetry results of Plastic Concrete samples show a bi-modal pore size distribution with two singular, age-dependant peaks, which have not been reported in the literature to date. In addition, the experimental boundaries of MIP testing, specifically for Plastic Concrete samples, are set out for the first time, with this study highlighting the key aspects to be considered regarding sample preparation (e.g drying temperature), porosimeter setup (e.g. calibration) and data analysis (e.g. measurement standard deviation). Furthermore, the obtained data shows a clear pore refinement over time, with the coarse porosity share dropping significantly over four years. In addition, this pore refinement positively correlates with a significant increase in compressive strength. In addition, the fine porosity peak clearly relates to the bentonite type and b:c-ratio used. XRD was also successfully performed on Plastic Concrete samples, confirming no unexpected crystalline phases form over 91 days. Overall the mix design, especially bentonite content and type, significantly influences the microstructural properties and compressive strength results and are clearly dependent on sample age, with significant material property changes far beyond the 28 day mark. Finally, the results presented here provide a solid basis for further research using MIP on high water content, low strength concrete samples such as Plastic Concrete.

All in all, the present study is the first to comprehensively investigate the effect of mix design, especially bentonite content and type, on the microstructural properties and compressive strength of Plastic Concrete. In addition, it has provided more profound insights into the time development of these properties over an extended study period of 4 years. Furthermore, these findings are of significant value for Plastic Concrete cut-off wall design since a more realistic and accurate time dependant design of Plastic Concrete cut-off wall design will be possible in future.

5.2. Future Research

Future research should be carried out to explore the effect of different sample preparation techniques on the measured porosity of Plastic Concrete using mercury intrusion porosimetry (MIP). It may hereby be expedient to use other sample preparation techniques such as solvent-exchange, vacuum-drying or freeze-drying [17, 18] compared to the direct drying method established in this study. However, whether these alternative techniques also work for high water content cementitious systems such as Plastic Concrete remains unclear. Other microstructural analysis techniques such as backscatter mode SEM [15] or Small-Angle X-Ray Scattering (SAXS) [13] may also provide further porosity measurements for Plastic Concrete samples. However, these are also technically more challenging and not available at all research institutions. Also, methods like isothermal calorimetry, Nuclear Magnetic Resonance (NMR), Thermogravimetric Analysis (TGA) and SAXS could provide new insights into whether bentonite has a nucleation effect on C-S-H crystallisation in Plastic Concrete [63]. In addition, XRD tests on Plastic Concrete with paste samples (without aggregate), as described in [58], could further confirm the assumption that no new mineral phases are developing during the hydration of Plastic Concrete. Finally, in-situ-XRD, as described by [64], could be beneficial to establish the early reaction mechanisms of Plastic Concrete more clearly since no sample drying and preparation is required. Based on the results of this study that similar compressive strengths can be achieved exhibiting different fine porosity (with different b:c-ratios and bentonite types), further research should be carried out to systematically study which fine porosity is most suitable for typical applications such as cut-off walls (e.g. which mix provides the lowest overall material permeability).

CRediT authorship contribution statement

David Alós Shepherd: Conceptualization, Methodology, Investigation, Validation, Formal Analysis, Writing - Original Draft, Writing - Review & Editing, Visualization, Project administration
Andreas Bogner: Validation, Writing - Review & Editing
Julia Bruder: Investigation, Visualization
Frank Dehn: Resources, Funding acquisition, Writing - Review & Editing

Declaration of competing interest

All authors of the paper declare no conflict of interest.

Acknowledgements

The authors of this article would like to thank Clariant AG for providing the bentonite materials and MAT Mischanlagentechnik GmbH for providing the bentonite mixer. In addition, the authors would like to thank the Institute of Applied Geosciences (AGW) at KIT for the support during the MIP testing campaign. Furthermore, the authors thank Prof. Katja Emmerich and Dr. Eleanor Bakker (CMM Karlsruhe/KIT) for their help in CEC testing and Astrid Hirsch (IMB/MPA Karlsruhe) for her support in XRD phase identification.

Funding

This research received no specific grant from funding agencies in the public, commercial, or not-for-profit sectors.

The authors acknowledge support from the KIT-Publication Fund of the Karlsruhe Institute of Technology (KIT) for the settlement of the Article Publishing Charge.

References

[1] D. Alós Shepherd, E. Kotan, F. Dehn, Plastic concrete for cut-off walls: A review, Construction and Building Materials 255 (2020) 119248. doi:10.1016/j.conbuildmat.2020.119248.

[2] D. A. Bruce (Ed.), Specialty construction techniques for dam and levee remediation, CRC Press, Boca Raton, 2013.

[3] P. P. Xanthakos, Slurry walls, McGraw-Hill, New York, 1979.

[4] U.S. Bureau of Reclamation, Design Standards No. 13: Embankment Dam, Chapter 16: Cutoff Walls, Revision 14 (2014/07).
URL https://www.usbr.gov/tsc/techreferences/designstandards-datacollectionguides/designstandards.html

[5] M. Ghazavi, Z. Safarzadeh, H. Hashemolhoseini, Response Of Plastic Concrete Cut-Off Walls In Earth Dams To Seismic Loading Using Finite Element Methods, in: Canadian Association for Earthquake Engineering (Ed.), Proceedings of the 13th World Conference on Earthquake Engineering, Vancouver, 2004.

[6] R. E. Grim, N. Güven, Bentonites: Geology, mineralogy, properties and uses, Vol. 24 of Developments in sedimentology, Elsevier, Amsterdam, 1978.

[7] P. von Soos, J. Engel, Eigenschaften von Boden und Fels – ihre Ermittlung im Labor, in: K. J. Witt (Ed.), Grundbau-Taschenbuch, Teil 1: Geotechnische Grundlagen, Ernst & Sohn, Berlin, 2008, pp. 123–218.

[8] S. Praetorius, B. Schößer, Bentonithandbuch: Ringspaltschmierung für den Rohrvortrieb, Bauingenieur-Praxis, Ernst & Sohn, Berlin, 2016.

[9] D. Koch, Eigenschaften und Einsatzmöglichkeiten von Bentonit/Zement-Mischungen im Speziealtiefbau, in: K. Eichler (Ed.), Spezialtiefbau, Kontakt & Studium, Expert Verlag, Renningen, 2015, pp. 170–189.

[10] K. Jasmund, G. Lagaly (Eds.), Tonminerale und Tone: Struktur, Eigenschaften, Anwendungen und Einsatz in Industrie und Umwelt, Steinkopff, Darmstadt, 1993. doi:10.1007/978-3-642-72488-6.

[11] F. Bergaya, G. Lagaly (Eds.), Handbook of Clay Science, Part A: Fundamentals, 2nd Edition, Developments in clay science, Elsevier, Burlington, 2013.

[12] K. Beckhaus, J. Kayser, F. Kleist, J. Quarg-Vonscheidt, D. Alós Shepherd, Design concept for sustainable cut-off walls made of highly deformable filling materials, in: R. Boes, P. Droz, R. Leroy (Eds.), Proceedings of the 12th ICOLD European Club Symposium 2023 (ECS 2023, Interlaken, Switzerland, 5-8 September 2023), CRC Press, Milton, 2023, pp. 641–650. doi:10.1201/9781003440420-72.

[13] A. Bogner, J. Schatz, F. Dehn, H. S. Müller, Influence of Drying on the Microstructure of Hardened Cement Paste: A Mercury Intrusion Porosimetry, Nitrogen Sorption and SAXS Study, Journal of Advanced Concrete Technology 18 (3) (2020) 83–94. doi:10.3151/jact.18.83.

[14] E. W. Washburn, Note on a Method of Determining the Distribution of Pore Sizes in a Porous Material, Proceedings of the National Academy of Sciences of the United States of America 7 (4) (1921) 115–116.

[15] S. Diamond, A discussion of the paper "Effect of drying on cement-based materials pore structure as identified by mercury porosimetry—a comparative study between oven-, vacuum-, and freeze-drying" by C. Gallé, Cement and Concrete Research 33 (1) (2003) 169–170. doi:10.1016/S0008-8846(02)00940-7.

[16] S. Diamond, Mercury porosimetry: An inappropriate method for the measurement of pore size distributions in cement-based materials, Cement and Concrete Research 30 (10) (2000) 1517–1525. doi:10.1016/S0008-8846(00)00370-7.

[17] C. Gallé, Effect of drying on cement-based materials pore structure as identified by mercury intrusion porosimetry, Cement and Concrete Research 31 (10) (2001) 1467–1477. doi:10.1016/S0008-8846(01)00594-4.

[18] F. Winnefeld, A. Schöler, B. Lothenbach, Sample preparation (Chapter 1), in: K. Scrivener, R. Snellings, B. Lothenbach (Eds.), A practical guide to microstructural analysis of cementitious materials, CRC Press, Boca Raton, Florida, 2016.

[19] C. Gallé, Reply to the discussion by S. Diamond of the paper "Effect of drying on cement-based materials pore structure as identified by mercury intrusion porosimetry: a comparative study between oven-, vacuum- and freeze-drying", Cement and Concrete Research 33 (1) (2003) 171–172. doi:10.1016/S0008-8846(02)00941-9.

[20] H. Ma, Mercury intrusion porosimetry in concrete technology: tips in measurement, pore structure parameter acquisition and application, Journal of Porous Materials 21 (2) (2014) 207–215. doi:10.1007/s10934-013-9765-4.

[21] C. Andrade, A. Martínez-Serrano, M. Á. Sanjuán, J. A. Tenorio Ríos, Reduced Carbonation, Sulfate and Chloride Ingress Due to the Substitution of Cement by 10% Non-Precalcined Bentonite, Materials 14 (5) (2021). doi:10.3390/ma14051300.

[22] M. L. Nehdi, Clay in cement-based materials: Critical overview of state-of-the-art, Construction and Building Materials 51 (2014) 372–382. doi:10.1016/j.conbuildmat.2013.10.059.

[23] J. K. Norvell, J. G. Stewart, M. C. Juenger, D. W. Fowler, Influence of Clays and Clay-Sized Particles on Concrete Performance, Journal of Materials in Civil Engineering 19 (12) (2007) 1053–1059. doi:10.1061/(ASCE)0899-1561(2007)19:12(1053).

[24] F. Solomon, S. O. Ekolu, Strength behaviour of clay-cement concrete and quality implications for low-cost construction materials, in: M. G. Alexander, H.-D. Beushausen, F. Dehn, P. Moyo (Eds.), Concrete repair, rehabilitation and retrofitting III, Proceedings of the 3rd International Conference on Concrete Repair, Rehabilitation and Retrofitting (ICCRRR), Cape Town, South Africa, September 3rd - 5th 2012, CRC Press, Boca Raton, FL, 2012, pp. 1420–1425.

[25] J. Ahmad, K. J. Kontoleon, M. Z. Al-Mulali, S. Shaik, M. Hechmi El Ouni, M. A. El-Shorbagy, Partial Substitution of Binding Material by Bentonite Clay (BC) in Concrete: A Review, Buildings 12 (5) (2022) 634. doi:10.3390/buildings12050634.

[26] H. Yang, D. Long, L. Zhenyu, H. Yuanjin, Y. Tao, H. Xin, W. Jie, L. Zhongyuan, L. Shuzhen, Effects of bentonite on pore structure and permeability of cement mortar, Construction and Building Materials 224 (2019) 276–283. doi:10.1016/j.conbuildmat.2019.07.073.

[27] M. A. Fam, J. C. Santamarina, Study of Clay-Cement Slurries with Mechanical and Electromagnetic Waves, Journal of Geotechnical Engineering 122 (5) (1996) 365–373. doi:10.1061/(ASCE)0733-9410(1996)122:5(365).

[28] Y. Shi, X. Chen, J. Li, X. Li, Z. Peng, Micro–macro properties of plastic concrete anti-seepage wall materials mixed with low-liquid limit clay, Advances in Mechanical Engineering 11 (5) (2019) 168781401984973. doi:10.1177/1687814019849736.

[29] T.-P. Chang, J.-Y. Shih, K.-M. Yang, T.-C. Hsiao, Material properties of portland cement paste with nano-montmorillonite, Journal of Materials Science 42 (17) (2007) 7478–7487. doi:10.1007/s10853-006-1462-0.

[30] X.-J. Niu, Q.-B. Li, Y. Hu, Y.-S. Tan, C.-F. Liu, Properties of cement-based materials incorporating nano-clay and calcined nano-clay: A review, Construction and Building Materials 284 (2021) 122820. doi:10.1016/j.conbuildmat.2021.122820.

[31] B. Tang, W. Cui, B.-z. Zhang, Z.-a. Jiang, The macroscopic mechanical characteristics and microscopic evolution mechanism of plastic concrete, Construction and Building Materials 391 (2023) 131898. doi:10.1016/j.conbuildmat.2023.131898.

[32] L. Flessati, G. Della Vecchia, G. Musso, Mechanical Behavior and Constitutive Modeling of Cement–Bentonite Mixtures for Cutoff Walls, Journal of Materials in Civil Engineering 33 (3) (2021). doi:10.1061/(ASCE)MT.1943-5533.0003584.

[33] B. Cao, J. Chen, A. Al-Tabbaa, Crack-resistant cement–bentonite cut-off wall materials incorporating superabsorbent polymers, Canadian Geotechnical Journal 58 (6) (2021) 800–810. doi:10.1139/cgj-2020-0181.

[34] V. A. Fernandes, P. Purnell, G. T. Still, T. H. Thomas, The effect of clay content in sands used for cementitious materials in developing countries, Cement and Concrete Research 37 (5) (2007) 751–758. doi:10.1016/j.cemconres.2006.10.016.

[35] C.-S. Barbu, A.-D. Sabau, D.-M. Manoli, M.-S. Serbulea, Water/Cement/Bentonite Ratio Selection Method for Artificial Groundwater Barriers Made of Cutoff Walls, Water 14 (3) (2022) 376. doi:10.3390/w14030376.

[36] Comité Européen de Normalisation, EN 197-1:2011-11 - Cement - Part 1: Composition, specifications and conformity criteria for common cements (German version).

[37] L. P. Meier, G. Kahr, Determination of the cation exchange capacity (CEC) of clay minerals using the complexes of Copper (II) ion with Triethylenetetramine and Tetraethylenepentamine, Clays and Clay Minerals 47 (3) (1999) 386–388.

[38] A. Steudel, Selection strategy and modification of layer silicates for technical applications, Dissertation, Karlsruhe Institute of Technology (2009). doi:10.5445/KSP/1000010748.

[39] Deutsches Institut für Normung, DIN 1045-2:2008-08 - Tragwerke aus Beton, Stahlbeton und Spannbeton - Teil 2: Beton - Festlegung, Eigenschaften, Herstellung und Konformität - Anwendungsregeln zu DIN EN 206-1 (in German).

[40] Comité Européen de Normalisation, EN 1008:2002-10 - Mixing water for concrete - Specification for sampling, testing and assessing the suitability of water, including water recovered from processes in the concrete industry, as mixing water for concrete (German version).

[41] L. Lei, M. Palacios, J. Plank, A. A. Jeknavorian, Interaction between polycarboxylate superplasticizers and non-calcined clays and calcined clays: A review, Cement and Concrete Research 154 (2022) 106717. doi:10.1016/j.cemconres.2022.106717.

[42] M. A. Fadaie, M. Nekooei, P. Javadi, Effect of Dry and Saturated Bentonite on Plastic Concrete, KSCE Journal of Civil Engineering 23 (8) (2019) 3431–3442. doi:10.1007/s12205-019-0835-2.

[43] S. Adjei, S. Elkatatny, A. Al-Majed, Effect of Bentonite Prehydration Time on the Stability of Lightweight Oil-Well Cement System, Geofluids 2021 (2021) 1–8. doi:10.1155/2021/9957159.

[44] Comité Européen de Normalisation, EN 12350-2:2019-09 - Testing fresh concrete - Part 2: Slump test (German version).

[45] Comité Européen de Normalisation, EN 12350-5:2019-09 - Testing fresh concrete - Part 5: Flow table test (German version).

[46] Comité Européen de Normalisation, EN 12350-6:2019-09 - Testing fresh concrete - Part 6: Density (German version).

[47] Comité Européen de Normalisation, EN 12350-7:2019:09 - Testing fresh concrete - Part 7: Air content - Pressure methods (German version).

[48] Comité Européen de Normalisation, EN 196-1:2016-11 - Methods of testing cement - Part 1: Determination of strength (German version).

[49] Comité Européen de Normalisation, EN 12390-2:2019-10 - Testing hardened concrete - Part 2: Making and curing specimens for strength tests (German version).

[50] Comité Européen de Normalisation, EN 15901-1:2016 - Evaluation of pore size distribution and porosity of solid materials by mercury porosimetry and gas adsorption - Part 1: Mercury porosimetry (German Version).

[51] E. Berodier, J. Bizzozero, A. C. A. Muller, Mercury intrusion porosimetry (Chapter 9), in: K. Scrivener, R. Snellings, B. Lothenbach (Eds.), A practical guide to microstructural analysis of cementitious materials, CRC Press, Boca Raton, Florida, 2016.

[52] Comité Européen de Normalisation, EN 13925-2:2003-07 - Non-destructive testing - X-ray diffraction from polycristalline and amorphous material - Part 2: Procedures (German Version).

[53] Comité Européen de Normalisation, EN 13925-1:2003-07 - Non-destructive testing - X-ray diffraction from polycristalline and amorphous material - Part 1: General principles (German Version).

[54] Comité Européen de Normalisation, EN 13925-3:2005-07 - Non-destructive testing - X-ray diffraction from polycristalline and amorphous material - Part 3: Instruments (German Version).

[55] Comité Européen de Normalisation, EN 1015-11:2020-01 - Methods of test for mortar for masonry - Part 11: Determination of flexural and compressive strength of hardened mortar (German Version).

[56] Deutsches Institut für Normung, DIN 4093:2015-11 - Bemessung von verfestigten Bodenkörpern - Hergestellt mit Düsenstrahl-, Deep-Mixing- oder Injektions-Verfahren (in German).

[57] D. Alós Shepherd, F. Dehn, Experimental Study into the Mechanical Properties of Plastic Concrete: Compressive Strength Development over Time, Tensile Strength and Elastic Modulus, Case Studies in Construction Materials 19 (2023) e02521. `doi:10.1016/j.cscm.2023.e02521`.

[58] H. Zhao, Y. Ma, J. Zhang, Z. Hu, H. Li, Y. Wang, J. Liu, K. Wang, Effect of clay content on shrinkage of cementitious materials, Construction and Building Materials 322 (2022) 125959. `doi:10.1016/j.conbuildmat.2021.125959`.

[59] L. N. Warr, IMA–CNMNC approved mineral symbols, Mineralogical Magazine 85 (3) (2021) 291–320. `doi:10.1180/mgm.2021.43`.

[60] R. Snellings, X-ray powder diffraction applied to cement (Chapter 4), in: K. Scrivener, R. Snellings, B. Lothenbach (Eds.), A practical guide to microstructural analysis of cementitious materials, CRC Press, Boca Raton, Florida, 2016.

[61] R. Fernández, A. Isabel Ruiz, J. Cuevas, Formation of C-A-S-H phases from the interaction between concrete or cement and bentonite, Clay Minerals 51 (2) (2016) 223–235. `doi:10.1180/claymin.2016.051.2.09`.

[62] S. Chatterji, A discussion of the paper "Mercury porosimetry—an inappropriate method for the measurement of pore size distributions in cement-based materials" by S. Diamond, Cement and Concrete Research 31 (11) (2001) 1657–1658. doi:10.1016/S0008-8846(01)00618-4.

[63] A. Bogner, J. Link, M. Baum, M. Mahlbacher, T. Gil-Diaz, J. Lützenkirchen, T. Sowoidnich, F. Heberling, T. Schäfer, H.-M. Ludwig, F. Dehn, H. S. Müller, M. Haist, Early hydration and microstructure formation of Portland cement paste studied by oscillation rheology, isothermal calorimetry, 1H NMR relaxometry, conductance and SAXS, Cement and Concrete Research 130 (2020) 105977. doi:10.1016/j.cemconres.2020.105977.

[64] P. R. de Matos, J. S. Andrade Neto, D. Jansen, A. G. de La Torre, A. P. Kirchheim, C. E. Campos, In-situ laboratory X-ray diffraction applied to assess cement hydration, Cement and Concrete Research 162 (2022) 106988. doi:10.1016/j.cemconres.2022.106988.

Paper 3

Experimental Study into the Mechanical Properties of Plastic Concrete: Compressive Strength Development over Time, Tensile Strength and Elastic Modulus

Publisher's version

Published in *Case Studies in Construction Materials*

Volume 19, 2023, pp. e02521

DOI: 10.1016/j.cscm.2023.e02521

Authors: **David Alós Shepherd**, Frank Dehn

Case Studies in Construction Materials 19 (2023) e02521

Contents lists available at ScienceDirect

Case Studies in Construction Materials

journal homepage: www.elsevier.com/locate/cscm

Experimental Study into the Mechanical Properties of Plastic Concrete: Compressive Strength Development over Time, Tensile Strength and Elastic Modulus

David Alós Shepherd [a,b,*,1], Frank Dehn [a,b]

[a] *Materials Testing and Research Institute Karlsruhe (MPA Karlsruhe), Gotthard-Franz-Str. 2/3, 76131 Karlsruhe, Germany*
[b] *Institute of Concrete Structures and Building Materials (IMB), Gotthard-Franz-Str. 3, Bldg. 50.31, 76131 Karlsruhe, Germany*

A R T I C L E I N F O

Keywords:
Plastic concrete
Compressive strength
Elastic modulus
fib MC 2020
Splitting tensile strength
Time development

A B S T R A C T

Plastic Concrete is a low-strength ($f_{cm,28d} \leq$ 1.0 MPa), low-stiffness, impervious concrete used for cut-off wall construction in earthen dams. To date, there has been no systematic study on the effect of mix design on the long-term time development of the mechanical properties (compressive strength, tensile strength, and elastic modulus) of Plastic Concrete. Therefore currently no Plastic Concrete specific constitutive law for cut-off wall design exists. The present study closes this gap. Ten Plastic Concrete mixes with two bentonite-cement ratios and three types of sodium bentonite were produced. Fresh concrete workability tests were performed for all mixes. Compressive strength tests were performed at ages 28 d, 56 d, 91 d and four years. Splitting tensile strength and elastic modulus tests were performed at 28 days. The workability results show a good linear correlation between slump and flow table tests. Plastic Concrete's compressive strength development over time is notably slower than that of ordinary concrete, and a new time development model following *fib* MC 2020 is established using a fitted s_C coefficient. The splitting tensile strength shows an overall good, linear correlation with compressive strength, with an approximate ratio of 0.135. Furthermore, the elastic modulus $E_{C,S}$ according to EN 12390-13 concrete tests show significantly higher elastic modulus than the available data, and a model approximation for the elastic modulus $E_{C,S}$ as a function of compressive strength is also provided. Overall, this study provides the first Plastic Concrete specific mechanical property models, confirming the critical role mix design plays on Plastic Concrete's short and long-term mechanical properties. Thus, the developed models enable a more realistic Plastic Concrete cut-off wall design and provide an important basis for future research.

1. Introduction

1.1. Background

Due to a significantly ageing infrastructure, dam remediation and repair is of increasing importance worldwide. Earthen dams,

* Corresponding author at: Materials Testing and Research Institute Karlsruhe (MPA Karlsruhe), Gotthard-Franz-Str. 2/3, 76131 Karlsruhe, Germany.

E-mail address: david.alosshepherd@kit.edu (D. Alós Shepherd).

[1] 0000-0001-9966-735

https://doi.org/10.1016/j.cscm.2023.e02521
Received 27 August 2023; Received in revised form 26 September 2023; Accepted 30 September 2023
Available online 2 October 2023

commonly used for hydropower generation, levees or flood retention basins, also show significant ageing, and their safety is of utmost importance for nearby urban areas. Therefore, earthen dams must also be remediated, whereby the most common solution for the remediation of earthen dams and levees is the design and construction of cut-off walls [1,2]. The planned cut-off wall, generally constructed as a slurry-trench wall [3], is extended into an underlying impervious stratum [4] and filled with a support fluid to stop the excavated trench from collapsing. The trench is then usually backfilled using the tremie method [1,2], whereby a wide range of backfill materials exist, with growing interest in Plastic Concrete due to the materials' suitable characteristics [1].

Plastic Concrete is hereby characterised by a high deformation capacity under load. This, in turn, decreases both rupture probability and crack opening width, reducing the probability of a permeability increase in the cut-off wall [1,2,5]. Plastic Concrete is, similar to ordinary concrete, composed of cement, water, aggregate, additions and admixtures, however, in differing proportions [1]. Most notably, Plastic Concrete is produced with a very high w/c-ratio (w/c $\geq$ 3.0) and water-binding additions (e.g. bentonite) to ensure fresh concrete stability and hereby obtain a highly ductile and impermeable material [1].

Despite its indisputably beneficial material properties, the mechanical behaviour of Plastic Concrete still needs to be widely studied [1]. Currently, the design of cut-off walls considers Plastic Concrete to be a linear-elastic material, with a defined compressive strength at 28 days [6], since no specific constitutive law for Plastic Concrete exists, which could account for the time development of the mechanical properties of Plastic Concrete [1]. This is not least due to the scarcely available systematic data in the literature, whereby the compressive strength, tensile strength and elastic modulus cannot be correlated from one mix design. The lack of a specific constitutive law also generally incurs higher cement contents than technically necessary, ensuring the strength criteria are permanently met in the linear-elastic design [6]. Thus, the material's full potential is only partially used and the inherent sustainability advantages do not come into effect [6]. The resulting increased costs may also significantly impede using Plastic Concrete in developing countries [7,8]. Therefore, in the following subsections, the current understanding of the mechanical behaviour of Plastic Concrete is summarised.

1.1.1. Compressive strength

In literature, various studies have tested the unconfined compressive strength of Plastic Concrete with varying mix design [9–12–15,16,17]. The studies show a gradual decline in Plastic Concrete strength with increasing w/c-ratio. However, since bentonite absorbs water into its structure, reducing the readily available water for cement hydration, the effective w/c-ratio is likely smaller. In literature there is no reference to the contending behaviour of cement and bentonite for the available water and possible interaction mechanisms in Plastic Concrete. In addition, compressive strength results are also dependent on the chosen loading speed and testing standard [18,19]. They must therefore be considered carefully to achieve measurable and precise data, avoiding any loading-speed induced effects [18,19]. The existing literature, however, does not systematically address these influencing parameters when studying the material behaviour of Plastic Concrete [1].

Furthermore, Plastic Concrete batching and casting are also of utmost importance for the material's performance. Various possibilities exist for batching [20,21], where a pre-hydrated bentonite slurry is most commonly added to cement and aggregates before mixing [1]. Especially the preparation of the bentonite slurry has a significant impact on Plastic Concrete performance, whereby the few available studies recommend a long mixing time with a high-RPM mixer [22] to ensure sufficient bentonite mixing. Regarding swelling time, current literature does not find significant differences in Plastic Concrete's performance with varying swelling times [21, 23].

Even though most reference testing for standard concrete is conducted at 28 days, it is common knowledge that the strength of concrete continues to increase beyond this mark. The knowledge of the long-term strength development of Plastic Concrete is of utmost importance since cut-off walls are constructed for design periods far exceeding 50 years. In addition, the water load application on cut-off walls occurs far beyond the 28-day mark; therefore, long-term strength development is essential to ensure accurate and realistic cut-off wall design. The curing speed of concrete is primarily influenced by factors such as water-cement ratio, type of cement and cement strength class [24]. For the latter, higher cement strength classes generally lead to faster strength development due to cement's increased fineness [18,24]. Code models like the *fib* Model Code 2010 [25] or *fib* Model Code 2020 [26] can be used to estimate the time function of concrete strength development (see Subsection 4.3). It is also known that, generally, the tensile strength develops faster than the corresponding compressive strength [26,27]. Literature data has, however, already shown that Plastic Concrete's compressive strength development is far slower than ordinary concrete, with a significant compressive strength increase beyond the 28-day mark [1,9,11,15,17]. This should be accounted for in Plastic Concrete cut-off wall design with a material-specific time development model, which, however, currently does not exist, and will therefore be studied in this paper.

1.1.2. Tensile strength

In concrete design, the uniaxial tensile strength (f_{ct}) is as important as the uniaxial compressive strength. For standard concrete, the uniaxial tensile strength is typically estimated to be 10% of the unconfined compressive strength f_{cu} [18]. However, this f_{ct}/f_{cu}-ratio is not constant and may decrease with increasing time and compressive strength f_{cu} [18,28]. Furthermore, the ratio is affected by the aggregate type, aggregate grading, curing conditions, and the type of tensile test performed [18,27].

According to *fib* MC 2010 [25], in turn based on the model by Heilmann [27,29], the tensile strength f_{ctm} can be estimated from the characteristic compressive strength f_{ck} following Equation (1) for concrete grades $\leq$ C50 [25].

$$f_{ctm} = 0.3 \cdot (f_{ck})^{2/3} \tag{1}$$

However, for a Plastic Concrete sample with a characteristic compressive strength f_{ck} of 1.5 MPa, this would incur in a mean tensile strength f_{ctm} of 0.39 MPa, suggesting a f_{ctm}/f_{ck}-ratio of 0.26, unlikely for Plastic Concrete samples. HEILMANN however shows that the factor 0.3 in Equation (1) may vary depending on the type of test used [27,29] and will therefore be studied in more detail in the present study.

On the other hand *fib* MC 2020 [26] suggests a new model, described in Equation (2).

$$f_{ctm} = 1.8 \cdot ln(f_{ck}) - 3.1 \tag{2}$$

However, this model is not applicable to Plastic Concrete since a negative tensile strength would be calculated for a characteristic compressive strength f_{ck} of 1.5 MPa. Therefore this model is not further pursued in the present study.

The tensile strength of concrete can be studied with various test methods. Most commonly, and due to the simple testing procedure, the so-called splitting tensile strength (also called "Brazilian test") standardised in EN 12390–6 [30] or ASTM C496 [31] is used. The splitting tensile test is usually performed on cylinders with a height-to-diameter ratio of 2, with smaller samples generally exhibiting higher strength [27]. It should be noted that tensile strength tests generally exhibit a higher standard deviation than compressive strength tests [18,24]. However, the sample size has a smaller influence on splitting tensile tests than on other tensile tests due to the stress induction mechanism and sample failure pattern [18,24]. The conversion factor α_{sp} for splitting tensile strength to uniaxial tensile strength for ordinary concrete is disputed in literature [24,28] and varies widely in existing international codes [26]; *fib* MC 2020 [26] therefore recommends using a conversion factor $\alpha_{sp} = 1.0$.

For Plastic Concrete, little research has been carried out on tensile strength. GAO ET AL. [32] performed splitting tensile strength tests on cubes with two sample sizes, showing a good correlation between the compressive strength and the tensile strength. KAHL ET AL. [33] studied a wide range of Plastic Concrete mixes at different ages using 6 in by 12 in cylinders, also finding a clear correlation between the achievable splitting tensile strength and the selected mix design. Finally KAYSER AND SCHULZ [34] performed few splitting tensile strength tests on 10 cm by 20 cm cylinders of hardened cement-bentonite slurries with different bentonites. In conclusion, the present paper must systematically study the tensile-to-compressive strength ratio, specifically for Plastic Concrete, and establish a new model for this purpose.

1.1.3. Elastic modulus

In Plastic Concrete cut-off wall design, the target elastic modulus should be similar to the surrounding soil's, and not exceed five times the latter, to ensure compatibility within the earthen dam [1,35]. The elastic modulus of concrete is hereby primarily determined by the elastic moduli of its components [18,19]. Similarly to ordinary concrete, the elastic modulus of Plastic Concrete increases with increasing compressive strength and thus with decreasing w/c-ratio or increasing cement content [1]. In literature, various studies have investigated the elastic modulus of Plastic Concrete [10,11,13,14,16,17,36]. Still, as reported by the authors in [1], the testing procedure used has a major influence on the test results. This is primarily due to the varying definitions of elastic modulus underlying the individual testing procedures and the different sample deformation measurement techniques used [1].

In concrete technology, elastic modulus testing is performed according to EN 12390-13 [37] or ASTM C469 [38], whereby the sample deformation is measured using dial gauges or LVDTs applied directly to the samples. On the other hand, geotechnical testing standards such as EN ISO 17892-7 [39] or ASTM D2166 [40] generally use machine displacement to obtain specimen deformation in a load-displacement curve. In addition, the definition of elastic modulus differs depending on the selected testing procedure and is, therefore, not directly comparable. Overall, the elastic modulus obtained through concrete technology testing procedures is expected to be higher than that from geotechnical standards. With the available data, the elastic modulus of Plastic Concrete based on geotechnical standards can be assumed to be in the range of 300–1500 MPa [1].

However, in the literature, no elastic modulus data is available for Plastic Concrete samples based on concrete technology testing procedures. Therefore, the present study aims to close this gap.

1.2. Focus & research questions

In conclusion, the existing literature fails to systematically study the effect of mix design, especially w/c-ratio, bentonite content and type, on the long-term time development of the mechanical properties of Plastic Concrete. In addition, no Plastic Concrete specific time development model exists to estimate the concrete strength development beyond the 28-day mark. Furthermore, Plastic Concrete's compressive-to-tensile strength ratio remains unclear, with limited data showing no distinct pattern. In addition, all elastic modulus data available to date has been obtained using the load-displacement curve of geotechnical compressive strength tests and not based on direct sample measurement techniques. However, these measurements also account for testing machine deformation and fail to study solely material behaviour as measured in situ on the samples. The successful application of elastic modulus testing according to EN 12390-13 [37] specifically on Plastic Concrete samples, remains to be reported.

Therefore, this paper aims to critically study the effect of Plastic Concrete mix design, especially bentonite content and type, on its mechanical properties. The focus also lies on the long-term time development (up to 4 years) of compressive strength of Plastic Concrete and the development of a Plastic Concrete specific compressive strength time development model. In addition, the fresh concrete properties of Plastic Concrete are tested using two separate testing methods (slump and flow table test) to establish a correlation between the two. In addition, splitting tensile tests are conducted for the corresponding compressive strength tests to determine a tensile-to-compressive strength ratio. Finally, the elastic modulus of Plastic Concrete is tested for the first time following EN 12390-13 [37] and provides realistic elastic modulus data for varying mix designs. The developed models are of key importance to ensure a more accurate and realistic Plastic Concrete cut-off wall design.

2. Materials and methods

2.1. Materials

The present study studied bentonite-based Plastic Concrete mixes consisting of cement, bentonite, aggregates and water, with a high w/c-ratio, as described in subsection 1.1.

2.1.1. Cement and bentonite

In the present study, a German OPC cement CEM I according to EN 197–1 [41] was used. Three activated sodium bentonites from different European deposits were used to study the corresponding effect on Plastic Concrete performance. These were Bentonil CV15, Bentonil WW4 and Tixoton, all produced and provided by CLARIANT Deutschland GmbH, were used. No further supplementary cementitious materials (SCMs) were added.

The chemical composition of the source materials, as determined through X-ray fluorescence analysis (XRF), is given in Table 1. The physical characteristics of the source materials are given in Table 2. In Table 3, the mineralogical composition, as determined through XRD, as well as the cation exchange capacity (CEC), as determined through Cu-trien method according to [42,43], of the bentonites used are shown.

2.1.2. Aggregates and water

The aggregates used were a combination of local Rhine sand and Rhine gravel from Graben-Neudorf, Germany. The maximum aggregate size was $d_{max} = 8$ mm, in line with considerations from literature [1]. The particle size distribution is shown Table 4 and lies between control sieve curve A8 and B8 according to DIN 1045–2 [44].

The mixing water used was mains water from Karlsruhe, previously tempered to 20°C, and in line with the requirements according to EN 1008 [45]. No admixtures were used since currently available PCE-based admixtures interact (negatively) with clay, rendering these ineffective [46].

2.2. Methods

2.2.1. Experimental setup and mix design

As mentioned in section 1, no systematic study has investigated the time development of compressive and tensile strength of Plastic Concrete. In addition no Plastic Concrete specific concrete models exist in literature. Therefore, this study investigates Plastic Concrete's compressive strength change over time as well as studying the splitting tensile strength of Plastic Concrete at 28 days with varying mix design. In addition, the fresh properties of concrete were tested. Finally, the elastic modulus of Plastic Concrete is determined in accordance with EN 12390-13 [37] at 28 days. A timeline of the experimental tests is shown in Fig. 1.

To further understand the changes in Plastic Concrete mechanical strength, the bentonite type and the bentonite content were varied. Three activated sodium bentonites were used (see Subsubsection 2.1.1). The bentonite to cement ratio (b:c-ratio) was varied between 1:1.5 and 1:6. An overview of the varying mix design factors and the corresponding designation of the mixes used for compressive strength, splitting tensile strength and fresh concrete testing is given in Table 5. For elastic modulus testing, only the 1:2 and 1:3 mixes were used.

It is well established in the literature that the bentonite to cement ratio (b:c-ratio), as well as the w/c-ratio, have a crucial influence on the material strength obtained for a Plastic Concrete mix [1,47]. With a Plastic Concrete target compressive strength between 0.5 and 2.5 MPa at 28 days, and based on previous studies conducted by the authors [1,23], a Plastic Concrete mix with 100 kg/m^3 of cement and a w/c-ratio of 4.0 was used. The mix designs of Plastic Concrete used in this study are shown in Table 6.

2.2.2. Concrete batching and fresh concrete testing

Based on the experimental setup developed in Subsubsection 2.2.1, and following considerations in [1], the Plastic Concrete mixes in this study were produced by combining the dry components (cement and aggregate) with the (pre-hydrated) bentonite slurry. Since no standardised batching procedure exists for Plastic Concrete, this process is described in more detail.

The bentonite slurry was produced in a batch suspension mixer type SC-20-K from MAT Mischanlagentechnik GmbH (Immenstadt, Germany). This mixer reaches a rotational speed of approx. 3000 rpm (50 Hz) and has a nominal power of 5.5 kW. The capacity of the mixer is approximately 20 litres. The batch suspension mixer was filled with 20 litres of water, and bentonite was added evenly to avoid clump formation [21]. The components were then mixed in the mixer for 6 min to achieve a homogeneous bentonite slurry [1, 22]. The slurry was then filled into buckets through a discharge pipe on the mixer. The 24-hour swelling process and storage also took

Table 1
Chemical composition of the cement and bentonites used, corrected by LoI.

		CaO	SiO_2	Al_2O_3	MgO	Fe_2O_3	Others	LoI
CEM I	(m.-%)	61.8	22.2	5.2	2.9	2.4	3.6	2.7
CV15	(m.-%)	2.3	59.8	12.0	1.9	2.2	3.4	15.7
WW4	(m.-%)	4.0	50.6	16.7	3.1	3.8	4.1	17.8
Tixoton	(m.-%)	3.9	49.2	17.5	2.5	5.3	5.4	18.2

Table 2

Physical characteristics of the cement and bentonite source materials used.

	PSD			density			specific surface
	$d_{10\%}$* (μ m)	$d_{50\%}$*	$d_{90\%}$*	no-dry (g/cm^3)	60°C	105°C	Blaine (cm^2/g)
CEM I	1.52	17.20	55.30	3.10	–	–	3.477
CV15	1.20	7.13	38.34	2.40	2.72	2.79	–
WW4	0.93	4.75	39.90	2.54	2.72	2.86	–
Tixoton	1.97	16.78	57.19	2.57	2.72	2.78	–

* Determination in water with $Na_4P_2O_7$

Table 3
Mineralogical composition determined by XRD and CEC of the bentonites used.

	CV15	WW4	Tixoton
Quartz	X	X	X
Carbonate (mainly calcite)	X	X	X
Illite / Mica (di)			X
Montmorillonite	X	X	X
Plagioclase	X	X	X
K-feldspar		X	X
CEC (cmol$^+$/kg)	61	88	65

"X" marks where the minerals are present

Table 4
Particle size distribution of aggregates used.

Sieve size	(mm)	0.125	0.25	0.5	1	2	4	8
Sieve passing	(m.-%)	0.5	8.8	21.0	30.2	40.0	63.2	97.2

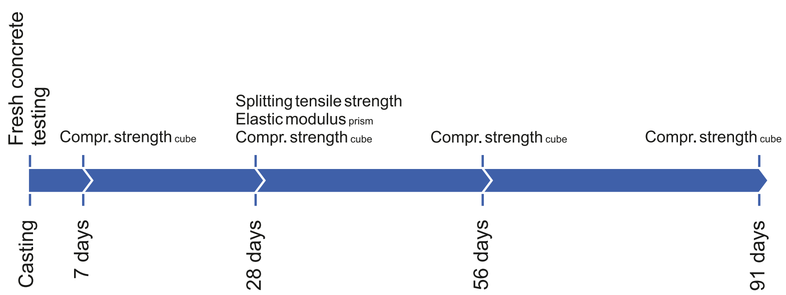

Fig. 1. Timeline of the experimental testing carried out in this study.

Table 5
Overview of the varying mix design factors and corresponding designation of the mix designs used.

b:c-ratio	Bentonite Type		
	Bentonil CV15	Bentonil WW4	Tixoton
1:1.5	C1:1.5	W1:1.5	T1:1.5
1:2	C1:2	W1:2	T1:2
1:3	C1:3	W1:3	–
1:4	C1:4	–	–
1:6	C1:6	–	–

place in these buckets, which were placed in a climate-controlled room with an air temperature of 20°C and a relative humidity of 65%.

The fresh Plastic Concrete was mixed using two different mixers depending on the concrete batch size. For batches up to 50 litres, a Zyklos ZZ 75 EH concrete mixer from Pemat Mischtechnik GmbH (Freisbach, Germany) was used. This mixer has a nominal power of 3.3 kW, a rotational speed of approximately 70 rpm and a capacity of 75 litres. For larger batches up to 240 litres, a pan concrete mixer from Teka Maschinenbau GmbH (Edenkoben, Germany) was used. This mixer has a nominal power of 15 kW, a rotor speed of

Table 6
Mix design of Plastic Concrete.

	Mix I (kg/m^3)	Mix II (kg/m^3)	Mix III (kg/m^3)	Mix IV (kg/m^3)	Mix V (kg/m^3)
Cement	100.0	100.0	100.0	100.0	100.0
Water	400.0	400.0	400.0	400.0	400.0
Bentonite	066.6	050.0	033.3	025.0	016.7
Sand (0–2 mm)	556.6	562.9	569.2	572.3	575.5
Gravel (2–8 mm)	873.5	883.4	893.3	898.2	903.1
b/c-ratio	1:1.5	1:2	1:3	1:4	1:6

approximately 17 rpm and a capacity of 375 litres. In addition, the ambient temperature in the laboratory was approximately 20˚C.

First, sand, gravel and cement were placed in the mixer drum and premixed for one minute. After that the bentonite slurry, with a prior 24 h swelling time, was added to the mixer drum. The Plastic Concrete was then mixed for 5 min until a homogeneous concrete mix was obtained. This is in line with the most common mixing procedure for Plastic Concrete [1] and also used in previous studies by the authors [23].

The finalised fresh concrete is then tested, with slump test according to EN 12350-2 [48] and flow table test according to EN 12350-5 [49] being performed immediately after mixing. Following on, fresh concrete density according to EN 12350-6 [50] and air content according to EN 12350-7 [51] were measured.

Thereafter, part of the concrete was cast into standard cubic (a=200 mm) and cylinder (l=300 mm, d=150 mm) steel moulds according to EN 12390-1 [52] and vibrated with a rod shaker with a 120 Hz frequency. In addition, the remaining part of the concrete was cast into standard 40 × 40 × 160 mm^3 steel prism moulds according to EN 196–1 [53] and vibrated on a shaking table with a 50 Hz frequency for 30 s. All samples were then stored in the moulds for 72 h (due to the low early age strength) at 20˚C under plastic foil and wet jute to avoid desiccation of samples following EN 12390-2 [54]. After this, the samples were demoulded and placed under water at 20˚C until testing.

2.2.3. Compressive strength testing

Most commonly, the compressive strength of concrete is determined according to EN 12390-3 [55] using cubic samples with an edge length of 150 mm. However, due to Plastic Concrete's very low strength properties, the minimum testing load of standard concrete uniaxial testing machines is not reached at Plastic Concrete sample failure. Therefore, cubes with an edge length of 200 mm were used, to increase test area and thus testing load. For any given age and mix, three cubes were tested. The cast cubes were removed from the water bath curing and surface dried using a cloth towel. The compressive strength was not tested thoroughly in compliance to EN 12390-3 [55] since the loading speed was reduced in line with the low strength requirements of Plastic Concrete. The loading speed was set to 0.05 MPa/s for all samples, as similarly described in DIN 4093 [56] for the testing of strengthened soil samples.

2.2.4. Splitting tensile strength testing

Furthermore, the tensile strength of specimens was studied using the splitting tensile test according to EN 12390-6 [30]. The tested cylinders were 300 mm in length and 150 mm in diameter. For any given age and mix, three cylinders were tested. The cast cylinders were removed from the water bath curing and surface dried using a cloth towel. Due to Plastic Concrete's very low strength properties, the splitting tensile strength was not tested thoroughly according to EN 12390-6 [30] since the loading speed had to be reduced. The loading speed was hereby set to 350 N/s (equivalent to 0.005 MPa/s).

2.2.5. Elastic modulus testing

Most commonly, the elastic modulus of concrete is determined according to EN 12390-13 [37] using cylinder samples with 150 mm diameter and 300 mm in length. However, due to Plastic Concrete's very low strength, standard concrete uniaxial testing machines are inadequate to test Plastic Concrete samples due to the minimum testing load. Therefore a specialised testing machine Zwick 010 from the manufacturer ZwickRoell GmbH & Co. KG (Ulm, Germany) was used. This electrical AC servomotor universal testing machine has a maximum load capacity of 10 kN and crosshead speed ranging between 0.0005 mm/min to 1000 mm/min, making the machine suitable for testing low-strength samples such as Plastic Concrete. The cast prisms were removed from the water bath curing and surface dried using a cloth towel. For any given age and mix, three prisms were tested. The prisms were placed vertically in the testing machine (testing cross-section 40 × 40 mm^2), and two oppositely placed DD1 strain transducers on a quick-action clamping device were used for sample deformation measurement. Thereafter the stabilised elastic modulus test according to EN 12390–13, procedure B [37] was performed. The loading speed was set to 0.01 MPa/s for all samples, with a pre-load stress of 0.06 MPa. Once elastic modulus testing was finalised, the clamping device with the strain transducers was removed from the samples, and the corresponding compressive strength was tested following EN 12390-3 [55] with an identical loading speed of 0.01 MPa/s. Deformation of the samples was hereby measured using the crosshead displacement.

3. Results

3.1. *Fresh concrete results*

As mentioned in Subsubsection 2.2.2, fresh concrete tests were performed on the concrete batches produced. Fig. 2 provides an overview of the fresh concrete workability results. In Fig. 3, the air content and fresh concrete density results are shown.

The results in Fig. 2 clearly show that an increase in bentonite content, i.e. increasing b:c-ratio, incurs lower Plastic Concrete workability, likely due to the water-binding capacity of bentonite and inline with results from other research [7,23,57–59]. It should be noted that mixes C1:6 and T1:2 (marked with * and hatched) displayed some minimal segregation and are therefore not considered for future analysis. In addition, at a constant b:c-ratio, the bentonite type used has a significant effect on concrete workability [23]. Finally, the results display a good correlation between the flow table and slump test results and will be further discussed in Subsection 4.1.

From Fig. 3, it becomes apparent that no clear correlation between b:c-ratio and the obtained air content exists, likely due to the known high scattering of air content test results. On the other hand, as would be expected for the selected mix designs (see Table 6), an increase in b:c-ratio incurs a lower concrete density, due to the intrinsic volumetric replacement of (heavier) aggregates with (lighter) bentonite. Nonetheless, variations in test execution can also affect the test results obtained, of particular importance with high b:c-ratio mixes, where a correct placement and compaction of the Plastic Concrete samples cannot be guaranteed due to the decreased workability.

3.2. *Compressive strength results*

As mentioned in Subsubsection 2.2.3, three cubes were tested on compression in accordance with EN 12390-3 [55] for every point in time and selected mix. In Fig. 4, the results from compressive strength tests at 28 days in dependence of the b:c-ratio are shown, whereby each point represents the mean value of three samples with its corresponding standard deviation.

Fig. 4 shows that the compressive strength at 28 days lies between 0.33 MPa and 0.79 MPa, aligning with the results expected in literature for the chosen mix [1,23,47]. Moreover, the results show a clear correlation between compressive strength and the b:c-ratio used, with compressive strength increasing with a higher bentonite content, due to a decreasing effective w/c-ratio [23,60,61]. The two mixes displayed in Fig. 4 with hollow symbols are not in line with this trend due to slight concrete segregation (see also Fig. 2) and subsequent concrete bleeding, increasing compressive strength of the remaining samples. Therefore it can be assumed that the b:c-ratio and compressive strength, for a given bentonite type, have a positive correlation.

The overall strength is, however, also dependent on the bentonite type used, for which literature is currently inconclusive. The cation exchange capacity (CEC), and thus bentonites' water absorption capacity, could affect the compressive strength of samples. However, as shown in Table 3, the CEC of WW4 bentonite is highest, but the samples exhibit lower strength than CV15 samples, contradicting this theory. In Fig. 5, the results from compressive strength testing are shown over time, whereby each point represents the mean value of three results, with corresponding standard deviation.

Fig. 5 shows that the compressive strength increases steadily from 28 days onwards. The compressive strength at 28 days lies between 0.58 MPa and 0.80 MPa, aligning with the results expected in literature for the chosen mix design [1,23,47]. In addition, the strength increase beyond 28 days is far greater than that of ordinary concrete due to Plastic Concrete's far higher w/c-ratio and reported slower cement hydration [20,61]. The compressive strength of Plastic Concrete samples tested here increases by approximately 30–50% between 28 days and 91 days due to continuous cement hydration and subsequent pore refinement over time [23]. These results will be further discussed in Subsection 4.3.

Moreover, a clear correlation between compressive strength and the b:c-ratio is visible, with the compressive strength of mixes with

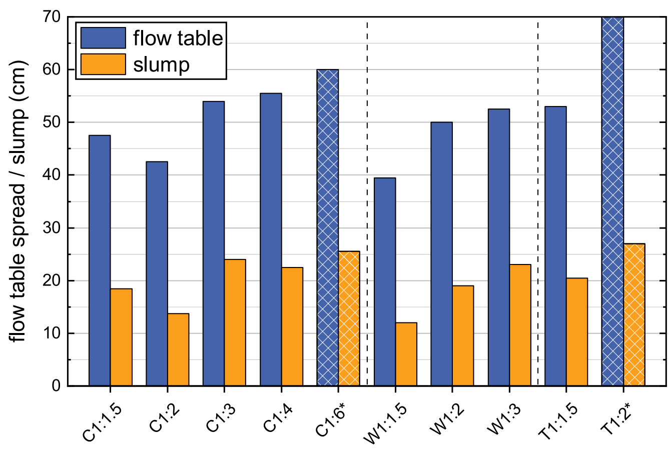

Fig. 2. Fresh concrete workability test results of all mixes.

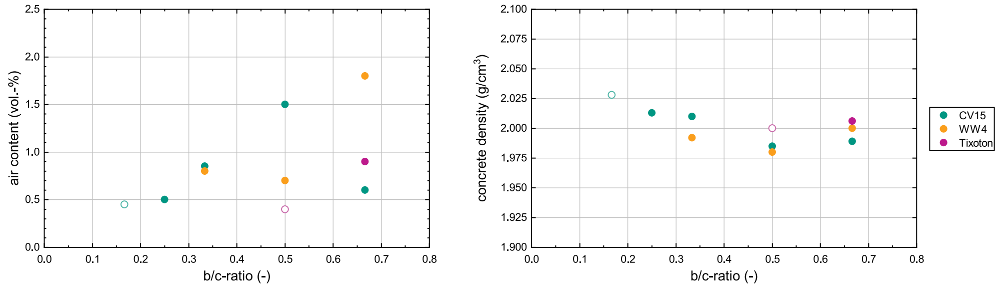

Fig. 3. Fresh concrete air content (left) and density (right) test results of all mixes.

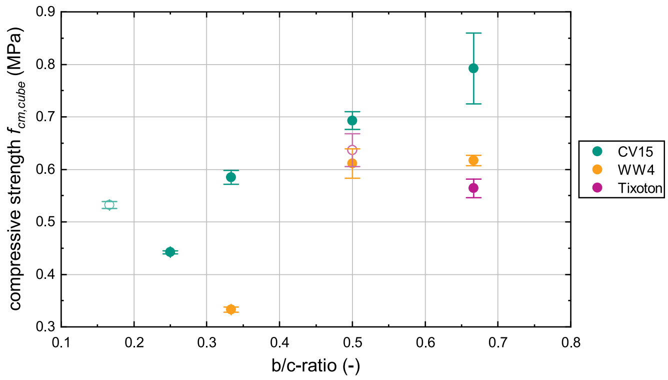

Fig. 4. Mean compressive strength (with standard deviation) of three cube samples (a = 200 mm) in dependence of b:c-ratio of Plastic Concrete at 28 days.

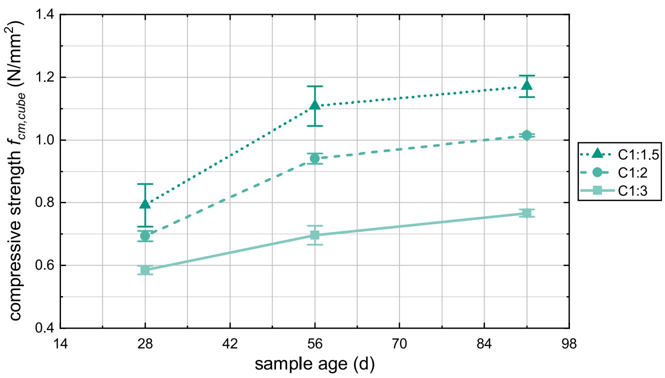

Fig. 5. Mean compressive strength (with standard deviation) of three cubes over time in dependence of Plastic Concrete mix design.

a 1:1.5 ratio lying above that of 1:3 mixes. Through a higher bentonite content in the mix, a lower effective w/c-ratio is incurred, allowing for a more dense cementitious matrix and, in turn, increasing the compressive strength [23,60,61].

3.3. Splitting tensile strength results

As described in Subsubsection 2.2.3, the splitting strength was tested according to EN 12390-6 [30] on three cylinders per mix design. In Fig. 6, the results from splitting tensile strength testing at 28 days in dependence of the b:c-ratio are shown, whereby each point represents the mean value of three samples with its corresponding standard deviation.

The results show that the splitting tensile strength at 28 days lies between 0.048 MPa and 0.103 MPa, aligning with the results expected in literature for the chosen mix [1]. Moreover, the results show some correlation between splitting tensile strength and the b:c-ratio used, with splitting tensile strength increasing with a higher bentonite content. However, the standard deviation of splitting tensile strength test results is far higher than that of compressive strength, as known from literature [24]. From the displayed results it remains inconclusive whether a dependency of splitting tensile strength on the bentonite type used exists and will be further studied in subsection 4.4.

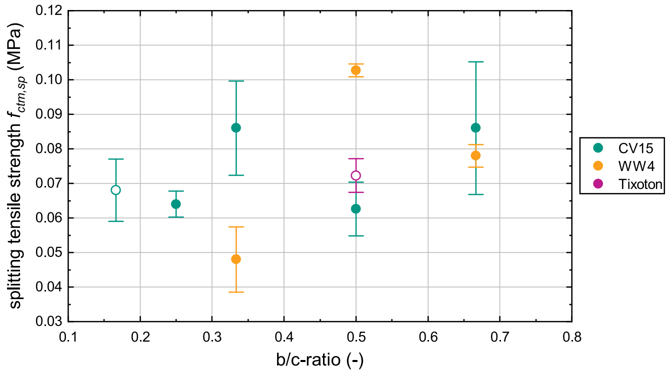

Fig. 6. Mean splitting tensile strength (with standard deviation) of three cylinder samples (l = 300 mm, d = 150 mm) in dependence of b:c-ratio of Plastic Concrete at 28 days.

3.4. Elastic modulus results

Elastic modulus tests according to EN 12390-13, procedure B [37] were performed on prism samples as described in Subsubsection 2.2.5. Thereafter, the corresponding compressive strength was tested following EN 12390-3 [55]. In Fig. 7, the elastic modulus $E_{C,S}$ test results are shown over the corresponding compressive strength, whereby each point represents one tested prism sample.

The results show that, as expected, an increase in compressive strength incurs in higher elastic modulus of Plastic Concrete samples. It is also apparent that neither bentonite type nor b:c-ratio significantly impact the achievable elastic modulus. Due to prism sample slenderness (h/d=4), most compressive strength results underestimate the correct compressive strength since the samples partially displayed shear failure. The results of the elastic modulus testing will be further discussed in Subsection 4.5.

4. Discussion

4.1. Slump and flow table correlation

As shown in Subsection 3.1, a positive correlation between the slump and flow table test results for Plastic Concrete seems to exist. Despite concrete being measured under different conditions with both tests (self-weight vs compaction), both test methods are suitable for testing high workability mixes [18,62]. To further analyse this correlation, the results from this study as well as a further study by the authors in [23], are plotted in Fig. 8 with the slump test results being displayed over flow table tests results.

It can be seen that, as expected, slump increases with increasing flow table spread, similar to results in ordinary concrete [63]. In addition, this trend occurs independently of the type of bentonite used. The results from this study have a marginally lower spread than those from [23]. The Guide to Tremie Concrete for Deep Foundations [62] states that the flow table test has a lower sensitivity while using dynamic impacts that may alter the obtained results. However, since no superplasticizing admixtures were used for the mix design the achieved workability is lower than standard tremie concrete and is therefore more appropriate for flow table testing. This is also in line with the limits defined in DIN Fachbericht 100 [64] where the presented results lay within the recommended limits for flow table testing (34–62 cm). The slump results lay slightly above the recommended limits (1–21 cm) [64].

Although Norvell et al. [57] suggest that concrete flowability correlates to the cation exchange capacity (CEC) of the bentonites used, the results presented in Fig. 2 and in Fig. 8 do no support this thesis, since nearly identical CECs of CV15 and Tixoton bentonite (see Table 3) incur in significantly different flow table results, despite identical mix designs. Fernandes et al. [59] describe a positive

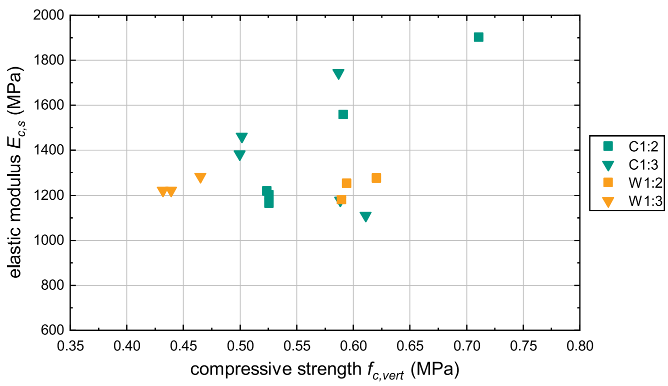

Fig. 7. Elastic modulus $E_{C,S}$ over compressive strength in dependence of Plastic Concrete mix design at 28 days.

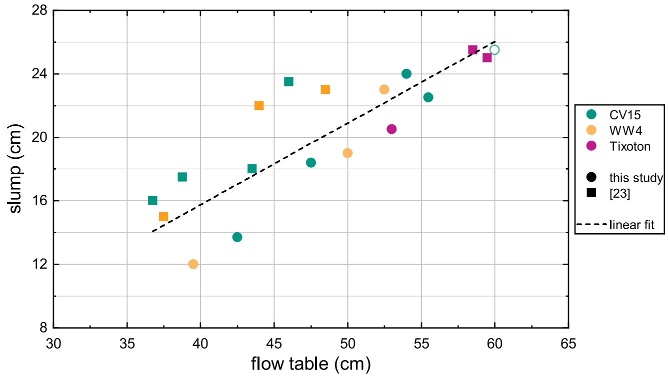

Fig. 8. Correlation between flow table and slump tests results for all mixes from this study and [23].

correlation between the moisture content (defined as the ratio by mass of water to solids) and the slump test results. However, in the present study, all mixes have an identical moisture content and thus, the varying workability of the mixes cannot be ascribed to this factor.

The linear trend of these results can be fitted and an approximate inclination of 0.52 is obtaine dwithin the tested data range displayed, i.e. that an increase in flow table spread of 10 cm incurs a 5.2 cm larger slump, inline with results presented in [62]. The coefficient of determination R^2 is only 0.646 due to the high, expected deviation of the fresh concrete test results. This high deviation is inherent with the applied fresh concrete test, reported to be $\pm$ 4 cm for flow table test results [62]. However, the overall trend can be accurately described with the displayed curve, where slump s correlates with flow table results ft according to Equation (3).

$$s = 0.52 \cdot (ft - 40 \text{ cm}) + 16 \text{ cm} \tag{3}$$

Future research should also measure the slump flow and slump flow velocity of Plastic Concrete mixes [62], since these results may display lower deviation for fresh tremie concrete properties.

4.2. *Influence of sample size and batching on compressive strength*

In this study, all compressive strength tests were conducted on cube samples with an edge length of 200 mm (as described in subsubsection 2.2.3). This, in turn, incurs a far more significant material consumption. Since the Plastic Concrete studied here has a maximum aggregate size d_{max} of 8 mm, it may therefore be more expedient to use prisms halves for compressive strength determination. Thus, within the scope of a previous study by the authors in [23], cube samples were cast to compare compressive strength results with prism halve samples. In addition, all samples from both studies were produced using the same batch of cement and bentonite, as well as aggregates from the same deposit, thus reducing the possible material scattering to a minimum. In Fig. 9, the results from this study and [23] are shown, whereby the strength is displayed over the corresponding mix design.

From this data it becomes apparent that cube samples have an overall repeatability since both studies provide similar compressive strength results. In addition, for most mix designs, the compressive strength of prism halve samples is close to that of cube samples, with both results lying within the standard deviation of one another. The data also shows that the standard deviation is approximately

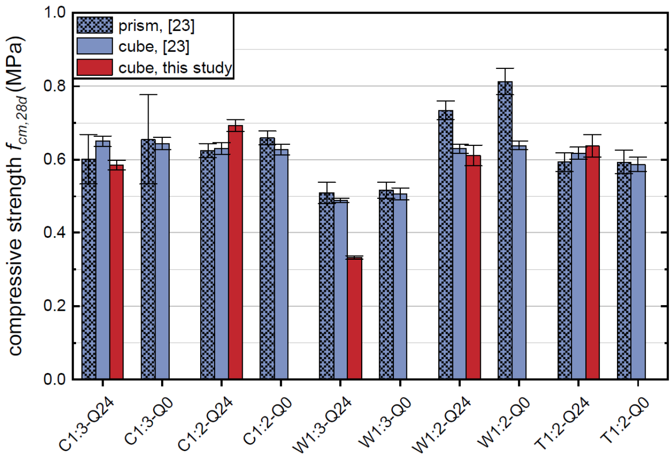

Fig. 9. Comparison of compressive strength of prism (40 × 40 mm²) and cube samples (200 × 200 mm²) from [23], with cube samples (200 × 200 mm²) from this study, at 28 days.

three times higher for the prism (0.0397 MPa) than cube (0.0143 MPa) samples, as would be expected due to the size and failure concentration effect based on the Weibull theory [18]. An average coefficient of the mean cube strength and prism strength can be calculated ($f_{cm,cube}/f_{cm,prism}$), with cubes strength being on average 0.963 × prism strength, in line with the expected theoretical correlation in literature [18]. Moreover, due to the chosen mix design (see subsubsection 2.2.1), the Plastic Concrete mixes tested in this study can all be considered water-dominated mixes [47]. Thus, the sample size has a less significant effect on compressive strength results than in standard concrete since cement particles are far further apart than in ordinary concrete, providing the same sample failure pattern (cross tensile failure) occurs. All in all, it can therefore be ascertained that the compressive strength of prism samples (40 × 40 mm^2) is approximately identical to that of cube samples (200 × 200 mm^2), despite higher standard deviation for prism samples. These results indicate that future research on Plastic Concrete compressive strength can be conducted using prism samples (providing $d_{max} \leq 8$ mm) due to the significant saving in the concrete volume needed for testing without significant influence on the compressive strength results. Furthermore, the results presented here should be further confirmed with more available research data in future.

4.3. *Compressive strength development over time*

In Subsection 3.2 the compressive strength results have been reported. However, the significant increase in compressive strength beyond the 28-day mark should be discussed in more detail.

For strength development of standard concrete, the *fib* Model Code 2010 [25] gives an approximation for the time function of the concrete strength development β_{cc} as a function of a cement-strength-class-dependant coefficient s and concrete age t, as shown in Equation (4).

$$\beta_{cc}(t) = \exp\left(s \cdot \left[1 - \left(\frac{28}{t}\right)^{0.5}\right]\right) \tag{4}$$

Few studies have examined the long-term strength of Plastic Concrete mixtures [9,11,15,17,65]. Therefore the results from this study as well as from [9,11,15,17] are shown in Fig. 10, where the relative compressive strength increase beyond 28 days ($f_{cm}(t)/f_{cm,28d}$) is shown as a function of time. For comparison, the *fib* MC 2010 model is also shown for a coefficient s of 0.20 and 0.38, respectively.

From Fig. 10, it becomes visible that the strength development over time is far more significant for Plastic Concrete samples than the *fib* MC 2010 predicts. The results from this study show a strength increase of 30–50% between 28 d and 91 d. It can also be seen that the compressive strength increase also clearly depends on the achievable compressive strength at 28 days and the w/c-ratio used, with a more substantial increase, the lower the corresponding compressive strength. From these results, changing the reference testing age for Plastic Concrete samples also seems expedient.

In *fib* MC 2020 [26], the time development function $\beta_{cc}(t)$ has been further extended in comparison to *fib* MC 2010 [25], whereby a different reference age t_{ref} can be further accounted for, as shown in Equation (5). If t_{ref} is set to 28 days, Equation (5) simplifies to Equation (4).

$$\beta_{cc}(t) = \exp\left\{s_C \cdot \left[1 - \left(\frac{t_{ref}}{t}\right)^{0.5}\right] \cdot \left(\frac{28}{t_{ref}}\right)^{0.5}\right\} \tag{5}$$

The s_C coefficient in *fib* MC 2020 [26] hereby depends on the speed of strength development and strength class of the selected concrete and has been updated in comparison to the s coefficient in *fib* MC 2010 [25]. For a compressive strength under 35 MPa according to Table 14.6–7 in [26,66] the s_C coefficient is selected to 0.3 (slow), 0.5 (normal) or 0.6 (slow) in accordance with corresponding strength development speed.

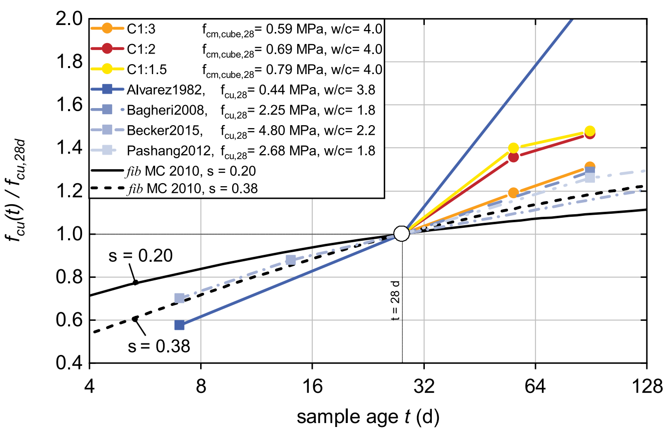

Fig. 10. Compressive strength of Plastic Concrete samples over time for this study and [9,11,15,17], with $t_{ref} = 28$ d.

Therefore in Fig. 11 the results from the present study and [23] are plotted over time using a reference age t_{ref} of 91 days. In addition, the *fib* MC 2020 time development function with $s_C = 0.50$ coefficient is plotted.

The results show that due to the high w/c-ratio used, the strength development of Plastic Concrete is still significantly slower than the *fib* Model Code 2020 [26] estimates. Therefore, adapting this model for Plastic Concrete may seem reasonable, using a best-fit approximation of the s_C coefficient for the data available. The results show that a best-fit approximation with the *fib* MC 2020 curve for $s_C = 1.75$ ($R^2 = 0.82$) incurs in an underestimation of the strength development, most significantly for early age. Therefore, subdividing the approximation into two data sets, before and after 91 days, may be more expedient. The best-fit approximation for these two subdivided data sets is also shown in Fig. 11.

It can be seen that through the split, best-fit approximation, a better correlation with the data can be achieved, with the early age strength development approximated with $s_C = 0.65$ ($R^2 = 0.90$) and the later age strength development approximated with $s_C = 1.98$ ($R^2 = 0.97$) providing a far better correlation to the presented data. With this, the best-fit approximation for the s_C coefficient at t_{ref} = 91 days can be achieved as shown in Equation (6).

$$s_C = \begin{cases} 0.65 & t < 91\text{ d} \\ 1.98 & t > 91\text{ d} \end{cases} \tag{6}$$

Although unexpected, such a differentiated compressive strength development can make sense for Plastic Concrete. The initial, somewhat faster, strength development coincides with the initial cement hydration [23]. The long-term, slower compressive strength development is likely caused by another strength development mechanism, possibly through a cement-bentonite interaction or another reaction, for which literature currently provides no explanation. A previous study by the authors [23] confirmed that a significant pore refinement and compressive strength increase occurs between 91 days and 4 years; however, no evidence of a further interaction mechanism could be obtained. Another possibility would be that, with increasing sample age and cement hydration, some of the water bound by the bentonite becomes entrapped and therefore increase compressive strength during testing due to the incompressibility of water. However, microstructural evidence of this has not yet been studied.

Overall, with the results presented here, a better approximation of the long-term strength development can be achieved, ensuring a better and more realistic design of Plastic Concrete cut-off walls.

4.4. Tensile to Compressive Strength Ratio

In Subsection 3.2 and Subsection 3.3 the results of compressive and splitting tensile strength testing are shown. It is common knowledge in concrete technology that the tensile strength correlates with the compressive strength of specimens and can generally be approximated to 1/10 of the compressive strength [18,24] (see also Subsubsection 1.1.2). In Fig. 12, the results from this study are shown, whereby the splitting tensile strength is plotted over the corresponding compressive strength. For comparison, the approximated correlation between splitting tensile strength and compressive strength ($f_{ctmm,\ psp} = 0.10 \cdot f_{cm}$) according to [18,24] is also shown.

From Fig. 12 it becomes apparent that Plastic Concrete also has an overall minimally higher tensile to compressive strength ratio than standard concrete, despite the overall higher standard deviation of splitting tensile test results [24].

In addition, some other authors have also published splitting tensile strength data for Plastic Concrete samples [32–34]. In Fig. 13, the splitting tensile strength is drawn over the corresponding compressive strength for the literature data [32–34] as well as the data from this study. In addition, best-fit modelling approaches following *fib* MC 2020 [26] / Heilmann [29] are shown, with the corresponding best-fit equation.

The results show a good correlation between splitting tensile strength and compressive strength results for Plastic Concrete samples over a broader range of compressive strength. The data furthermore lies above the expected ratio of 1/10. If a linear fit is applied, the splitting tensile can be approximated to Equation (7), with a ratio of 0.135. The coefficient of determination R^2 is 0.983, providing an overall excellent accordance for this data.

$$f_{ctm,sp} = 0.135 \cdot f_{cm} \tag{7}$$

Alternatively an approximation in line with *fib* MC 2020 [26]/Heilmann [29] can be calculated. The resulting approximation is shown in Equation (8). The coefficient of determination R^2 is 0.895, providing an overall good accordance for this data. However, as can be seen in Fig. 13, the tensile strength would be overestimated for low compressive strengths (0 - 1.5 MPa) and underestimated for higher compressive strengths (4 - 10 MPa) with this model.

$$f_{ctm,sp} = 0.179 \cdot f_{cm}^{2/3} \tag{8}$$

It should be noted that the specimen size, shape and testing standard used for the splitting tensile tests shown above are not identical for all samples. The sample size and shape are known to have a small effect on splitting tensile strength results due to sample failure pattern [18,24], which might slightly affect model prediction accuracy. Nevertheless, it seems reasonable to adapt the models to the available data to better account for Plastic Concrete mechanical behaviour, since no material-specific tensile strength prediction model currently exists. In this sense, the linear prediction model (Equation (7)) currently provides the more accurate results, especially at very low compressive strengths, and should therefore be preferred and used for future Plastic Concrete cut-off wall design. In future, more data should be obtained to optimise the prediction accuracy of the proposed model.

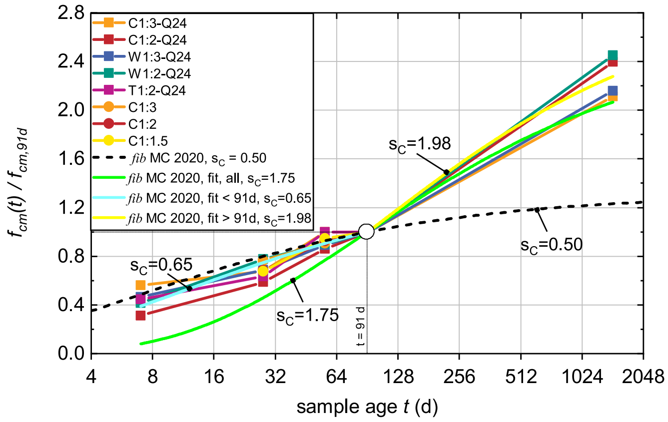

Fig. 11. Compressive strength of Plastic Concrete samples over time for this study and [23], as well as *fib* MC 2020 function, with $t_{ref} = 91$ d.

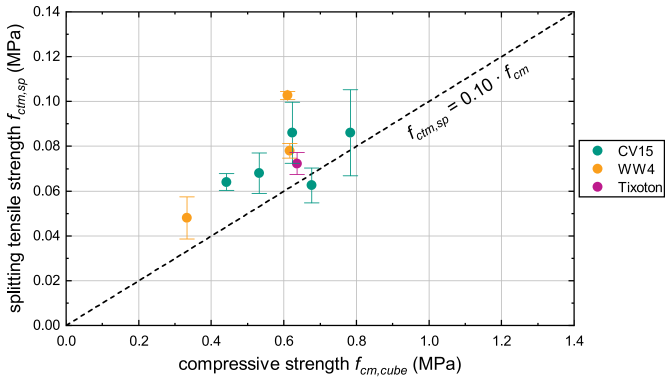

Fig. 12. Splitting tensile strength over compressive strength results at 28 days.

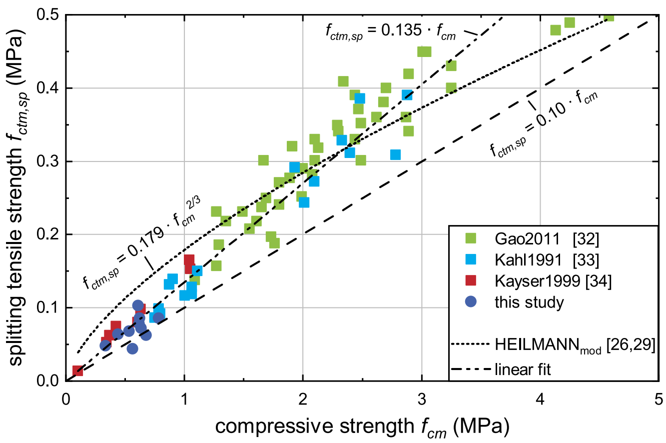

Fig. 13. Splitting tensile strength over compressive strength from this study and [32–34] as wells as modelling approximations in accordance with [26,29].

4.5. Discussion of elastic modulus results

In Subsection 3.4 the results of the elastic modulus testing are shown. As described, the testing procedure used clearly influences the obtained elastic modulus, in-line with varying definitions of elastic modulus underlying the individual testing procedures [1] (see also Subsubsection 1.1.3). This is generally caused by the deviating deformation measurement techniques used [1]. Therefore, in the present study, the stabilised elastic modulus $E_{C,S}$ (hereinafter “stabilised modulus”) was tested according to EN 12390-13, procedure B [37] with deformation measurement through two oppositely placed DD1 strain transducers on a quick-action clamping device. In addition, during subsequent compressive strength testing, the sample deformation was measured using the testing machines' cross-head displacement. A load-displacement curve is obtained with the latter, which can be further used to analyse sample deformation. Based on the *fib* MC 2020 [26], the initial elastic modulus E_{ci} can be obtained as the maximum tangent slope of the load-displacement-curve (hereinafter "tangent modulus"). In addition, the secant elastic modulus E_{c1} can also be obtained as the secant modulus from the origin to the peak compressive stress (hereinafter "secant modulus"). In the present study, the origin is here established as the intersection of the tangent modulus and the displacement axis to remove any contact effects in the load-displacement curve. In Fig. 14, the results of the present study with the stabilised elastic modulus $E_{C,S}$, the tangent elastic modulus E_{ci} and the secant elastic modulus E_{c1} are shown against the corresponding compressive strength. In addition the available literature data reported in [1] and based on [10,11,13,14,16,17,36] is shown in grey.

From the results in Fig. 14 it becomes clear that the testing scheme, especially the deformation measurement technique, plays a crucial role in the obtained elastic modulus results. The stabilised elastic modulus $E_{C,S}$ lies far above the other elastic moduli due to the direct deformation measurement of the samples and, therefore, also represents the "real" material behaviour. This testing incurs the lowest overall deformation and, thus, the highest elastic modulus, especially since deformation measurement occurs only in the middle third of the sample. When fitting the results, a linear approximation between the stabilised elastic modulus $E_{C,S}$ and the compressive strength f_c provides the best approximation with a coefficient of determination R^2 of 0.975 and is shown in Equation (9).

$$E_{C,S} = 2385 \cdot f_c \tag{9}$$

The results also show that the secant modulus $E_{c,i}$ and the tangent modulus E_{c1} provide similar results and are, as expected, in line with the results shown in literature from geotechnical testing standards. The tangent modulus is consistently higher than the secant modulus, which relates to the secant modulus accounting for the higher, plastic deformation of the Plastic Concrete samples. The present results provide the first comprehensive study of the elastic modulus of Plastic Concrete samples and a pioneering comparison between various testing methods. The results show that the stabilised elastic modulus $E_{C,S}$ is approximately 5.5x higher than the tangent modulus E_{ci} determined through the load-deformation curve. This suggests that, to date, cut-off wall design significantly underestimates Plastic Concrete material stiffness. However, since Plastic Concrete should provide a similar stiffness to the surrounding soil [1,35], and the soil stiffness is established as the tangent modulus in a load-displacement curve (see subsubsection 1.1.3), the tangent modulus E_{ci} may be the most appropriate value for geotechnical cut-off wall design. This is not least because the settlement calculations, and thus the load transfer onto the cut-off wall, use soil stiffness (i.e. tangent modulus) as input parameters. Once the design loads are obtained, these can be used as input for the Plastic Concrete cut-off wall stress analysis and wall design. The stress analysis can then be performed following available concrete design codes, and the newly developed models from this study, using the stabilised elastic modulus $E_{C,S}$.

5. Conclusions

The present study aimed to determine the effect of Plastic Concrete mix design on its mechanical properties over time and develop appropriate models. In addition, the present study also aimed to model the tensile-to-compressive strength ratio specifically for Plastic Concrete. Finally, the elastic modulus of Plastic Concrete was to be tested for the first time following EN 12390-13 [37] and related to the corresponding compressive strength.

This study's results show a good correlation between slump and flow table tests and can be estimated according to Equation (3). In addition, a wide range of compressive strength data is obtained for varying mix design and b:c-ratio. The compressive strength results for prism halve samples is shown to closely correlate to the corresponding cube strength, as seen in Fig. 9. Furthermore, a new time development model following *fib* MC 2020, specifically for Plastic Concrete, is developed exhibiting a significantly slower compressive strength increase over time, as described by the s_C coefficient in Equation (6). Furthermore, the splitting tensile strength shows an

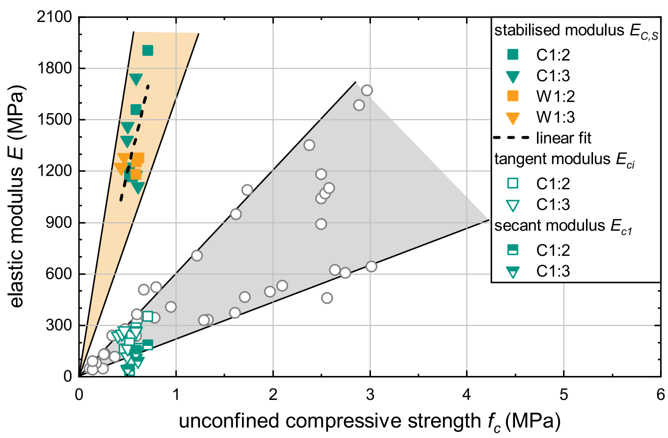

Fig. 14. Elastic modulus testing results ($E_{C,S}$, E_{ci}, E_{c1}) over corresponding unconfined compressive strength in comparison to literature results [1,10,11,13,14,16,17,36] (in grey) with varying mix design.

overall good, linear correlation with compressive strength with an approximate ratio of 0.135, as also shown in Fig. 13. Moreover, the elastic modulus $E_{C,S}$ concrete tests according to EN 12390-13 [37] show significantly higher elastic modulus than the available data (see Fig. 14), and a model approximation for the elastic modulus $E_{C,S}$ in dependence of compressive strength is given in Equation (9). All in all, this paper has provided a deeper insight into the understanding of Plastic Concrete's mechanical properties with varying mix design. In addition, the first Plastic Concrete specific mechanical property models have been developed,enabling a more realistic Plastic Concrete cut-off wall design and provide an essential basis for future research.

Future research should be carried out to explore the effect of the long-term strength increase in Plastic Concrete samples and further understand possible cement-bentonite interactions enhancing compressive and tensile strength time development models. In addition, further data should be acquired to adapt the newly developed models to a variation in source materials (e.g. CEM III or other SCMs) and also varying w/c-ratios. Finally, additional elastic modulus tests with varying mix design and sample ages should be performed to further develop the understanding of Plastic Concrete's elastic modulus. For this, novel measurement techniques such as digital image correlation (DIC) [67] could be explored, providing further insights into Plastic Concrete's mechanical behaviour.

Funding

This research did not receive any specific grant from funding agencies in the public, commercial, or not-for-profit sectors. The authors acknowledge support by the KIT-Publication Fund of the Karlsruhe Institute of Technology (KIT) for the settlement of the Article Publishing Charge.

CRediT authorship contribution statement

David Alós Shepherd: Conceptualization, Methodology, Investigation, Validation, Formal analysis, Writing – original draft, Writing – review & editing, Visualization, Project administration. **Frank Dehn**: Resources, Funding acquisition, Writing – review & editing.

Declaration of Competing Interest

The authors declare that they have no known competing financial interests or personal relationships that could have appeared to influence the work reported in this paper.

Data availability

Data will be made available on request.

Acknowledgements

The authors of this article would like to thank Clariant AG for providing the bentonite materials and MAT Mischanlagentechnik GmbH for providing the bentonite mixer. In addition, the authors would like to thank Ms. Anja Husel, Mr. Stefan Weber and Ms. Liv Wittkopf-Bertsch (IMB Karlsruhe/KIT) for their support during the testing campaign as part of their Bachelor's and Master's thesis. Furthermore, the authors thank Prof. Katja Emmerich and Dr. Eleanor Bakker (CMM Karlsruhe/KIT) for their help in CEC testing and their feedback regarding bentonite properties and behaviour.

References

[1] D. AlósShepherd, E. Kotan, F. Dehn, Plastic concrete for cut-off walls: a review, Constr. Build. Mater. 255 (2020), 119248, https://doi.org/10.1016/j.conbuildmat.2020.119248.
[2] D.A. Bruce (Ed.), Specialty Construction Techniques for Dam and Levee Remediation, CRC Press, Boca Raton, 2013.
[3] P.P. Xanthakos, Slurry walls, McGraw-Hill,, New York, 1979.
[4] U.S. Bureau of Reclamation Design Standards No. 13: Embankment Dam, Chapter 16: Cutoff Walls, Revision 14 (2014/07) (2014). ⟨https://www.usbr.gov/tsc/techreferences/designstandards-datacollectionguides/designstandards.html⟩.
[5] M. Ghazavi, Z. Safarzadeh, H. Hashemolhoseini, Response of plastic concrete cut-off walls in earth dams to seismic loading using finite element methods (Canadian Association for Earthquake Engineering (Ed.)). Proceedings of the 13th World Conference on Earthquake Engineering, Vancouver, 2004.
[6] K. Beckhaus, J. Kayser, F. Kleist, J. Quarg-Vonscheidt, D. Alós Shepherd, Design concept for sustainable cut-off walls made of highly deformable filling materials, in: R. Boes, P. Droz, R. Leroy (Eds.), Proceedings of the 12th ICOLD European Club Symposium 2023 (ECS 2023, Interlaken, Switzerland, 5-8 September 2023), CRC Press, Milton, 2023.
[7] F. Solomon, S.E. Ekolu, Strength behaviour of clay-cement concrete and quality implications for low-cost construction materials, in: M.G. Alexander, H.-D. Beushausen, F. Dehn, P. Moyo (Eds.), Concrete repair, rehabilitation and retrofitting III, Proceedings of the 3rd International Conference on Concrete Repair, Rehabilitation and Retrofitting (ICCRRR), Cape Town, South Africa, September 3rd - 5th 2012, CRC Press, Boca Raton, FL, 2012, pp. 1420–1425.
[8] M.L. Nehdi, Clay in cement-based materials: critical overview of state-of-the-art, Constr. Build. Mater. 51 (2014) 372–382, https://doi.org/10.1016/j.conbuildmat.2013.10.059.
[9] A.R. Bagheri, M. Alibabaie, M. Babaie, Reduction in the permeability of plastic concrete for cut-off walls through utilization of silica fume, Constr. Build. Mater. 22 (6) (2008) 1247–1252, https://doi.org/10.1016/j.conbuildmat.2007.01.024.
[10] J. Sadrekarimi, Plastic Concrete Mechanical Behaviour, J. Inst. Eng. India Civ. Eng. Div. 82 (FEV) (2002) 201–207.
[11] A. Becker, C. Vrettos, Laboruntersuchungen zum Materialverhalten von Tonbeton (in German), Bautechnik 92 (2) (2015) 152–160, https://doi.org/10.1002/bate.201400064.

[12] J.C. Evans, E.D. Stahl, E. Drooff, Plastic concrete cutoff walls, in: R.D. Woods (Ed.), Geotechnical practice for waste disposal 1987, Geotechnical Special Publications, ASCE, New York, 1987, pp. 462–472.

[13] S. Hinchberger, J. Weck, T. Newson, Mechanical and hydraulic characterization of plastic concrete for seepage cut-off walls, Can. Geotech. J. 47 (4) (2010) 461–471, https://doi.org/10.1139/T09-103.

[14] A. Mahboubi, A. Ajorloo, Experimental study of the mechanical behavior of plastic concrete in triaxial compression, Cem. Concr. Res. 35 (2) (2005) 412–419, https://doi.org/10.1016/j.cemconres.2004.09.011.

[15] Y. PashangPisheh, S.M. MirMohammadHosseini, Stress-strain behavior of plastic concrete using monotonic triaxial compression tests, J. Cent. South Univ. 19 (4) (2012) 1125–1131, https://doi.org/10.1007/s11771-012-1118-y.

[16] S. Kazemian, S. Ghareh, L. Torkanloo, To investigation of plastic concrete bentonite changes on it's physical properties, Procedia Eng. 145 (2016) 1080–1087, https://doi.org/10.1016/j.proeng.2016.04.140.

[17] L. Alvarez, J. Larenas, A. Bernal, J.A. Marin, Characteristics of the plastic concrete of the diaphragm wall of Convento Viejo Dam. International Commission On Large Dams (Ed.), 14th International Congress on Large Dams in Rio de Janeiro, Brazil, Vol. IV, 1982, pp. 371–389.

[18] A.M. Neville. Properties of Concrete, 5th edi., Pearson,, Harlow, 2011.

[19] H.-W. Reinhardt. Ingenieurbaustoffe (in German), 2nd ed., Ernst & Sohn,, Berlin, 2010.

[20] M.A. Fam, J.C. Santamarina, Study of clay-cement slurries with mechanical and electromagnetic waves, J. Geotech. Eng. 122 (5) (1996) 365–373, https://doi.org/10.1061/(ASCE)0733-9410(1996)122:5(365).

[21] M.A. Fadaie, M. Nekooei, P. Javadi, Effect of dry and saturated bentonite on plastic concrete, KSCE J. Civ. Eng. 23 (8) (2019) 3431–3442, https://doi.org/10.1007/s12205-019-0835-2.

[22] S. Adjei, S. Elkatatny, A. Al-Majed, Effect of bentonite prehydration time on the stability of lightweight oil-well cement system, Geofluids 2021 (2021) 1–8, https://doi.org/10.1155/2021/9957159.

[23] D. AlósShepherd, A. Bogner, J. Bruder, F. Dehn, Experimental Study into the Time Development of the Microstructural Properties of Plastic Concrete: Material Insights & Experimental Boundaries (In Review), Case Studies in Construction Materials (CSCM) (2023).

[24] P. Grübl, H. Weigler, S. Karl, Beton: Arten, Herstellung und Eigenschaften (in German). Handbuch fur Beton-, Stahlbeton- und Spannbetonbau, 2nd ed., Ernst & Sohn,, Berlin, 2001.

[25] International Federation for Structural Concrete (Ed.), fib Model Code for Concrete Structures 2010, 1st ed., Ernst & Sohn,, Berlin, 2013.

[26] International Federation for Structural Concrete (Ed.), fib Model Code for Concrete Structures 2020: Final Draft, May 2023, unpublished Edition, Lausanne, 2023/05.

[27] H.W. Reinhardt, Factors affecting the tensile properties of concrete, in: J. Weerheijm (Ed.), Understanding the tensile properties of concrete, Woodhead Publishing series in civil and structural engineering, Woodhead Publishing, Oxford, 2013, pp. 19–51, https://doi.org/10.1533/9780857097538.1.19.

[28] V. Malárics, Ermittlung der Betonzugfestigkeit aus dem Spaltzugversuch an zylindrischen Betonproben (in German): Dissertation, Vol. 69 of Karlsruher Reihe Massivbau, Baustofftechnologie, Materialprüfung, KIT Scientific Publishing,, Karlsruhe, 2011.

[29] H.G. Heilmann, Relations between tensile and compressive strength of concrete (in German), Beton 19 (2) (1969) 68–70.

[30] Comité Européen de Normalisation, EN 12390–6:2010–09 - Testing hardened concrete - Part 6: Tensile splitting strength of test specimens (German version).2023.

[31] ASTM International, ASTM C496/C496M-17 - Test Method for Splitting Tensile Strength of Cylindrical Concrete Specimens.2023.

[32] D.Y. Gao, S.Q. Song, L.M. Hu, Relationships of Strengths and Dimensional Effect of Plastic Concrete, Adv. Mater. Res. 306 307 (2011) 1029–1037, https://doi.org/10.4028/www.scientific.net/AMR.306-307.1029.

[33] T.W. Kahl, J.L. Kauschinger, E.B. Perry, Plastic Concrete Cut-Off Walls for Earth Dams, Technical Report REMR-GT-15, USACE, Vicksburg, MS, 1991.⟨https://apps.dtic.mil/sti/citations/ADA234566⟩.

[34] J. Kayser, T. Schulz, Spannungs-Verformungs-Verhalten erhärteter Bentonit-Zement-Suspensionen (in German), Bautechnik 76 (9) (1999) 747–756, https://doi.org/10.1002/bate.199904870.

[35] International Commission On Large Dams, Filling materials for watertight cut off walls, Bulletin 51 (1985).

[36] P. Zhang, Q. Guan, Q. Li, Mechanical properties of plastic concrete containing bentonite, research, J. Appl. Sci., Eng. Technol. 5 (4) (2013) 1317–1322.

[37] Comité Européen de Normalisation, EN 12390-13:2014-06 - Testing hardened concrete - Part 13: Determination of secant modulus of elasticity in compression (German version).2023.

[38] ASTM International, ASTM C469/C469M-14 - Test Method for Static Modulus of Elasticity and Poissons Ratio of Concrete in Compression.2023.

[39] Comité Européen de Normalisation, EN ISO 17892-7:2018–02 - Geotechnical investigation and testing – Laboratory testing of soil – Part 7: Unconfined compression test (German version).2023.

[40] ASTM International, ASTM D2166/D2166M-16 - Test Method for Unconfined Compressive Strength of Cohesive Soil.2023.

[41] Comité Européen de Normalisation EN 197–1:2011-11 - Cement - Part 1: Composition, specifications and conformity criteria for common cements (German version).2023.

[42] L.P. Meier, G. Kahr, Determination of the cation exchange capacity (CEC) of clay minerals using the complexes of Copper (II) ion with Triethylenetetramine and Tretraethylenepentamine, Clays Clay Miner. 47 (3) (1999) 386–388.

[43] A. Steudel, Selection strategy and modification of layer silicates for technical applications, Dissertation, Karlsr. Inst. Technol. (2009), https://doi.org/10.5445/KSP/1000010748.

[44] Deutsches Institut für Normung DIN 1045–2:2008–08 - Tragwerke aus Beton, Stahlbeton und Spannbeton - Teil 2: Beton - Festlegung, Eigenschaften, Herstellung und Konformität - Anwendungsregeln zu DIN EN 206–1 (in German).2023.

[45] Comité Européen de Normalisation EN 1008:2002–10 - Mixing water for concrete - Specification for sampling, testing and assessing the suitability of water, including water recovered from processes in the concrete industry, as mixing water for concrete (German version).2023.

[46] L. Lei, M. Palacios, J. Plank, A.A. Jeknavorian, Interaction between polycarboxylate superplasticizers and non-calcined clays and calcined clays: A review, Cem. Concr. Res. 154 (2022), 106717, https://doi.org/10.1016/j.cemconres.2022.106717.

[47] C.-S. Barbu, A.-D. Sabau, D.-M. Manoli, M.-S. Serbulea, Water/cement/bentonite ratio selection method for artificial groundwater barriers made of cutoff walls, Water 14 (3) (2022) 376, https://doi.org/10.3390/w14030376.

[48] Comité Européen de Normalisation EN 12350-2:2019-09 - Testing fresh concrete - Part 2: Slump test (German version).2023.

[49] Comité Européen de Normalisation EN 12350-5:2019-09 - Testing fresh concrete - Part 5: Flow table test (German version).2023.

[50] Comité Européen de Normalisation EN 12350-6:2019-09 - Testing fresh concrete - Part 6: Density (German version).2023.

[51] Comité Européen de Normalisation EN 12350-7:2019:09 - Testing fresh concrete - Part 7: Air content - Pressure methods (German version).2023.

[52] Comité Européen de Normalisation EN 12390-1:2021-09 - Testing hardened concrete - Part 1: Shape, dimensions and other requirements for specimens and moulds (German version).2023.

[53] Comité Européen de Normalisation EN 196-1:2016-11 - Methods of testing cement - Part 1: Determination of strength (German version).2023.

[54] Comité Européen de Normalisation EN 12390-2:2019-10 - Testing hardened concrete - Part 2: Making and curing specimens for strength tests (German version).2023.

[55] Comité Européen de Normalisation EN 12390-3:2009-07 - Testing hardened concrete - Part 3: Compressive strength of test specimens (German version).2023.

[56] Deutsches Institut für Normung DIN 4093:2015-11 - Bemessung von verfestigten Bodenkörpern - Hergestellt mit Düsenstrahl-, Deep-Mixing- oder Injektions-Verfahren (in German).2023.

[57] J.K. Norvell, J.G. Stewart, M.C. Juenger, D.W. Fowler, Influence of clays and clay-sized particles on concrete performance, J. Mater. Civ. Eng. 19 (12) (2007) 1053–1059, https://doi.org/10.1061/(ASCE)0899-1561(2007)19:12(1053).

[58] J. Ahmad, K.J. Kontoleon, M.Z. Al-Mulali, S. Shaik, M. HechmiElOuni, M.A. El-Shorbagy, Partial substitution of binding material by bentonite clay (BC) in concrete: a review, Buildings 12 (5) (2022) 634, https://doi.org/10.3390/buildings12050634.

[59] V.A. Fernandes, P. Purnell, G.T. Still, T.H. Thomas, The effect of clay content in sands used for cementitious materials in developing countries, Cem. Concr. Res. 37 (5) (2007) 751–758, https://doi.org/10.1016/j.cemconres.2006.10.016.
[60] B. Cao, J. Chen, A. Al-Tabbaa, Crack-resistant cement–bentonite cut-off wall materials incorporating superabsorbent polymers, Can. Geotech. J. 58 (6) (2021) 800–810, https://doi.org/10.1139/cgj-2020-0181.
[61] H. Zhao, Y. Ma, J. Zhang, Z. Hu, H. Li, Y. Wang, J. Liu, K. Wang, Effect of clay content on shrinkage of cementitious materials, Constr. Build. Mater. 322 (2022), 125959, https://doi.org/10.1016/j.conbuildmat.2021.125959.
[62] European Federation of Foundation Contractors. Deep Foundations Institute, Guide to Tremie Concrete for Deep Foundations, 2nd edition.,, 2018. ⟨https://www.effc.org/media_corner/effc-dfi-guide-to-tremie-concrete-for-deep-foundations-2nd-edition/⟩.
[63] G.A. Smith, S.W. Benham, A study of the flow-table and the slump test, Acids J. Proc. 27 (1) (1931) 420–438, https://doi.org/10.14359/8194.
[64] Deutsches Institut für Normung e.V., DIN-Fachbericht 100:2010–03 - Beton - Zusammenstellung von DIN EN 206–1 Beton - Teil 1: Festlegung, Eigenschaften, Herstellung und Konformität und DIN 1045–2 Tragwerke aus Beton, Stahlbeton und Spannbeton - Teil 2: Beton; Festlegung, Eigenschaften, Herstellung und Konformität; Anwendungsregeln zu DIN EN 206–1 (in German).2023.
[65] F. Jafarzadeh, S.H. Mousavi, Effect of specimenas age on mechanical properties of plastic concrete walls in dam foundations, Electron. J. Geotech. Eng. 17 (D) (2012) 473–482. ⟨http://www.ejge.com/2012/Abs12.042.htm⟩.
[66] H.S. Müller, M. Boumaaza, Modeling concrete properties: new approaches in MC2020, Struct. Concr. (2023), https://doi.org/10.1002/suco.202201231.
[67] D. AlósShepherd, S. Bruckschlögl, E. Kotan, F. Dehn, Untersuchungen zur Anwendbarkeit optischer Verformungsmessverfahren bei Plastic Concrete, Bautechnik 97 (3) (2020) 171–179, https://doi.org/10.1002/bate.201900071.